Titre: Title:	Controllability limitations of TMP-refining processes
Auteur: Author:	Ilich Lama Bustinza
Date:	2006
Type:	Mémoire ou thèse / Dissertation or Thesis
Référence: Citation:	Lama Bustinza, I. (2006). Controllability limitations of TMP-refining processes [Thèse de doctorat, École Polytechnique de Montréal]. PolyPublie. https://publications.polymtl.ca/7747/

UNIVERSITÉ DE MONTRÉAL

CONTROLLABILITY LIMITATIONS OF TMP-REFINING PROCESSES

ILICH LAMA BUSTINZA
DÉPARTEMENT DE GÉNIE CHIMIQUE
ÉCOLE POLYTECHNIQUE DE MONTRÉAL

THÈSE PRÉSENTÉE EN VUE DE L'OBTENTION
DU DIPLÔME DE PHILOSOPHIAE DOCTOR
(GÉNIE CHIMIQUE)
AVRIL 2006

Your file Votre référence
ISBN: 978-0-494-17979-6
Our file Notre référence
ISBN: 978-0-494-17979-6

UNIVERSITÉ DE MONTRÉAL

ÉCOLE POLYTECHNIQUE DE MONTRÉAL

Cette thèse intitulée :

CONTROLLABILITY LIMITATIONS OF TMP-REFINING PROCESSES

présentée par : LAMA BUSTINZA Ilich
en vue de l'obtention du diplôme de : Philosophiæ Doctor
a été dûment acceptée par le jury d'examen constitué de :

M. TANGUY Philippe, Ph.D., président
M. STUART Paul, Ph.D., membre et directeur de recherche
M. PERRIER Michel, Ph.D., membre et codirecteur de recherche
M. SRINIVASAN Bala, Ph.D., membre
M. RITALA Risto Kalevi, Ph.D., membre

A Gisella, mi trébol de cuatro hojas...

"Nature uses only the longest threads to weave her patterns, so that each small piece of her fabric reveals the organization of the entire tapestry"
Richard Feynman (1918-1988)

REMERCIEMENTS

Je voudrais remercier mon directeur de recherche, le professeur Paul Stuart et mon co-directeur le professeur Michel Perrier pour leurs conseils et les discussions fructueuses que nous avons eus tout au long de ces années mémorables. L'appui que j'ai toujours reçu de leur part s'est révélé critique dans l'élaboration de cette thèse.

Je voudrais également remercier la Chaire Industrielle d'Intégration de Procédés pour l'aide financière reçue pendant mes études à Polytechnique. De même, je tiens à remercier le Conseil de Recherches en Sciences Naturelles et en Génie du Canada (CRSNG) et le Fonds Québécois de la Recherche sur la Nature et les Technologies (FQRNT) pour le support financier alloué à mon projet de recherche.

Le travail effectué dans cette thèse a été enrichi, dans sa forme et son contenu, par la précieuse collaboration de Monsieur Alain Roche. Ses idées, toujours innovatrices, précises et surtout généreuses, ont été importantes dans le développement de mes travaux. De même, je voudrais remercier Abitibi Consolidated Inc., en particulier, Pascal Hébert et Marc Dalton pour leur implication, ainsi que Martin Fairbank pour la critique constructive de plusieurs articles techniques formant la base du présent travail.

Mon remerciement sincère à Mme Agnès Dévarieux-Martin pour son appui constant et son attitude proactive. Ses qualités personnelles la rendent littéralement indispensable à tous les égards.

J'exprime ma gratitude à Monsieur José-Antonio Orccotoma pour l'occasion qui m'a été offerte, il y a déjà six ans, de découvrir le Canada et par la suite d'entreprendre des études en cycles supérieurs. Son accueil et ses conseils ont été un point d'appui considérable dont je lui serai toujours reconnaissant.

Un remerciement spécial au groupe d'étudiants de la Chaire, à ceux qui ne sont plus là et à ceux qui y restent. Chacun et chacune par leurs qualités, par leur personnalité et par ses gestes ont pour moi, redéfini et exalté la signification de l'amitié.

Un gracias capital pour ma famille au Pérou, mon père César et ma mère Maggy ainsi que mon cher frère José Carlos. Ils représentent la base essentielle de tout ce que je suis. Leur appui et présence sont aussi frais dans mon coeur que le jour de mon départ et m'inspirent à atteindre des sommets toujours plus hauts.

Finalement, les remerciements les plus tendres et mérités vont à Gisella, ma femme. Avec ses sourires, sa générosité et son encouragement, elle est sans aucun doute la pièce maîtresse de cette réalisation. Je t'aime.

RÉSUMÉ

Au Canada, l'industrie des pâtes et papier est l'un des secteurs industriels les plus importants, notamment celui de la production de papier journal à partir de la pâte thermomécanique (PTM). La variabilité excessive de la qualité de la pâte peut causer des casses de la feuille sur la machine à papier, une diminution de la vitesse de la machine ainsi que la production de papier qui est hors spécification. En particulier, la variabilité associée aux limitations inhérentes du procédé ne peut pas être atténuée même avec le système de contrôle le plus avancé, à moins d'entreprendre des changements de conception ou de redéfinir des conditions d'opération courantes. Cette variabilité n'a pas encore été étudiée dans une perspective de boucle ouverte, telle que l'analyse de contrôlabilité. La contrôlabilité est une propriété inhérente du procédé puisqu'elle ne dépend pas du système de contrôle. Elle indique la facilité avec laquelle une usine peut être maintenue à un régime permanent malgré des perturbations externes et des incertitudes. L'analyse de contrôlabilité a été appliquée à une grande variété de procédés chimiques pour examiner des solutions au niveau de la conception ou pour choisir les configurations de contrôle les plus appropriées. En ce qui concerne les procédés de raffinage de la PTM en deux étapes, aucune étude de contrôlabilité n'a été publiée à ce jour.

L'objectif principal de la thèse est de développer une méthodologie par modèles pour élucider le potentiel inhérent d'atténuation de la variabilité dans les opérations de raffinage de la PTM. En particulier, la méthodologie détecte dans quelles conditions une usine atteint une opération à faible variabilité, en plus de déterminer le rapport entre cette opération et ses limitations de contrôlabilité. Un aspect important de l'approche est qu'elle est indépendante de la configuration de contrôle utilisée.

La méthodologie commence par la collection des données pour une année complète afin de capturer une grande plage de conditions d'opération. Ces données sont nettoyées des points aberrants pour leur utilisation dans la modélisation du procédé de raffinage de la PTM. Un des avantages importants de la procédure de modélisation est que l'identification conventionnelle en utilisant des échelons n'est pas nécessaire puisque l'information est extraite à partir de l'opération courante. Avec le modèle en place, la directionalité des interactions principales ayant lieu dans des procédés raffinage de la PTM est discutée. Les résultats fournissent un aperçu sur la façon d'opérer des raffineurs PTM par rapport à l'usure des plaques et son impact sur la qualité de la pâte. D'où la prochaine étape qui consiste en la formulation d'un problème d'optimisation. Ceci évalue l'effet à long terme de l'usage des plaques sur la minimisation de l'énergie nécessaire pour produire de la pâte dans les spécifications désirées. Cette structure d'optimisation nous sert à évaluer le potentiel pour réduire la consommation d'énergie de raffinage en opérant autour des conditions alternatives. La conclusion la plus importante de cette étape est que la plus grande opportunité d'économiser de l'énergie se présente lorsque l'on opère avec de vieilles plaques. Ensuite, le modèle est linéarisé autour des points d'opération actuel et alternatif afin de comparer leurs limitations de contrôlabilité par rapport à l'atténuation de la variabilité. Les résultats indiquent que l'opération, autour des conditions alternatives, implique plus de potentiel pour l'atténuation de la variabilité. Finalement, puisque la plupart des usines contrôlent seulement un paramètre de qualité de la pâte, à savoir l'égouttage, la dernière étape de notre méthodologie discute des raisons de ce choix et propose, par analyse de contrôlabilité, une configuration décentralisée tenant compte des interactions du procédé. Les résultats indiquent que l'égouttage est une variable plus convenable à contrôler que le contenu de fibre longue et c'est donc en elle que réside un plus grand potentiel d'atténuation de la variabilité.

L'application de la méthodologie à l'étude de cas donne des contributions thématiques importantes concernant l'effet de l'âge des plaques et de la qualité du bois sur la

contrôlabilité des opérations de raffinage de la PTM. Deux des contributions les plus importantes figurent ci-dessous:

- La contrôlabilité de l'opération de raffinage avec de vieilles plaques est limitée à cause de sa proximité aux contraintes du procédé. Ainsi, plus les plaques deviennent usées dans les raffineurs, plus il est difficile d'atténuer les variations dans la qualité du bois à plus long terme. La raison est que l'âge diminue la sensibilité du procédé aux changements des entrées manipulées et donc, aux fréquences où le contrôle est nécessaire, l'effort de manipulation pourrait atteindre la saturation. D'ailleurs, nos résultats indiquent que quand les plaques sont vieilles, l'opération de raffinage devient de plus en plus mal conditionnée, c'est-à-dire potentiellement plus difficile à contrôler. D'autre part, l'âge des plaques réduit également l'effet des perturbations sur les sorties de procédé et donc, il se pourrait que le raffinage n'ait pas besoin de contrôle pour certaines fréquences et conditions de variabilité dans la densité et humidité du bois.

- Indépendamment de l'âge des plaques, la perturbation la plus problématique se produit lorsque la densité et l'humidité du bois changent dans des directions opposées. En revanche, si l'un des deux change et pas l'autre, il est beaucoup plus facile de rejeter l'effet sur le système de la densité que celui de l'humidité du bois avec un contrôle décentralisé.

Finalement, étant donné le compromis entre optimalité et contrôlabilité sous certaines conditions, l'atténuation de la variabilité peut être fortement limitée par le montant additionnel d'énergie spécifique que l'opération est disposée à consommer afin d'avoir plus de manoeuvrabilité pour le contrôle. Ce travail est ainsi un point de départ vers le développement d'un système de contrôle optimal capable de gérer l'effet de l'usure des plaques et des variations du bois sur la qualité de la pâte.

ABSTRACT

In Canada, the pulp and paper industry is by many measures the most important industry sector, and of particular relevance is newsprint production from thermo-mechanical pulp (TMP). Excessive variability in pulp quality most likely results in paper machine breaks, reduced paper machine speed and paper off-spec. In particular, variability associated to process-inherent limitations cannot be overcome by even the most advanced control system unless design changes are undertaken or current operating conditions are redefined. This type of variability is yet to be approached from an open-loop perspective such as controllability analysis. Controllability is a property of the process that accounts for the ability to remain at a specified operating regime despite bounded external disturbances and uncertainties, and regardless of the control system imposed on it. So far, controllability analysis has been used in a variety of chemical engineering applications to screen flowsheet alternatives or select the best control configurations. No controllability studies have been reported to date on two-stage TMP-Refining processes.

The main objective of the present thesis is to develop a model-based methodology that elucidates the inherent potential for variability attenuation in TMP-Refining operations. In particular, the methodology detects when and under what conditions the plant was able to achieve a low variability operation, and determines how far that operation is from its inherent controllability limitations. An important aspect of the approach is that it is independent of the control configuration currently in place.

The methodology starts by collecting over a year worth of data so as to account for a wide range of operating conditions. This data is outlier-cleaned and used to model the TMP-Refining process. One major advantage of the modeling procedure is that conventional bump testing is not necessary since process information is extracted from

routine operation. With the model in place, the directionality of the main interactions taking place in TMP-Refining processes is discussed. Results provide an insight into how TMP refiners can be operated as plates wear and the associated impact on pulp quality. Hence, the next step is to formulate an optimization problem that accounts for the long-term effect of plate wear on the minimization of the energy necessary to produce pulp within specifications. Using this optimization framework, we evaluate the potential for reducing energy consumption by operating around alternative conditions. The most important conclusion from this application is that the largest opportunity to save energy arises when operating with old plates. Next, the model is linearized around both the current and the alternative operating points so as to compare their controllability limitations for variability attenuation. Results indicate that operation around alternative conditions involves more potential for variability attenuation. Finally, given that most plants control only one pulp quality parameter, namely freeness, the purpose of the last stage in our methodology is to investigate the reasons behind this selection, and propose – via controllability analysis - a decentralized configuration aware of process interactions. Results indicate that freeness is a more suitable controlled variable than long fibre content, and therefore has more potential for variability attenuation.

The application of the methodology to the case study has given rise to important thematic contributions regarding the effect of wood quality and plate age on the controllability of TMP-Refining operations. Below the two most important:

- The controllability of the operation with old plates is limited given its proximity to constraints. Accordingly, the older the plates in both refiners, the harder the attenuation of wood moisture and density variations becomes in the longer term. The reason is that age reduces the sensitivity of the process to input changes, and thus at frequencies where control is actually needed the manipulated effort may reach saturation. Furthermore, our findings indicate that when plates are old the

refining plant becomes increasingly ill-conditioned, i.e. potentially hard to control. On the other hand, plate age also reduces the effect of disturbances on process outputs, and consequently refining may not require control at certain frequencies and wood variability conditions.

- Regardless of plate age, the most problematic disturbance occurs when wood moisture and wood density enter the system in opposite directions. Individually, wood density is much easier to reject than wood moisture under decentralized control.

Finally, given the inherent trade-off between optimality and controllability under certain disturbance and plate age conditions, variability attenuation may be strongly limited by the additional amount of specific energy the operation is willing to consume in order to have more manoeuvrability for control. This work is thus an initial step towards developing an optimal control system capable of handling the effect of wood variations and plate wear upon pulp quality.

CONDENSÉ EN FRANÇAIS

L'industrie des pâtes et papiers est un secteur cyclique et compétitif, où les améliorations de productivité même minimes sont critiques. Au Canada, elle est l'un des secteurs industriels les plus importants, notamment pour la production de papier journal à partir de pâte thermomécanique (PTM). La variabilité excessive de la qualité de la pâte peut causer des casses de la feuille sur la machine à papier, une diminution de la vitesse de la machine ainsi qu'une production de papier hors spécification.

La variabilité, associée à des caractéristiques inhérentes au procédé, n'a pas encore été étudiée dans une perspective boucle ouverte. Ce type de variabilité ne peut pas être atténué même avec le système de contrôle le plus avancé, à moins que des changements de conception soient entrepris ou que des conditions d'opération courantes soient redéfinies. Dans ce travail, nous explorons des points d'opération alternatifs qui possèdent une bonne contrôlabilité, plutôt que des changements au niveau de la conception qui entraînent en général des coûts d'investissement importants.

La contrôlabilité est une propriété inhérente au procédé, qui indique la facilité avec laquelle une usine peut être maintenue à un régime permanent, malgré des perturbations externes et des incertitudes, et ce, indépendamment du système de contrôle. L'analyse de contrôlabilité a été appliquée à une grande variété de procédés chimiques pour examiner des solutions au niveau conception, ou pour choisir les configurations de contrôle les plus appropriées. À ce jour, en ce qui concerne les procédés de raffinage de la PTM en deux étapes, aucune étude de contrôlabilité n'a été publiée.

L'objectif principal de la thèse est de développer une méthodologie par modèles, pour élucider le potentiel inhérent d'atténuation de la variabilité dans les opérations de

raffinage de la PTM. En particulier, la méthodologie doit détecter dans quelles conditions une usine atteint une opération à faible variabilité, en plus de déterminer le rapport entre cette opération et ses limitations de contrôlabilité. Un aspect important de l'approche est qu'elle est indépendante de la configuration de contrôle utilisée.

La méthodologie comprend sept étapes: collecte de données, modélisation mécaniste, étude de la directionnalité des interactions, optimisation par modèles, détermination des points alternatifs d'opération pour réduire la consommation d'énergie de raffinage, détection du potentiel d'atténuation de la variabilité et proposition d'un système de contrôle décentralisé. Les paragraphes suivants expliquent brièvement chacune de ces étapes.

Dans un premier temps, les valeurs moyennes horaires de chaque donnée d'opération ont été collectées sur une année, afin de capturer une grande plage de conditions opératoires. Une technique de filtrage robuste est appliquée aux données pour enlever des points aberrants. Les frontières de la collecte de données incluent les raffineurs et le cuvier de latence.

L'étape de modélisation est divisée en deux parties. Dans la première partie, nous proposons une procédure pour modéliser la charge du moteur, en fonction de l'âge des plaques et des entrées normalement manipulées pour contrôler les raffineurs. Des techniques d'identification de régimes permanents, ainsi que des données d'opération à court terme non comprimées, sont utilisées pour estimer la dynamique des raffineurs. La deuxième partie est axée sur la modélisation de la qualité de la pâte. Ce modèle estime les caractéristiques de la pâte en termes d'égouttage et de classification de fibres. Les deux modèles sont ensuite couplés en se basant sur des relations mécanistes, des données d'opération courantes et des essais en laboratoire. Les prédictions données par le modèle suivent les tendances et les dérives réelles à long terme. Un des avantages importants de la procédure est que l'identification conventionnelle en

utilisant des échelons n'est pas nécessaire, puisque l'information est extraite à partir de l'opération courante.

La nature interactive des procédés de raffinage de la PTM est l'une des sources les plus importantes de variabilité dans la qualité de la pâte. Avec le modèle en place, la troisième étape consiste à déterminer la directionalité des interactions principales dans le procédé en question. Les résultats fournissent un aperçu sur la façon d'opérer des raffineurs de PTM, en tenant compte de l'usure des plaques et de son impact sur la qualité de la pâte.

La quatrième étape de la méthodologie utilise le modèle pour optimiser l'opération de raffinage de la PTM à mesure que les plaques s'usent. Le problème d'optimisation tient donc compte de l'effet à long terme de l'usure des plaques sur la minimisation de l'énergie nécessaire pour produire de la pâte dans les spécifications désirées. La sensibilité de l'opération optimale, vis-à-vis de changements importants des contraintes du procédé et des conditions de qualité du bois, est également soulignée.

Dans une usine intégrée de papier journal, la quantité d'énergie de raffinage représente environ 70-75% de la totalité des besoins en énergie électrique. Dans ce contexte, la structure d'optimisation développée nous sert à évaluer le potentiel de réduction de cette consommation. En particulier, la procédure détecte sous quelles conditions l'usine atteint une opération à faible variabilité, par l'intermédiaire de l'identification de régimes permanents, et ensuite vérifie si une condition d'opération alternative optimale, peut être trouvée. Les résultats sont donnés pour des conditions spécifiques de l'âge des plaques dans les deux raffineurs et de la qualité du bois. La conclusion la plus importante est que la plus grande opportunité d'économiser d'énergie se présente lorsque l'on opère avec de vieilles plaques.

Les caractéristiques variables du bois, l'âge des plaques dans les raffineurs, les limites au niveau conception et opération et les interactions internes du procédé, toutes contribuent à la variabilité dans le raffinage du bois. Dans l'étape six, le modèle est linéarisé autour des points d'opération actuel et alternatif afin de comparer leurs limitations de contrôlabilité par rapport à l'atténuation de la variabilité. Les contraintes du procédé, les interactions internes fondamentales, l'âge de plaque et les variations du bois (humidité et densité) sont intégrées dans la formulation du problème. Les solutions sont indépendantes de la configuration de contrôle utilisée, et sont analysées du point vue statique et dynamique. Les graphes, utilisés pour représenter le potentiel d'atténuation de la variabilité, permettent d'identifier le niveau de variabilité maximale, au niveau de la qualité du bois que le procédé serait capable de gérer sous l'action du système de contrôle. Les résultats indiquent que l'opération autour de ces conditions alternatives donne un meilleur potentiel d'atténuation de la variabilité.

Étant donné que la plupart des usines contrôlent uniquement un paramètre de qualité de la pâte, à savoir l'égouttage, la dernière étape de notre méthodologie discute des raisons du choix et propose, par analyse de contrôlabilité, une configuration décentralisée tenant compte des interactions du procédé. Les résultats indiquent que dans un système décentralisé où les charges du moteur sont contrôlées par les pressions hydrauliques, et où les consistances le sont par les débits de dilution, l'égouttage est une variable plus convenable à contrôler que le contenu de fibre longue. En effet, l'impact des interactions en boucle fermée, sur la boucle qui contrôle l'égouttage, est favorable pour l'atténuation de la variabilité.

L'application de la méthodologie à l'étude de cas donne des contributions thématiques importantes, concernant l'effet de l'âge des plaques et de la qualité du bois sur la qualité de la pâte et la contrôlabilité des opérations raffinage de la PTM. Les contributions les plus importantes sont les suivantes:

- Pour des conditions données d'âge des plaques, de dilution et de taux de production, un contenu de fibre longue et égouttage élevés sont atteints en appliquant de haut split d'énergie (par rapport au raffineur primaire) à basse énergie totale.

- L'âge des plaques augmente le split d'énergie ainsi que l'intensité de raffinage dans les deux raffineurs. En outre, plus les plaques s'usent, plus l'application d'énergie sur la pâte est difficile. Si les deux raffineurs commencent leur opération avec des plaques neuves, la fenêtre d'opération se déplace graduellement vers des zones de bas égouttage et de bas faible de fibre longue.

- L'augmentation de l'humidité du bois et des conditions de dilution déplacent la fenêtre d'opération principalement vers des zones de bas contenu de fibre longue.

- À égouttage constant, du bois à haute densité favorise l'économie d'énergie. En outre, le raffinage optimal du bois à haute densité produit, à mesure que les plaques s'usent, de la pâte avec un égouttage et un contenu de fibre longue plus élevés.

- À égouttage constant, et en supposant que l'humidité du bois représente des conditions saisonnières, l'opération hivernale permet une économie supérieure par rapport à l'opération estivale, mais produit un contenu de fibre longue inférieur.

- À égouttage constant, la relaxation des limites inférieures de la charge du moteur primaire, réduit considérablement la consommation d'énergie par rapport à une opération avec des limites plus serrées. Par ailleurs, quand les plaques commencent à vieillir, ces conditions relaxées permettent d'atteindre des valeurs d'égouttage plus élevées. En revanche, des contraintes inférieures plus serrées permettent d'atteindre des contenus de fibre longue plus élevés à égouttage constant.

- Les spécifications d'égouttage inférieures plus relaxées impliquent des économies d'énergie et un contenu de fibre longue plus élevés, surtout lorsque les plaques sont relativement neuves.

- La contrôlabilité de l'opération de raffinage avec de plaques vieilles est limitée à cause de la proximité des contraintes du procédé. Ainsi, plus les plaques deviennent usées dans les raffineurs, plus il est difficile d'atténuer à plus long terme les variations dues à la qualité du bois. En effet, l'âge diminue la sensibilité du procédé aux changements des entrées manipulées et donc, aux fréquences où le contrôle est nécessaire, l'effort de manipulation pourrait atteindre la saturation. D'ailleurs, nos résultats indiquent que, quand les plaques sont vieilles, l'opération de raffinage devient de plus en plus mal conditionné, c'est-à-dire potentiellement plus difficile à contrôler. L'âge des plaques réduit également l'effet des perturbations sur les sorties de procédé, et il se pourrait donc que le raffinage n'ait pas besoin de contrôle pour certaines fréquences et conditions de variabilité dans la densité et l'humidité du bois.

- Indépendamment de l'âge des plaques, la perturbation la plus problématique se produit lorsque la densité et l'humidité du bois changent dans des directions opposées. En revanche, si l'un des deux change et pas l'autre, il est beaucoup plus facile de rejeter l'effet sur le système de la densité, que celui de l'humidité du bois avec un contrôle décentralisé.

- L'âge des plaques n'a pas un effet important sur les interactions de procédé avec un contrôle décentralisé. En fait, le changement de l'effet des perturbations provoqué par le contrôle décentralisé ne varie pas avec l'âge des plaques.

Quant aux travaux futurs à entreprendre, les opportunités suivantes ont été identifiées.

En ce qui concerne la modélisation, il serait intéressant d'étudier s'il y a un changement important, du à l'âge des plaques, dans les constantes de temps décrivant la dynamique de la charge du moteur. Un autre aspect à explorer est l'introduction de la distribution granulométrique des copeaux et l'humidité du bois dans la structure du modèle décrivant la charge du moteur. Des développements récents, au niveau des systèmes de gestion de copeaux et des mesures de qualité du bois en ligne, pourraient aider à clarifier comment ces caractéristiques du bois affectent non seulement la charge du moteur mais la qualité de la pâte en général.

En ce qui concerne la méthodologie, l'identification de régimes permanents est un aspect important. L'application de cette technique dans le contexte de cette thèse se base sur l'hypothèse qu'une seule variable (la charge du moteur) peut jouer le rôle d'indicateur de régimes permanents pour le système en entier. Des travaux futurs pourraient éviter cette hypothèse et appliquer directement des techniques d'identification multivariables en autant que les variables choisies ne soient pas corrélées.

Afin de simplifier les calculs durant les optimisations, nous avons fait l'hypothèse que l'égouttage reflète la quantité de fines dans la pâte. Des travaux futurs devraient inclure explicitement le contenu de fines dans l'application de la méthodologie générale, en plus de l'égouttage et du contenu de fibre longue. Ainsi, des propriétés physiques du papier, telles que la résistance à la traction ou l'indice de déchirement, pourront faire partie de la formulation du problème. En plus, nous avons également supposé lors de l'optimisation en fonction de l'âge des plaques que, les deux étapes de raffinage commencent l'opération avec des plaques neuves. Dans ce contexte, il serait intéressant de considérer la problématique de changement de plaques. Le modèle présenté dans cette thèse peut être utilisé à cette fin, puisque sa structure permet de simuler différentes conditions de plaques dans chaque raffineur.

Finalement, étant donné le compromis entre optimalité et contrôlabilité sous certaines conditions, l'atténuation de la variabilité peut être fortement limitée par le montant additionnel d'énergie spécifique que l'opération est disposée à consommer, afin d'avoir plus de manoeuvrabilité pour le contrôle. Ce travail est ainsi un point de départ vers le développement d'un système de contrôle optimal, capable de gérer l'effet de l'usure des plaques et des variations du bois sur la qualité de la pâte. Pour cela, il faudrait d'abord caractériser la relation entre l'usure de la plaque et l'âge de la plaque.

TABLE OF CONTENTS

LIST OF TABLES

LIST OF FIGURES

LIST OF APPENDICES

LIST OF SYMBOLS AND ABBREVIATIONS

a_o = plate age constant

A = plate age factor

A_o = plate age residual constant

A_{TOT} = specific surface area, m^2/g

Bauer14 = Bauer McNett fraction +14, %

Bauer28 = Bauer McNett fraction +14/28, %

B_1 = probability that when shives are broken down, that the broken fibres will become long fibres

C = consistency, %

CN = condition number

CSF = pulp freeness, mL

d = vector of process disturbances

dc = Volumetric design capacity of the transfer screw feeder for a given chip size distribution and chip packing, m^3/hr/RPM

D = total basic density of wood mix, o.d.kg/m^3

D_u = diagonal scaling matrix for manipulated inputs

D_y = diagonal scaling matrix for process outputs

D_d = diagonal scaling matrix for process disturbances

e = vector of offsets or control errors

e_{loss} = heat losses, fraction

f_i = refining intensity factor

f_{CSF}, f_{LF}, f_{MF} = corrective factors accounting for the direct plate age effect on pulp quality

F_c = dry production rate, TN/d

F_d = setpoint to the dilution flowrate control loop, L/min

F_{dil} = dilution mass flowrate, TN/d

FF_{PQM} = estimated fine PQM fraction, %

F_{seal} = seal water mass flowrate, TN/d

G = process transfer matrix

G_d = disturbance transfer matrix

G_{ref} = transfer function representing the dynamics inside the refiner

G_{reg} = transfer function of a regulatory loop

H = water content of the pulp entering the refiner or wood moisture, %

JP_{mix} = mass fraction of Jack Pine in the low density wood mix

K_f = factor quantifying the degree of surface development in the pulp

K = matrix of process gains

K_{ML} = motor load gain

L = average fibre length, mm

L_{48} = cumulative weighted average fibre length at Bauer McNett fraction +48, mm

L_e = enthalpy of saturated steam at a given casing pressure P_{ref}, J/kg

LF = long fibre content after latency chest, %

LF_{28} = long fibre content (fraction Bauer McNett +28), %

LF_{PQM} = estimated long fibre PQM fraction, %

L_s = latent heat of steam at a given casing pressure P_{ref}, J/kg

MF_{PQM} = estimated medium fibre PQM fraction, %

ML = motor load, MW

NI = Niederlinski index

p = proportion of wood species in furnish, %

P_{age} = refiner plate age, hr

P_{agemax} = maximum recorded plate lifetime, hr

P_c = setpoint to the hydraulic pressure control loop, KPa

P_{ref} = casing pressure (refiner's outlet pressure), psig

PVA = potential for variability attenuation

Q_{dil} = "big" dilution flowrate to the latency chest, L/min

Q_{RP} = flowrate of primary screens' rejects, L/min

Q_{RS} = flowrate of secondary screen's rejects, L/min

R_{48} = Bauer McNett fraction +28/48, %

RDG = relative disturbance gain

r = vector of setpoint changes

r_{int} = inlet ratio of the refining zone, m

r_{ext} = outlet ratio of the refining zone, m

S_{SVo} = nominal selection parameter representing the probability that a shive will undergo comminution

S_{LFo} = nominal selection parameter representing the probability that a long fibre fraction will undergo comminution

SE = specific energy, kW-hr/TN

SET = total specific energy (both refiners), kW-hr/TN

$splitPR$ = power split (with respect to primary refiner), fraction

spw = specific refining power (a measure of refining intensity), kJ/kg/sec

SV = shives content, %

tss = setpoint to the transfer screw speed control loop, RPM

u = vector of manipulated inputs

U = matrix of output singular vectors

U_{min} = smallest input effort

V = matrix of input singular vectors

W_s = saturated steam mass flowrate leaving the refiner, TN/d

x = tuning parameter for freeness prediction

y = vector of process outputs

y_{loss} = yield loss due to sulfonation or transportation leaks, %

α = constant parameter (obtained from mill data) accounting for the effect of transfer screw speed on motor load

β = constant parameter (obtained from mill data) accounting for the effect of hydraulic pressure on motor load

χ = distribution cutting point for long fibre PQM

γ = constant parameter (obtained from mill data) accounting for the effect of dilution flowrate on motor load

η = motor efficiency, fraction

λ_1, λ_2 = distribution cutting points for medium fibre PQM

Λ = matrix of relative gains (RGA)

μ_r = radial friction coefficient between pulp and plates

μ_t = tangential friction coefficient between pulp and plates

θ = delay time of regulatory loops, sec

ρ = oven dry density of the wood species, kg/m^3

Σ = matrix of nonnegative singular values

$\overline{\sigma}$ = maximum singular value

$\underline{\sigma}$ = minimum singular value

τ_{ref} = residence time spent by the pulp inside the refiner, sec

τ_T = time constant of regulatory loops, sec

ω = rotational speed of the plate, RPM

Subscripts

1 = primary refiner

2 = secondary refiner

3 = pulp after small dilution point

BF = Balsam Fir

BS = Black Spruce

dil = dilution water

final = final quality estimations

HD = High density wood (almost entirely Black Spruce)

HW = hardwood

inlet	=	refiner's inlet
JP	=	Jack Pine
LD	=	low density wood
outlet	=	refiner's outlet
PQM	=	fibre quality given in Pulp Quality Management units
ref	=	refiner
seal	=	seal water

Other symbols

^	=	unscaled value
$^{-1}$	=	pseudo inverse of matrix
^{T}	=	transpose of matrix

CHAPTER 1: INTRODUCTION

"When the number of factors coming into play in a phenomenological complex is too large scientific method in most cases fails."
Albert Einstein (1879 - 1955)

1.1. Problem statement

Pulp and paper industry is a global, cyclical and competitive sector where minimal productivity improvements are critical. In Canada, the pulp and paper industry is by many measures the most important industry sector, and of particular relevance is newsprint production from thermo-mechanical pulp (TMP).

Paper machine runnability is strongly affected by the operation of the TMP-Refining plant which is responsible for transforming wood chips into pulp. Indeed, excessive variability in pulp quality most likely results in paper machine breaks, reduced paper machine speed and paper off-spec.

The problem of process variability in existing plants has been mostly addressed from a closed-loop standpoint, i.e. either by control loop assessment and troubleshooting, or via multivariate statistical analysis. On the other hand, variability associated to process-inherent characteristics is yet to be approached from an open-loop perspective. This type of variability cannot be overcome by even the most advanced control system unless design changes are undertaken or current operating conditions are redefined.

Design changes normally entail high capital costs, and thus in this work we explore alternative operating points with good controllability properties.

A process is controllable if it is able to remain at a specified operating regime despite bounded external disturbances and uncertainties, and regardless of the control system imposed on it. In this context, controllability analysis integrates both process design and control concepts, with the goal of increasing productivity by holding an acceptable control performance. So far, controllability tools have been used in screening flowsheet alternatives or selecting the best control configurations. The applications vary from distillation columns to reactors, to heat-exchanger networks and buffer tanks, and to benchmark plants such as the Tennessee-Eastman process. As for newsprint processes, unsurprisingly it is the paper machine that has received most of the attention, while no controllability studies on two-stage TMP-Refining processes have been reported to date.

The present thesis introduces for the first time a model-based methodology that detects when and under what conditions a TMP-Refining plant is able to achieve an operation with low variability, and then determines how far that operation is from its inherent controllability limitations. The methodology is independent of the control configuration currently in place. The most important thematic contributions resulting from the application are: a methodology to model TMP-Refining processes, an insight on the directionality of process interactions involved in refining, the effect of refiner plate age on operation and pulp quality, and the proposal of a decentralized control structure based on controllability analysis.

1.2. Hypothesis

The main hypothesis of this thesis is that the inherent potential for variability attenuation in a given TMP-refining process can be determined by analyzing the controllability limitations of its operation under different conditions of wood quality and refiner plate age.

1.3. Objectives

The problem statement and the hypothesis call for the development of a systematic methodology to determine the inherent potential for variability attenuation. This methodology is illustrated by case study at an existing TMP-Refining plant and involves the following objectives:

- *To develop a model describing a TMP-Refining process in mechanistic terms.*
- *To understand the directionality of the interactions taking place in TMP-Refining processes.*
- *To optimize, using a model-based approach, the TMP-Refining operation over the long term, specifically as plates wear.*
- *To determine alternative operating points having the potential for reducing current energy consumption levels.*
- *To detect the potential for further variability attenuation around alternative operating points.*
- *To propose an alternative control configuration and analyze its controllability characteristics.*

1.4. Overall methodology

The overall methodology used in this thesis is depicted in Figure 1.1 and consists of seven major stages:

1) **Data collection and pre-treatment**

   Hourly average operating data for both refiners and the latency chest are collected over a year so as to take into account a wide range of operating conditions. A robust technique based on the Hampel filter (Hampel, 1974; Liu et al., 2004) is applied to clean the data. The filter removes the outliers and replaces them with a value that is more representative of the shape of the data. More specifically, the filter estimates the distance between a given data point and the median of the data inside the moving window wherein the detection takes place. If this distance is greater than a given threshold –which is based on the median absolute deviation- the data point is believed to be an outlier and is replaced by the corresponding median.

2) **Process modeling: CHAPTER 3 and CHAPTER 4**

   TMP-Refining processes are, by nature, non-stationary. Indeed, process dynamics change as the quality of the wood fed to the plant varies, and as the refiner plates that defiberize this wood wear out. Consequently, a model able to accurately estimate process targets (notably, motor load) and pulp quality is required. The model explicitly accounts for plate age and very important wood characteristics such as moisture, density and species proportions.

3) **Analysis of the directionality of process interactions: CHAPTER 5**

   This analysis provides an insight into how TMP refiners can be operated as plates wear and the associated impact on pulp quality.

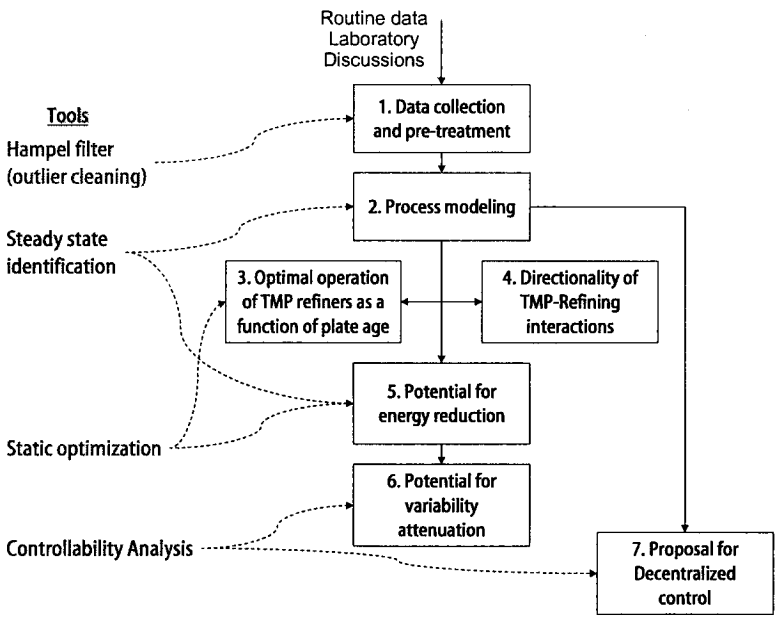

Figure 1.1. Overall methodology

4) **Optimal operation of TMP refiners as a function of plate age: CHAPTER 6**

An optimization framework is developed to minimize – for a given plate age condition - energy consumption while keeping process targets and pulp quality within pre-specified limits. Optimal operating profiles are obtained as a function of plate age by concatenation of static solutions.

5) **Determination of potential for energy reduction around alternative operating points: CHAPTER 7**

Using the optimization framework proposed above, the purpose is to evaluate the potential for energy reduction under low variability conditions detected beforehand via steady state identification. Accordingly, alternative operating points can be calculated for specific conditions of plate age in both refiners and wood quality.

6) **Determination of potential for variability attenuation: CHAPTER 8**
   The model is linearized around both the current and the alternative operating points so as to compare their controllability limitations for variability attenuation.

7) **Proposal for a decentralized control configuration: CHAPTER 9**
   Given that most plants control only one pulp quality parameter, namely freeness, the purpose here is to investigate the reasons behind this selection, and propose – via controllability analysis - a decentralized configuration aware of process interactions.

1.4.1. Steady state identification

Identification of steady state regimes plays a major role in our methodology. It is specifically used in CHAPTER 3 to model motor load, and later on in CHAPTER 7 to detect operating regimes of low variability. The steady state identification technique used in this thesis is based on the *R*-statistic method (Cao and Rhinehart, 1995). This method uses a statistical test (*R*-statistic) to determine whether a given data point is at steady state or not. This metric represents the ratio of variances estimated on the same set of data by two different methods. The variance in the numerator is estimated from deviations between individual data and a filtered value. The variance in the denominator is estimated from deviations between successive data. A data point is likely to be "not at steady state" if its *R*-statistic is larger than a critical value, R_{crit}. Hence, intervals wherein $R < R_{crit}$ are deemed here steady state intervals. Calculations also require the knowledge of the noise variance which can be extracted via process signal analysis (e.g. wavelet transforms, moving average filters, etc.).

Strictly speaking, a given process is at steady state if all its variables are simultaneously at steady state. In practice, detecting steady states with precision is fairly difficult given the lack of measurements of key process variables, the intrinsic uncertainty of available

measurements, and the different dynamic scales involved in most processes. Furthermore, all variables selected to represent a steady state condition cannot be cross-correlated, i.e. variations on each variable must be independent of other variables (Brown and Rhinehart, 2000). In order to overcome the above mentioned issues, throughout this work only one variable is chosen to represent a steady state condition on the basis of its impact upon the operation. Accordingly, *motor load* is selected since it substantially affects refining intensity, energy consumption and pulp quality.

1.4.2. Process constraints

The constraints of the process are presented in Table 1.1. These limits are used throughout the thesis, notably when performing model-based optimizations in CHAPTER 6, CHAPTER 7 and CHAPTER 8.

Table 1.1. Process constraints

Decision variables (manipulated inputs), u	u_{lower}	u_{upper}
Transfer screw speed, *tss* (RPM)	68	80
Hydraulic Pressure Primary Ref., Pc_1 (KPa)	6500	10500
Dilution flowrate Primary Ref., Fd_1 (L/min)	180	200
Hydraulic Pressure Secondary Ref., Pc_2 (KPa)	5000	10000
Dilution flowrate Secondary Ref., Fd_2 (L/min)	80	100
Output variables, y	y_{lower}	y_{upper}
Motor load Primary Ref., ML_1 (MW)	18	19
Consistency Primary Ref., Co_1 (%)	44	57
Consistency Secondary Ref., Co_2 (%)	45	62
Power split ratio to Primary Ref., $splitPR = \frac{ML_1}{ML_1 + ML_2}$	0.54	0.61
Long fibre content, *LF* (%)	30	34
Freeness, *CSF* (mL)	220	250

CHAPTER 2: LITERATURE REVIEW

"An expert is a person who has made all the mistakes that can be made in a very narrow field."
Niels Bohr (1885 - 1962)

2.1. Newsprint and pulp quality

Newsprint plays a fundamental role in the spreading of information on a massive scale. This type of paper is primarily made from fresh wood pulp that requires certain characteristics to allow for an efficient papermaking operation[1].

The quality characteristics of wood pulp considered in this work are *freeness* and *long fibre content*. The former accounts for the resistance of a fibre mat to the flow of water, i.e. it measures water drainage which has a direct impact on fibre bonding (Saltin and Strand, 1993), paper strength (Kaunonen and Luukkonen, 1992; Qian and Tessier, 1995) and thus, on paper machine runnability. The latter is closely related to fibre flocculation, sheet formation, and also paper strength (Saltin and Strand, 1993; Stoere et al., 2001). Freeness is generally considered to be a good measure of pulp quality, however high freeness may not imply good strength, and therefore monitoring of long fibre content is essential to guarantee acceptable quality. It is worthwhile to note that in order to simplify calculations we have assumed in CHAPTER 6, CHAPTER 7, CHAPTER 8, and CHAPTER 9 that freeness indirectly reflects the amount of fines.

[1] The final pulp stock furnished to papermaking contains virgin fibre, recycled fibre and sometimes chemical pulp.

The Canadian Standard Freeness (CSF) is defined as the number of mL of water collected from the side orifice of the standard tester when a pulp suspension drains through the screen plate at 0.3% consistency and 20°C. Long fibre content is obtained by classifying the pulp into different length fractions using screens. In practice, most plants measure pulp characteristics on-line using Pulp Quality Management (PQM) or Pulp Expert (PE) systems.

It is worthwhile to note that pulp quality parameters can be used to estimate important paper properties. Thus, average fibre length relates very good with tear index and light scattering, whereas freeness is a good tool for estimating tensile and burst strength (Kaunonen and Luukkonen, 1992; Qian and Tessier, 2000). These paper properties are not discussed in this work.

2.2. Wood quality

In most mill facilities, information on pulp quality is scarce. Measurements all limited to only few wood characteristics typically, density, species proportions and moisture. These variables are inputs to the model presented in CHAPTER 3 and CHAPTER 4.

Variations in wood density result in quality variations for mechanical pulps (Rudie et al., 1994; Sundholm, 2000). The main impact of wood density is on production rate (dry pulp throughput) and therefore on the applied specific energy which is ultimately a decisive variable in controlling pulp quality (Brill, 1985; Sundholm, 2000).

In this work, three types of softwood are considered: *Black Spruce*, *Balsam Fir* and *Jack Pine*. Hardwood is also added to the wood mix to improve the optical properties of the pulp. However, given the short average length of its fibre the amount of hardwood in the mix is much smaller than that of softwood.

Wood moisture depends on density, heartwood and resin content, and the conditions under which chips are procured and stored (Sundholm, 2000). The moisture content of the chips has a critical effect on pulp quality since uncontrolled variations affect pulp consistency inside the refiner, and therefore the intensity of the operation.

2.3. Thermomechanical pulping (TMP) process

The TMP process starts by softening the wood chips - that have been previously washed and screened – with pressurized steam so as to facilitate comminution during *refining*. Refining separates the fibre from the chips via attrition and abrasion. Pulp fibres are sent to a chest full of hot water for a while before undergoing screening. Finally, the pulp is thickened and sometimes bleached before heading to the papermaking area. Figure 2.1 depicts in a simplified manner the main line of typical TMP process and highlights the sub-section of interest, i.e. wood refining.

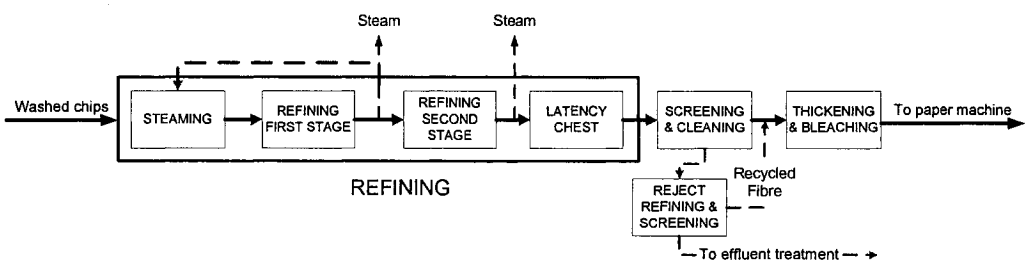

Figure 2.1. Block diagram of a typical TMP process

2.3.1. Wood refiners

Typically, softened chips enter the refining phase at about 40-50% consistency. The refiner is a rotating unit –propelled by an electric motor- that uses hard steel alloy

plates (discs) to defiberize the wood. A representative plate is depicted in Figure 2.2. The plates have three regions of different bar[2] design: breaker bars, intermediate bars and fine bars. The breaker bars are coarse and widely spaced, while intermediate and fine bars have narrower bar width and smaller pitch. The plates are paired face to face with a small interval or gap between them to ensure that the pulp moves evenly toward the periphery.

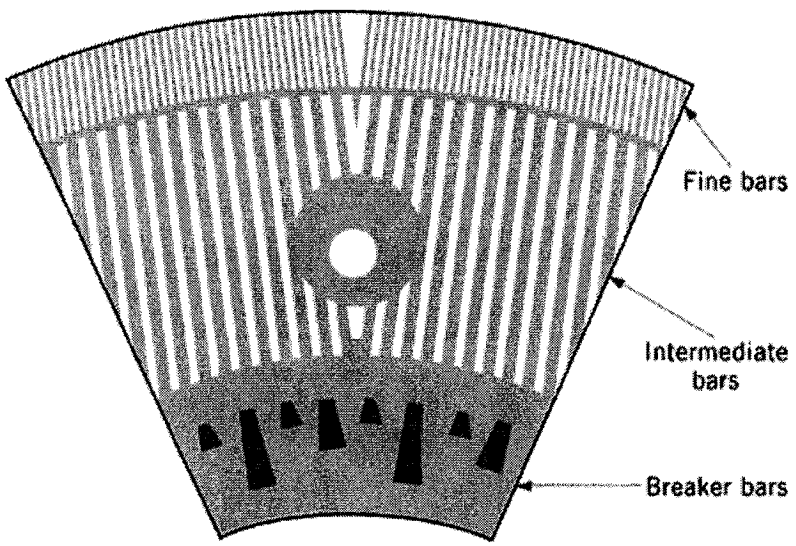

Figure 2.2. Refiner plate design

Refiners can have either a single plate (disc) rotating opposing a stationary plate, or two plates rotating in opposite directions. In either case, defiberization starts with the chips being introduced by a screw feeder into the open eye of the refiner. As the chips move toward the periphery, they undergo attrition and coarse shredding (breaker bars), being progressively broken down into smaller bundles (intermediate bars), and eventually into single fibres (fine bars). Water is supplied to the eye of the refiner to

[2] The length of each bar varies with the type of refiner.

control pulp consistency, which is about 20-40%. At this consistency, a considerable amount of steam is developed because of the heat generated in the fibre material as a result of frictional processes. The pulp exits with the steam, which is removed by means of blow cyclones. The steam is used elsewhere in the plant whether to produce hot water or as a supply in the drying section of the paper machine.

The plant under study in this work operates with Twin refiners. These refiners can handle large production rates and consist of a rotating double-sided plate mounted between two stationary plates which balance the axial thrust on both sides of the rotating plate. This configuration results in two flat refining zones in a single refiner casing (hence the denomination Twin refiner). In the eye of the refiner, wood is fed into the parallel refining zones, one on each side of the rotating plate. The loading of the refiner is accomplished by high hydraulic pressures applied to each end of the refiner. A typical Twin refiner is depicted in Figure 2.3.

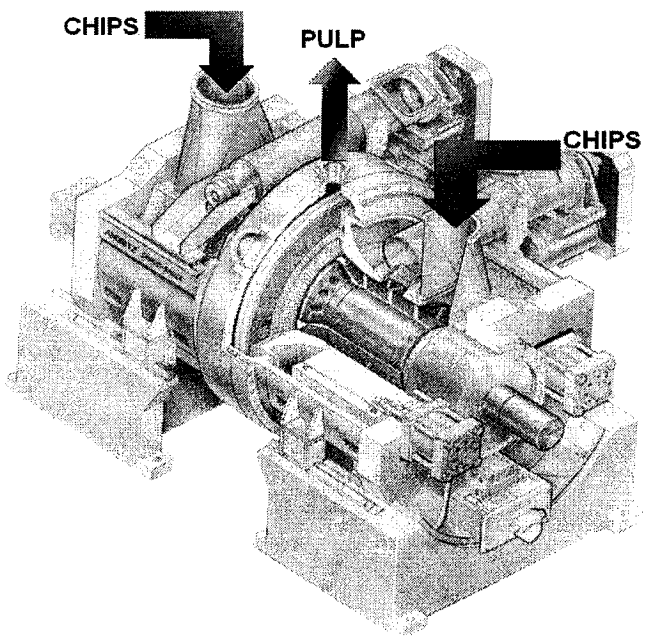

Figure 2.3. Twin-refiner

2.3.2. TMP Refining – Process description

A simplified flowsheet of the two-stage refining process under consideration is depicted in Figure 2.4. Wood chips are fed volumetrically into a steaming vessel (SV). The softened chips leaving SV are sent to the primary refiner (R1) by means of a transfer screw feeder. R1 typically uses more than half of the total energy consumed by both stages to progressively break down the chips into smaller bundles and eventually into single fibres. The pulp exits R1 and passes through a blow cyclone (C1) to separate the steam and then into a secondary refiner (R2) which operates similarly to the primary refiner. In the secondary stage fibres are further developed. As in the first stage, a blow cyclone (C2) is placed after R2 to remove the steam. The fibres in the pulp leaving C2 remain twisted, kinked and curled. This deformed state is known as latency. Latency is removed by heating the pulp (for about 30 to 50 minutes) inside a stirred chest full of hot water (TK). During this period, fibres progressively straighten. The pulp leaving TK is diluted to about 3-6% consistency. It is at this point where pulp quality parameters, namely freeness and long fibre content are measured.

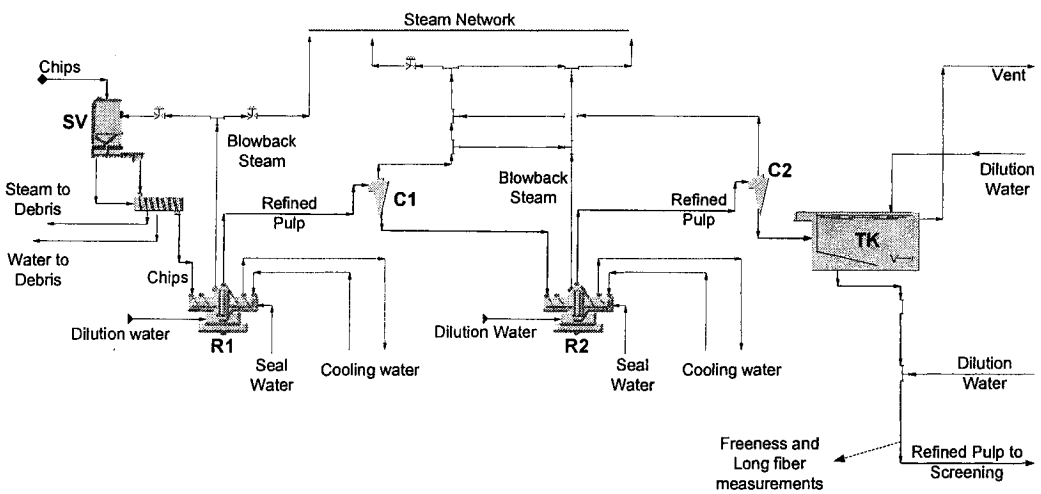

Figure 2.4. Two-stage TMP-refining plant.

2.4. Variability

Every process has some amount of variability. Variability may be reduced by process redesign, better use of process control, or via changes in operating conditions. Process variability and poor control performance can be attributed to variations in raw material, controller tuning, sudden changes in supply utilities, equipment malfunction, process design, or control configuration (Blevins et al., 2003; Tseng et al., 1999; Bialkowski, 1999; Bialkowski, 2001; Bialkowski, 2000; Bialkowski, 2002a; Bialkowski, 2002b; Bialkowski, 2003).

Process control and process design aim at handling inevitable sources of variability. In particular, because of process-inherent dynamic limitations, feedback control can eliminate variability only to some extent. Low process variability can only be achieved if disturbances can be prevented from reaching the process in the first place, whether by implementing feedforward control or by modifying the process itself. In fact, compensating for the above mentioned sources of variability is difficult as variability extends over a large frequency spectrum. Variability associated to process control develops within relatively low frequency ranges. On the other hand, higher frequency disturbances can only be attenuated by changing the design of the process. In any case, if variability cannot be reduced in the upstream processes it will eventually appear in the final product.

2.4.1. Variability Detection and Diagnosis

Process understanding is fundamental in detecting new sources of variability. In addition, there are several statistical tools that help in performing a sound variability assessment. Below, some of the most utilized in industry (Blevins et al., 2003; Aft, 1988; Leiviskä, 1999; Stanfelj et al., 1993):

- *Cause and Effect Analysis*: It showcases all the variables (or factors) involved in the problem under study by tracing back the origin of a given event. The most famous representations are the Ishikawa diagrams (Fishbone chart).

- *Histograms*: They indicate the average value and the statistical distribution of a given variable. The disadvantage is that they do not show its timely development.

- *Pareto Chart*: It identifies the major sources of variability by showing the relative frequency of the occurrences in relation to their corresponding causes. It uses the common 80/20 rule, i.e. 20% of reasons cause 80% of defects.

- *Power Spectrum*: This tool illustrates how variability is distributed over different frequencies. Such information may be helpful for instance, in determining the magnitude and frequency of process noise, or the frequency of disruptions caused by loop interaction or upstream processes.

- *Control Charts*: Useful to follow the timely development of quality variables. In particular, it depicts the variation of the mean within pre-specified upper and lower limits. These charts showcase possible drifts or major operating changes.

- *Autocorrelation graphics*: Depict the state of the current control system performance in respect to the minimum variance possible.

- *Cross-correlations*: These representations reveal dependencies between two process variables. For instance, the influence of other control loops and upstream conditions on the variability of a control loop may be determined through cross-correlation.

- *Multivariate statistical Analysis*: This type of analysis has gained attention due mainly to vast amount of data currently available in most mills. Among the most often used we have: Principal component analysis (PCA) and Partial Least Squares (PLS). The main asset of all these tools is the identification of plant variables that are the major contributors to variability. They are a powerful alternative to cross-correlation techniques.

- *Univariate variability metrics*: The most commonly used metrics are the standard deviation, and the process capability and performance indices (Shunta, 1996). The process capability index quantifies the capacity to overcome variability under ideal control, i.e. when the only variability is due to common causes such as short-term random upsets inherent to the process (e.g. process noise). The index removes the effect of long-term drifts, shifts, and cycles that one normally sees in the plant. On the other hand, the process performance index quantifies the process capacity to overcome variability during normal operation, i.e. includes drifts, cycles, and variability from all causes, whether removable or inherent to the process. The comparative analysis of these two indices can provide an insight on the nature of the improvement to make. Accordingly, results could either show an opportunity to revamp controls, or on the contrary indicate that current variability is about the best the process can achieve. In the latter case, process design changes are usually recommended.

- *Control performance assessment*: It has its origins in the pioneering work of (Harris, 1989) on minimum variance control (MVC). In principle, all available approaches evaluate statistical metrics that reflect the quality of the current control performance and compare them against a MVC benchmark. The reader is referred to (Jelali, 2006) for a complete review on recent developments in the area, and specifically to (Kammer et al., 2005) for applications in the pulp and paper industry.

2.4.2. Variability in TMP-newsprint processes

Papermaking operations aim at producing uniform paper from variable wood. Unlike other type of industries, product uniformity cannot be obtained by blending various batches of product, and thus variability must be removed – or at least kept to a minimum possible - within the manufacturing operation limits (Pikulik and Crotogino, 2001). Some of the variability sources mentioned in p. 14 can be eliminated through proper equipment maintenance or plant changes, whereas other sources are unavoidable, such as input variability (Tseng et al., 1999). Input variability is associated with the fact that raw material properties vary due to their origin and/or storage conditions. In turn, this variability can be profoundly affected by the way in which raw material is processed. Accordingly, paper quality variability is a function of both wood quality variations and the variability associated with the operations upstream of the paper machine. In the context of our work these operations are limited to the two-stage TMP-Refining process.

The major sources of input variability in TMP-Refining are wood origin, and wood density and moisture. The efficiency of the entire process is measured by the quality of the fresh pulp delivered to the papermaking operation. The paper machine essentially requires a pulp with adequate consistency, freeness, and fibre strength. Excessive variability in those pulp quality parameters is eventually translated in impaired paper machine runnability and paper quality as mentioned in section 2.1 (p. 8).

2.5. Process Controllability

Nowadays, higher standards in plant's efficiency are driven by increasingly tighter environmental regulations, rapid changes in customer demands, and minimal consumption of utilities. Ensuring plant's controllability is crucial as the operation is continuously subject to internal interactions, disturbances and all sort of uncertain

events. A brief introduction in certain aspects of plant behaviour is required before thoroughly tackling the concept of process controllability. Accordingly, notions such as operability, stability, resiliency, and performance are presented next.

2.5.1. Important preliminary notions

Operability

According to (Fisher et al., 1988) the goal of operability analysis is to assume that there is an adequate amount of equipment over-design to satisfy all process constraints. Their definition was associated to the minimization of operational and over design costs. (Pedersen et al., 1998) define operability as the ability of the plant to provide acceptable static and dynamic operational performance.

Stability

The main objective of any process control system is stability. Stability refers to the capacity for holding a given response within certain bounds: "A system is stable if any bounded input produces a bounded output for all bounded initial conditions" (Goodwin et al., 2001). The same system is termed internally or asymptotically stable if all the states remain bounded to any bounded disturbances (Mohideen et al., 1997). Hence, an effective control strategy should ultimately bring the output response to its desired setpoint value.

Resiliency

Resiliency measures how well a given process can meet its design objectives in spite of external disturbances and uncertainties in its design parameters (Lewin, 1999), (Solovyev and Lewin, 2001).

Performance

Performance concerns the quality of the closed-loop response. In particular, our interest in this work is to address the issue of acceptable performance. Generally, an acceptable closed-loop performance must guarantee stability and allow the system output to reach the desired setpoint in neither sluggish nor oscillatory way (Ogunnaike and Ray, 1994). An acceptable closed-loop performance is measured through the output's response characteristics. In addition, these response requirements have to be accomplished while avoiding input saturation i.e. by using only those manipulated variables that are capable to perform a control action without violating their physical constraints (Havre and Skogestad, 1998; Skogestad and Postlethwaite, 1996).

2.5.2. The evolution of the controllability concept

In the early 1940s, (Ziegler and Nichols, 1943) developed methods to characterize process dynamics, and so they defined controllability as the "ability of the process to achieve and maintain the desired equilibrium value". In the 1960s, (Kalman, 1960) introduced the term *state controllability* thereby associating for a while the concept of controllability to the field of systems theory. State controllability is defined as the ability to bring a system from a given initial state to a final state within a finite time. Nevertheless, this definition does not account for the trajectory of the response between and after these two states. In fact, (Rosenbrock, 1970) affirmed that most plants are controlled quite satisfactorily even though they are not state controllable. Thus, he referred to controllability as the ability to "achieve the specified aims of control whatever these may be" thereby establishing a new definition, *functional controllability*. The idea behind this concept is to find inputs and conditions under which a desired trajectory for a given set of outputs may be specified. Up to this point in time, the problem of controllability was approached mostly from the mathematical point of view. In the early 1980s, the issue of controllability was regarded from the

goal-oriented standpoint as opposed to the state space-oriented or mathematical perspective. It was (Morari, 1983) who introduced the concept of *dynamic resilience* to account for the best "quality of the regulatory and the servo behaviour which can be obtained for the plant by feedback". In order to quantify this dynamic resilience, he assumed "perfect control" as a target to assess process controllability. In doing so, his process-inherent approach did not need to rely on controller information to account for the best achievable closed-loop behaviour. Accordingly, controllability was assessed by identifying the limitations of the process itself namely, manipulated variable constraints, non-minimum phase behaviour (RHP zeros and time delays) and model uncertainty (Holt and Morari, 1985a; Holt and Morari, 1985b; Skogestad and Morari, 1987a). In this context, controllability cannot be altered by any change in the control algorithm but only by changing either the process design or the control strategy (Skogestad and Postlethwaite, 1996).

(Skogestad and Postlethwaite, 1996) proposed the term *input-output controllability* inspired in the following questions: How well the plant can be controlled? What control structure should be used? How might the process be changed to improve control? All these questions are associated to the inherent control characteristics of the process itself. Hence, they defined input-output controllability as "the ability to achieve acceptable control performance; that is to keep the outputs within specified bounds from their references in spite of unknown but bounded variations, such as disturbances and plant changes, using available inputs and available measurements". Other controllability definitions often invoked in the literature are the one provided by (Lewin, 1999): "Controllability can be defined as the ease with which a continuous plant can be held at a specified steady state", and the one stated by (Jorgensen et al., 1999): "Controllability may be viewed as a property of the plant which indicates how easy it is to control the plant to achieve the desired performance". In light of the various concepts and definitions revised here, the concept of controllability can be synthesized as follows: *Controllability is an inherent property of the process that*

accounts for the ease with which a continuous plant can be held at a specified operating regime despite bounded external disturbances and uncertainties, and regardless of the control system imposed on such a process.

2.6. Controllability Analysis

As stated above, plants are always subjected to disturbances and uncertainties during operation. Determining the inherent-process characteristics that enable the plant to operate with acceptable performance is the ultimate objective of any controllability analysis. Accordingly, this analysis is independent of the control system imposed to the plant.

2.6.1. The Role of Controllability in Design and Control Integration

The integration of design and control objectives entails the design of a process and its operability. The motivating issues to integrate design and control issues are the presence of uncertainties, the external disturbances that may degrade performance and the trade-offs involved in achieving at the same time, steady state economic objectives and acceptable plantwide operability. Thus, the operability of a process is certainly a function of the structure and configuration of its control system, but above all it depends on the limitations imposed by the process' physics and design, i.e. it relies on the *controllability* of the process.

The traditional way to evaluate controllability properties was based on experience, i.e. through trial-and-error procedures that consisted of selecting a control structure, adjusting controller parameters, and validating the resulting configuration by means of numerous closed-loop simulations. In fact, the design of the control system was only attempted when the design of the process was completed (Russell and Perkins, 1987). As a result, plants were over-designed and energy inefficient. Furthermore, the

numerous surge drums that were installed to compensate for disturbances also compromised the plant's capacity to rapidly change product specifications. Nevertheless, this approach proved to be relatively successful that is, up to the 1960's. The oil crisis that stroke the world in the early 1970's, the environmental concerns that came along and the evermore varying nature of the market demands changed forever the industry, and thereby the way in which the plant had to be designed.

Nowadays, plant design involves the integration of mass an energy networks in order to accomplish operational cost savings and also to meet increasingly tighter environmental, safety and product specifications. However, and regardless of its economic advantage, process integration does involve operability problems, being the most important the deterioration of control performance due to recycle interactions (Luyben, 1993; Wolff and Skogestad, 1994; Semino and Giuliani, 1997; McAvoy, 1999). In addition, process integration may result in extra capital cost as it involves also a larger *back-off* to avoid violation of constraints. Back-off is the movement of an operating point away from the boundaries of the feasibility region by considering the controllability of the process, i.e. the effect of the expected disturbances on plant operation (Arbiza et al., 2003). In this context, controllability analysis should be performed before undertaking the design of the control system so that the resulting plant is less difficult to control. There are different approaches to account for controllability issues when designing a process. These approaches can be classified by the type of models they use in their analysis (Pedersen et al., 1998), namely linear and nonlinear. In this work, only linear-based methods are discussed. References on nonlinear approaches for assessing controllability can be found in (Pedersen et al., 1998; Lewin, 1999; Bogle andFraga, 2000; Ma and Bogle, 2001; Kuhlmann et al., 1997; Lewin and Bogle, 1996).

2.6.2. Linear-based controllability Analysis

This type of analysis relies on transfer functions, i.e. it is performed in the frequency domain. The application of these measures requires a great deal of process understanding as each controllability indicator usually considers only one controllability characteristic at a time. These methods are widely used when selecting control structures and configurations.

The linear controllability approach has its origins in the *dynamic resilience* concept introduced by (Morari, 1983) and subsequently used by (Holt and Morari, 1985a) and (Holt and Morari, 1985b). The focus was to developed linear tools for assessing the effect of process-inherent limitations on achievable closed-loop performance. Since then, several tools and concepts have emerged relying on adequate linear approximations of process dynamics. In a linearized model, the open-loop response of n process outputs (vector y) is related to the variations of m manipulated inputs (vector u) and q disturbances (vector d), via G and G_d which represent respectively, the process and the disturbance transfer function matrices:

$$\hat{y}(s) = \hat{G}(s) \cdot \hat{u}(s) + \hat{G}_d(s) \cdot \hat{d}(s) \tag{2.1}$$

where symbol ^ denotes unscaled values, and s represents the frequency domain, which means that all vectors and matrices in equation (2.1) are given in their Laplacian form. The offset, e is expressed as:

$$\hat{e}(s) = \hat{r}(s) - \hat{y}(s) \tag{2.2}$$

where r denotes a setpoint change. All vectors in the above equation ($\hat{e}, \hat{y}, \hat{r}$, $\hat{u}$, and $\hat{d}$) are given in their deviation form[3]. In this work, only frequency-based tools are considered given their extensive use in control applications. The reader is referred to the work done by (Johansson, 2002; Meeuse and Huesman, 2002) for detailed developments on controllability tools in the time domain.

The ultimate objective of controllability analysis is to account for the upper limit of achievable control performance. Most controllability tools assume *perfect control*[4] in their formulations. The consideration of perfect control was outlined by (Morari, 1983) and it regards the controller[5] simply as the inverse of the plant. Accordingly, any limitation on constructing the process inverse (G^{-1}) results in a limitation upon achievable ("perfect") control performance. The most used linear controllability indices - based on perfect control - are presented in the next section (2.6.2.1). Using these tools a systematic procedure is proposed in CHAPTER 9 to select a decentralized control structure for the TMP-Refining process under study.

Scaling

Some of these indices require the use of scaled (normalized) linear models. Scaling is made by dividing each variable –in its deviation form- by its maximum "expected" or "allowed" change so that all variables are equal or less than one in magnitude (Skogestad and Postlethwaite, 1996). In case the allowed variation is not symmetric with respect to its nominal value, the smallest allowed variation is selected.

---

[3] Deviation variable: perturbation from nominal (steady state) operating point, i.e. x_i-x_{nom}

[4] The output is identical to the setpoint at all frequencies.

[5] The controller was based on the concept of Internal Model Control (IMC, (Garcia and Morari, 1982)) which poses no limitation as for the type of controller to be used.

In multivariable systems, all scaled variables are obtained by multiplying the corresponding unscaled variables ($\hat{y},\hat{u},\hat{d}$) by the inverse of the diagonal scaling matrices (D_y, D_u, D_d) which contain the maximum expected or allowed deviations (Δy_{max} , Δu_{max} , Δd_{max}):

$$y = D_y^{-1}\hat{y},\ u = D_u^{-1}\hat{u},\ d = D_d^{-1}\hat{d} \tag{2.3}$$

Finally, the scaled gain matrices are obtained as follows:

$$G = D_y^{-1}\hat{G}D_u,\ \ G_d = D_y^{-1}\hat{G}_d D_d \tag{2.4}$$

2.6.2.1. Controllability indices for control structure selection

The controllability indices presented in this section relate to the following aspects: stability, process interaction, directionality and resiliency. They do not require any knowledge about the actual controller's internal-laws and have been extensively used for decades in control system design. References for various applications can be found in (Seider et al., 1999; Skogestad and Postlethwaite, 1996).

2.6.2.1.1. Relative Gain Array (RGA)

The Relative Gain Array (Bristol, 1966) is one of the most widely applied methods for assessing controllability and control structure selection (variable pairing) in multivariable systems. It was introduced as a quantification of steady state interaction for decentralized control. The RGA-matrix is calculated using the steady state process gain matrix G:

$$\Lambda(G) = G \otimes (G^{-1})^T \tag{2.5}$$

The symbol $\otimes$ denotes an element-by-element multiplication and ^{T} denotes the transpose of the pseudo inverse $^{-1}$ of matrix G. In general, pairing on RGA-elements close to 1 should result in an almost non-interacting system. In general, systems that possess large RGA-elements are difficult to control because of sensitivity to input uncertainties (Grosdidier et al., 1985; Skogestad and Morari, 1987a; Skogestad and Morari, 1987c; Skogestad and Havre, 1996). If $\lambda_{ij} = 0$, manipulation of input j has no effect whatsoever upon output i. In particular, the pairing rule suggests not to pair on negative values as the effect of input j upon output i will be counteracted by a more dominant retaliatory (interactive) effect from the other loops thereby provoking closed-loop instability.

2.6.2.1.2. Niederlinski Index (NI)

The Niederlinski index (Niederlinski, 1971) gives a measure of the system's closed-loop stability for all possible pairings using only steady state gains, i.e. matrix $K = G(0)$. The Niederlinski theorem states that the closed-loop system consisting of a multivariable process K and a multi-loop control layer is structurally monotonic unstable[6], if and only if:

$$NI = \frac{\det(K)}{\prod_{i=1}^{N} K_{ii}} < 0 \tag{2.6}$$

[6] i.e. the closed-loop system will be unstable for any controller setting.

where det(K) is the determinant of K and $\prod_{i=1}^{N} K_{ii}$ is the product of the diagonal elements of K (provided variable pairings are placed along the diagonal). The theorem is valid provided that (a) each element of K is open loop stable and proper (or strictly proper), (b) the plant K is assumed square, (c) all feedback controllers have integral action, and (d) controllers are designed in such a way that each SISO (Simple-Input-Simple-Output) control loop is stable when all the other are open. For 2-by-2 systems the theorem is both necessary and sufficient. For larger systems the theorem is only necessary.

2.6.2.1.3. Necessary conditions for decentralized closed-loop integrity (DCLI)

A decentralized control system possesses integrity if it can be stabilized by a controller with integral action and can maintain its nominal stability in the face of any combination of failures in its sensors and/or actuators (Chiu and Arkun, 1990). As formulated, these necessary conditions require only steady state information from the process. Chiu and Arkun have proposed the following stepwise procedure to select pairings on the basis of RGA and NI:

1. Select pairings with positive $\lambda_{ii}(K)$
2. Check the sign of NI(K).
    a. If NI(K) > 0, the selected pairing possesses integrity against single-loop failure. Set $l = k$ -2. ($k = n, n$ -1, …, 2).
    b. If NI(K) ≤ 0, return to step 1 as pairing selection is not acceptable.
3. If l = 0 or 1 then pairing selection is acceptable and the procedure terminates here, otherwise go to step 4.

4. Check:

   a. $\lambda_{ii}(K_{J_l}) > 0$, for $l = 2 \ldots k\text{-}2$.

   or

   b. $NI(K_{J_l}) > 0$, for $l = 2 \ldots k\text{-}2$

   where K_{J_l} is an l x l square matrix that is a subset of K.

   If neither (4a) nor (4b) are satisfied then the pairing selection is not acceptable, otherwise plant K possesses integrity with the selected pairing for any combination of (k-l) loop failures. If so, set $l = l$ -1, and return to step 3.

2.6.2.1.4. Singular Value Decomposition

Every process G can be factorized via singular value decomposition as follows:

$$G = U \cdot \Sigma \cdot V^T \tag{2.7}$$

where Σ is a matrix of nonnegative singular values, $\sigma_i(G) = \sqrt{\lambda_i(G^T G)}$, arranged in descending order along its diagonal; the other entries are zeros (G^T is the complex conjugate transpose of G); $\lambda_i(\cdot)$ indicates *eigenvalues* which are the n solutions of the nth order characteristic equation: $\det(G - \lambda \cdot I) = 0$; U, is a matrix of output singular vectors (output directions), u_i; V, is a matrix of input singular vectors (input directions), v_i.

The singular value decomposition allows us to analyze gains and directionality of multivariable plants, i.e. the singular values measure the gains in different directions with respect to different outputs. Thus, the first column of matrix U represents the output direction in which the inputs are most effective while, the first column of V represents the input direction with the largest amplification. On the other hand, the last

column of U represents the output direction in which the inputs are least effective while, the last column of V represents the input direction with the smallest amplification. This interpretation of directionality is related to matrix Σ which provides with the *minimum and maximum singular values*, ($\underline{\sigma}(G)$ and $\overline{\sigma}(G)$ respectively) placed at the "corners" of the diagonal:

$$\Sigma = \begin{bmatrix} \overline{\sigma}(G) & 0 & 0 & 0 & 0 \\ 0 & \ddots & 0 & 0 & 0 \\ 0 & 0 & \ddots & 0 & 0 \\ 0 & 0 & 0 & \ddots & 0 \\ 0 & 0 & 0 & 0 & \underline{\sigma}(G) \end{bmatrix} \tag{2.8}$$

Thus, the maximum and minimum singular values represent respectively the largest and the smallest gain for any input direction. This aspect leads to the definition of Condition Number (CN).

2.6.2.1.5. Condition Number (CN)

The Condition Number is a scale-dependent indicator of directionality of the process gain and it is calculated as follows:

$$CN(G) = \frac{\overline{\sigma}}{\underline{\sigma}} \tag{2.9}$$

The main use of the condition number is to account for *model uncertainty* as it quantifies the sensitivity to uncertainties in matrix G. A process is called *ill-conditioned* if the condition number is large (CN >10). Physically, this means that the gain of the process is strongly dependent on input direction (Skogestad and Morari, 1987a). However, large CN do not necessarily mean a process sensitive to uncertainty

under all circumstances. In fact, only small sensitiveness is guaranteed. Thus, large condition numbers *may* indicate control problems[7], whereas small condition numbers, preferably close to 1 (typically CN < 2), are *definitely* an indication that plant-model mismatches are far from being amplified and hardly serious (Skogestad and Postlethwaite, 1996).

2.6.2.1.6. Minimum singular value ($\underline{\sigma}$)

Mathematically, the magnitude of $\underline{\sigma}$ is a measure of the minimum distance to the nearest singular matrix i.e. it measures the invertibility of the system. We want $\underline{\sigma}$ as large as possible (Morari, 1983). Physically, $\underline{\sigma}$ provides information about the effect of constraints on closed-loop performance. Hence, if $\underline{\sigma}$ is small, in order to achieve acceptable control, the controller would have to supply very large input signals in the suitable direction and thereby it may violate some input constraints (Morari, 1983; Skogestad and Postlethwaite, 1996). Conversely, plants with large $\underline{\sigma}$ are desirable as they are less susceptible to input saturation when achieving acceptable control performance.

2.6.2.1.7. Relative Disturbance Gain (RDG)

The Relative Disturbance Gain (RDG) (Stanley et al., 1985) was originally introduced as a steady state tool to provide a better understanding on how disturbances affect control-loop operability. The RDG provides an indication on whether the presence of internal interactions between loops is favorable for disturbance rejection. For a particular disturbance d_k, the RDG is defined for each manipulated variable (u_j) as follows:

---

[7] The RGA rather than the *CN(G)* gives a more reliable measure of the plant's sensitivity to diagonal input uncertainty (Skogestad and Morari, 1987c)

$$RDG_{jk} = \frac{\left.\frac{\partial u_j}{\partial d_k}\right|_{y_i}}{\left.\frac{\partial u_j}{\partial d_k}\right|_{y_j, u_{j\neq i}}} \tag{2.10}$$

The numerator represents the change in manipulated variable u_j required to perfectly counteract disturbance d_k and bring all outputs y_i back to their setpoints (perfect disturbance rejection). The denominator represents the change in manipulated variable u_j required to perfectly reject disturbance d_k in output y_j only, while keeping the other manipulated variables $u_{j\neq i}$ constant. As shown in the above equation, the RDG is similar to the RGA in that it involves a ratio of perfect control effects to open-loop effects, and thus it is also a scale-independent measure. For multiple disturbances, the RDG-matrix can be calculated using the following equation (Skogestad and Morari, 1987b):

$$RDG_{jk} = \frac{\left[\tilde{G}G^{-1}G_d\right]_{jk}}{\left[G_d\right]_{jk}} \tag{2.11}$$

where G_d is the open-loop transfer matrix from disturbances to outputs and $\tilde{G}$ denotes the matrix consisting of the diagonal elements of G. The division sign denotes element by element division. It is desirable to have small RDG elements, as this means that internal interactions reduce the "apparent" effect of the disturbance, so that no high closed-loop gains in the individual loops j are needed (Skogestad and Postlethwaite, 1996). Incidentally, the numerator in equation (2.11) represents the closed-loop disturbance gain as proposed by (Skogestad and Hovd, 1990):

$$\text{CLDG} = \Gamma G_d \tag{2.12}$$

where $\Gamma = \widetilde{G}G^{-1}$ represents the performance relative gain, PRGA (Hovd and Skogestad, 1992) which accounts for one-way interactions that may arise as a result of control[8]. Accordingly, the RDG predicts the change in the effect of the disturbance caused by decentralized control.

The RDG used in conjunction with the RGA provides with valuable information in terms of screening control schemes with poor resiliency. In fact, for a qualitative assessment of control configurations, four different cases are possible, depending on the size of the RDG and RGA (Marino-Galarraga et al., 1987). As depicted in Table 2.1 small values for both RDG and RGA are preferred. By accounting for the effect of disturbances, the RDG overcomes the major limitation of the RGA which merely describes internal interaction. Thus, the RDG distinguishes between clearly unfavorable control schemes and those which may result in acceptable transient performance when expected disturbances occur (Stanley et al., 1985).

Table 2.1. Assessment of Control Schemes - RDG and RGA(*)

	Large RGA (>5)	Small RGA (≤5)
Large RDG (>2)	• RGA: Response to individual disturbance paths is very sluggish. • RDG: Unfavorable effect of interaction, disturbance paths do not cancel each other.	• RGA: Response to individual disturbance paths is rapid. • RDG: Unfavorable effect of interaction, disturbance paths do not cancel each other.
Small RDG (≤2)	• RGA: Response to the individual disturbance paths is very sluggish • RDG: Favorable effect of interaction, disturbance paths cancel each other	• RGA: Response to individual disturbance paths is fast • RDG: Favorable effect of interaction, disturbance paths cancel each other

(*) Synthesized from (Marino-Galarraga et al., 1987).

[8] Note that although RDG is scale-independent, both PRGA (diagonal excepted) and CLDG depend on output scaling. In addition, CLDG is disturbance scale-dependent

2.6.2.2. Acceptable control: Minimum manipulated effort

In order to quantify the minimum manipulated effort for acceptable control (offset $\|e\|_\infty \leq 1$), all matrices and vectors need to be expressed in their scaled forms as indicated in section 2.6.2. The issue here is to determine whether achieving acceptable control is possible and if so, what would be the smallest input effort $u = U_{min}$ (best input direction) necessary to keep the offset $\|e\|_\infty$ at least equal to 1 once the worst-case disturbance ($\|d\|_\infty = 1$) enters the system. If any element in $\|G_d\|$ is larger than 1 then control is definitely needed.

2.6.2.2.1. Exact solution

Since no setpoint changes are involved, from equation (2.2): $\|e\|_\infty = \|y\|_\infty$, and thus the formulation for this problem can be stated as (Wolff, 1994):

$$
\begin{aligned}
& U_{\min} = \max_{d}\left(\min_{u}\|u\|_\infty\right) \\
& s.t. \\
& \quad \|d\|_\infty \leq 1 \\
& \quad \|u\|_\infty \leq 1 \\
& \quad \|e\|_\infty \leq 1
\end{aligned}
\qquad (2.13)
$$

Attenuation of current offsets is limited by the presence of constraints, internal interactions and maximum expected variations in wood density and moisture. In particular, depending on how these disturbances are aligned, their effect on the outputs may either lead to constraint violations or tend to cancel each other. Acceptable control is possible if $0 < \|U_{\min}\|_\infty < 1$.

2.6.2.2.2. Approximate solution

Exact conditions involve the solution of an optimization problem that becomes computationally intensive when having several decision variables to work with and a space of different disturbance scenarios. (Skogestad and Postlethwaite, 1996) propose an approximate method to find $\| U_{\min} \|_\infty$ using the singular value decomposition (SVD) of the plant G:

$$\| U_{\min} \|_\infty = \left\| \Sigma^{-1} \left(\left| U^T G_d d \right| - e_{\max} \right) \right\|_\infty \tag{2.14}$$

where $e_{\max} = [1\ 1\ 1\ 1\ 1\ 1]^T$ ($e_{\max}$ is a constant vector containing as many ones as the number of process outputs, n), and U and Σ are the matrix of output singular vectors and singular value matrix, respectively obtained from SVD decomposition of G.

Remarks:

1. Matrix and vector dimensions: G (n x m), U (n x n), Σ (n x m), G_d (n x q), d (q x 1), $e_{\max}$ (n x 1).
2. In equation (2.14), if any of the first m elements of $\left| U^T G_d d \right|$ is smaller than 1, then the corresponding elements of $U_{\min}$ is set to 0 (Skogestad and Postlethwaite, 1996).
3. Being G a non-square matrix, the pseudo-inverse of Σ yields a matrix with only zeros in the last (n^{th}) column, and consequently the last (n^{th}) element of vector $\left| U^T G_d d \right|$ does not take part in the computations.

2.6.3. Methodology frameworks for controllability analysis

There are basically three types of methodology frameworks that aim at improving the controllability of a given plant flowsheet: *Simulation-based, Optimization-based* and *Sequential.*

Simulation-based frameworks make use of exhaustive closed-loop dynamic simulations to improve control performance. This type of framework not only requires a specific controller design but also long hours in performing several runs. Furthermore, since controllability is upgraded via simultaneous changes in both the process and the control system, one cannot identify whether the nature of the improvement results from having overcome an inherent process limitation.

In *optimization-based* frameworks the problem is formulated as a mathematical superstructure capable of attaining a given steady state economic objective while respecting at the same time dynamic operability, model uncertainty, and the synthesis of optimal controllers. Hence, both the process and the controller are simultaneously optimized. Naturally, the solution of superstructures is difficult and time consuming requiring most of the time of a simplified process model to avoid numerical intractability. Superstructures may include linear controllability measures as part of their formulations. See (Lewin, 1999; Pedersen et al., 1998) for a survey on this approach.

Sequential frameworks use linear controllability indices to account for the inherent limitations of the process in terms of acceptable control performance. These frameworks use simulations only as a tool for model identification or for closed-loop validation. Linear analysis is normally performed around a nominal operating condition. This condition is normally the most common operating regime in the plant, but can also be calculated from a prior static optimization of the process. The reader is

referred to (Weitz and Lewin, 1996; Dimian et al., 1997; Seider et al., 1999; Groenendijk et al., 2000) for sequential methodologies to assess controllability of process flowsheets.

The methodology proposed in this thesis is based on a sequential approach. Hence, in CHAPTER 7 an optimal operating point of low variability is calculated, and then linear analysis is used in CHAPTER 8 to determine controllability limitations.

2.7. Controllability analysis in pulp and paper processes

So far, controllability Analysis tools have been mostly developed and applied on heat-exchanger networks, processes based on distillation columns and reactors, or benchmark plants such as the Tennessee-Eastman Process or the Hydrodealkylation of toluene process (HDA), whether to account for process interactions and resiliency or for selecting control structures and configurations (see review by (Pedersen et al., 1998)). In contrast, research in controllability of pulp and paper processes has not been that profuse. The main reasons for that may be attributed to the lack of robust process models[9] and also to the type of unit operations employed. Indeed, units such as chip refiners or paper machines are exclusive property of pulp and paper mills, thus precluding their exploitation as controllability benchmarks. Nevertheless, we have found in the literature some references on controllability of pulp and paper processes which can be divided in two basic areas: *control structure selection* and *controllability for better resiliency*.

[9] i.e. compared to models developed in the oil or pharmaceutical industry for example.

2.7.1. Control structure selection

(McAvoy, 1983) used the RGA to propose a control configuration for a headbox. The RGA suggested different configurations at high and low frequencies. Thus, at low frequencies the (steady state) RGA called for pairing the *feedstock valve* with the *total head (pressure)* and the *air valve* with the *level*, whereas at high frequencies the RGA suggested reverse pairings. The pairings used in practice are precisely those suggested at high-frequency as the response of the head pressure to a change in air flow is very fast. Although, this work provided with the physical interpretation involved in pairing process variables, it did not present the repercussions that such pairing would have in terms of wet-end stability or paper machine runnability. In fact, no context as for papermaking operation was established whatsoever, and the headbox application was merely regarded as an example for the application of dynamic RGA.

(Castro and Doyle III, 2002) proposed a plantwide control system design of the fibre line of a pulp mill process (over 5000 state variables). They used heuristics to select the controlled variables, and controllability analysis (specifically the RGA) to determine the control pairings for decentralized control. They had to deal with an open-loop unstable process, and therefore straightforward application of the standard RGA was impossible. Given the complexity of the flowsheet, instead of using the Jacobian of the process (linearization), they calculated the RGA by using open-loop simulations of the nonlinear model. From the steady state RGA analysis they concluded that most interactions were associated to the digester. Hence, frequency-dependent RGA was used to select the appropriate pairings for the digester. Once the pairings were selected, they proceeded to design the actual controllers. Although the selection of the control pairings based on the RGA was thoroughly carried out, the controllability analysis did not take into account the effect of disturbances on the main outputs (i.e. in terms of a particular resiliency index such as the RDG for instance) which might have either reinforced the selected configuration or even disregarded it for a more resilient one.

(Lama et al., 2003) applied the self-optimizing stepwise procedure for control structure selection proposed by (Skogestad, 2000) to a subsystem within an integrated newsprint mill, namely the *short recirculation loop*. They incorporated the steady state RGA and the Niederlinski Index into the procedure to select the control configuration. The application of the technique resulted in agreement with the current control implementation and proved to be conceptually extendable to more complex newsprint processes. The main drawbacks in their work reside in the simplicity of the flowsheet, namely a 2x2 system, and also on the selection of the objective function which in turn determines the configuration. Indeed, different objective functions, as well as larger systems may result in diverse control configuration alternatives. Moreover, the selection of the control structure did not account for any dynamic aspects as it was carried out on a steady state basis.

2.7.2. Controllability for better resiliency

(Orccotoma, 1997) examined controllability analysis specifically in the context of newsprint mills. He developed a methodology for applying controllability theory over the wet-end section of a newsprint mill. By using a modeling approach he quantified the effect of disturbances (consistency and fines content in the furnish pulp) in a newsprint machine and determined its input-output controllability. In doing so, the problems associated with the control of the main variables in a paper machine (First-Pass Retention and Basis Weight) were satisfactorily explained. The work done by Orccotoma is probably the most complete study to date on the controllability of a newsprint wet-end section, yet due to a reduction in the complexity of the model the linear analysis ultimately focused only on a single-input-single-output (SISO) system.

(Cui, 2000) studied the dynamics and controllability of processes with recycle. As a case study a pulp bleaching process was chosen. By combining dynamic simulations

with input-output controllability analysis, the effect of partial filtrate recycling on the dynamics of the bleaching stage was investigated. In the light of her results, she recommended to include the entire bleaching plant, and thus account for more interactions and multivariable recycles.

(Hauge et al., 2002) presented a case study wherein they stabilized the wet-end of a particular paper machine. Although the objective was to implement multivariable predictive control (MPC), an input-output controllability analysis was performed to account for the process' ability to achieve acceptable control performance. According to their results, neither input saturation, nor model uncertainty or the external disturbances appear to represent and obstacle for the implementation of their modified MPC version. In addition, they explained – also through controllability analysis - why process operators were necessary to act on measured disturbances. However, they failed in synthesizing the advantages of knowing the process-inherent limitations before undertaking an MPC implementation. In fact, their study would have been of more value if they showed the behaviour of the control system beyond the limits determined by the controllability analysis.

From the above review it is clear that controllability methodologies currently available address the controllability problem at the conceptual design stage only, and thus there is an opportunity to apply these concepts in retrofit to address the issue of process variability. Finally, concerning pulp and paper applications available literature does not report any controllability analysis performed upon two-stage TMP-Refining processes.

CHAPTER 3: EMPIRICAL MODELING OF MOTOR LOAD

"When you know a thing, to hold that you know it; and when you do not know a thing, to allow that you do not know it - this is knowledge."
Confucius

3.1. Introduction

Motor load is defined as the electrical energy applied to a refiner (Du, 1998). Provided the refiner is operated within a region wherein linear conditions can be assumed, most theorists and practitioners agree on the behaviours between manipulated inputs and motor load depicted in Figure 3.1 (Sundholm, 2000).

In reality, motor load behaviour has a nonlinear and non-stationary nature. Indeed, motor load gains vary with plate age and operating conditions (Dumont and Astrom, 1988; Sundholm, 2000). Derivation of first principle equations to predict motor load (Di Ruscio, 1993) has received little attention mainly because the solution entails heavy computational demands. Instead, most of the work done in this area has been focused on empirical modeling. Qian and Tessier propose a nonlinear equation relating motor load, transfer screw speed, and hydraulic pressure (Qian and Tessier, 1995). Other nonlinear (Fu and Dumont, 1993; Du et al., 1995; Schwartz et al., 1996) and linear models (Dumont and Astrom, 1988; Allison et al., 1995; Evans et al., 1995; McQueen et al., 1999) also use hydraulic pressure and/or dilution flowrates to predict motor load. Although most of these models are adaptive in nature, and thus indirectly take into account plate wear, their formulations have been structured so as to be used for

regulatory control purposes (Dumont and Astrom, 1988; Fu and Dumont, 1993; Allison et al., 1995; Du et al., 1995; Evans et al., 1995; McQueen et al., 1999).

In this chapter, a methodology is proposed to predict motor load changes using steady state identification techniques and uncompressed short-term data from operations. Unlike previous work, the effect of plate age on motor load is explicitly considered in the model formulation. Accordingly, the inputs to the model are the refiner plate's age, wood species proportions and respective densities, and the setpoints to the transfer screw speed, the hydraulic pressures and the dilution flowrates for both primary and secondary refiners. The methodology is tested in Twin refiners.

One major advantage of the procedure is that conventional bump testing is not necessary since process information is extracted from routine operation. In addition, the model provides information on refiner dynamics and can be used to elucidate how motor load gains vary at different operating regimes and plate conditions.

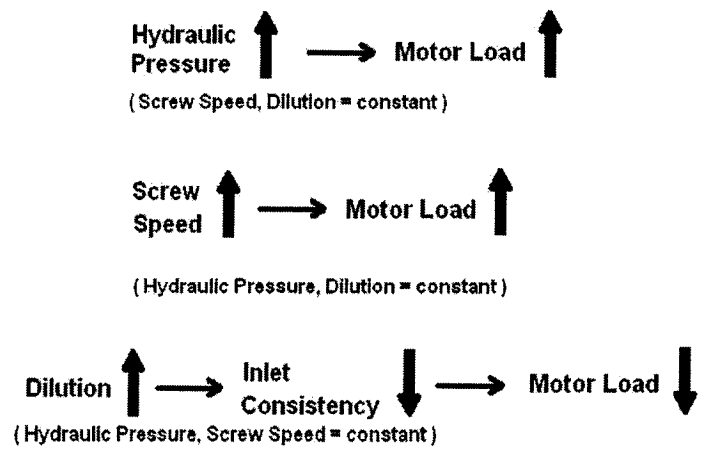

Figure 3.1. Typical behaviour of refiner motor load

3.2. Methodology for modeling motor load

The proposed methodology has two major parts. First, motor load gains are calculated based on steady state or long-term information. In order to do so, a *space of nominal operating points (SNOP)* needs to be determined. This nonlinear space represents virtually all available combinations of plate age and manipulated inputs from which motor load can be calculated at various steady state conditions. The construction of this space involves the use of long term averages and the application of a steady state detection technique. The nonlinear equation describing this space is then used to calculate the process gains that relate motor load, plate age and all the manipulated inputs. The second part involves the development of a short-term model from routine uncompressed data. This model captures the first order dynamics –essentially time constants- produced as a result of input manipulation.

3.2.1. Long-term model: Determination of motor load gains

As shown in Figure 3.2, the procedure uses outlier clean steady state data to compute motor load gains. Steady state data is generated via the method given in section 1.4.1.

a. **Calculation of nominal values for the manipulated inputs:** The median of each of the three manipulated inputs - i.e. setpoints to the transfer screw speed, hydraulic pressure and dilution flowrate loops - is calculated at every steady state interval.

b. **Space of nominal operating points (SNOP):** A least-square regression is performed to obtain the model for the SNOP. The static relationships between motor load and the three manipulated inputs have been assumed to follow a power law and only describe the modus operandi of the plant below the limits associated with fibre cutting (Sundholm, 2000):

$$ML = A \cdot F_c^{\alpha} \cdot P_c^{\beta} \cdot F_d^{\gamma} \tag{3.1}$$

where P_c and F_d are respectively, the setpoints to the hydraulic pressure and dilution flowrate regulatory loops, and F_c denotes dry production rate.

Because of the significant uncertainty associated with the measurement of production rate – or the lack of it - most refining plants calculate their throughput by simply multiplying the transfer screw speed by a proportionality factor. In that regard, Qian and Tessier (Qian and Tessier, 1995) have proposed a model that also includes wood basic density. In this work, we have extended that idea to include the proportion of each species in the mix. Hence, the production rate is not only a function of the refiner's screw speed but it also depends on the volumetric design capacity and the variations in the density of each species involved in the wood furnish:

$$F_c = \frac{24}{1000} \cdot dc \cdot tss \cdot D \tag{3.2}$$

where *tss* is the setpoint to the regulatory loop controlling the transfer screw speed. The design capacity of the refiner's transfer screw feeder is – for the plant under study – equal to dc = 0.41 m^3/hr/RPM and is valid for a given chip size distribution and chip packing in this plant. The total basic density of the wood mix is represented by D and accounts for the wood species and their respective proportions in the feed. Provided that volumetric flow is an additive variable, the total basic density of the wood D is calculated as follows:

$$D = \frac{1}{\frac{p_{BS}}{\rho_{BS}} + \frac{p_{LD} \cdot \left(JP_{mix} \cdot \rho_{BF} + (1 - JP_{mix}) \cdot \rho_{JP}\right)}{\rho_{JP} \cdot \rho_{BF}} + \frac{p_{HW}}{\rho_{HW}}} \tag{3.3}$$

where ρ_{BS}, ρ_{LD} and ρ_{HW} denote respectively, the oven dry density of Compartment 1, 2 and 3 (see section 5.4.2). These three sources of wood are fed to the refining section in fractional mass proportions p_{BS}, p_{LD}, and p_{HW}, respectively. JP_{mix} is the fraction of Jack Pine in Compartment #2. Fractional proportions are calculated from the recorded tonnage at the plant. The oven dry densities of Jack Pine and Balsam Fir are denoted by ρ_{JP} and ρ_{BF}, respectively.

The factor accounting for the effect of plate age on motor load A is calculated as follows:

$$A = A_o \cdot \exp\left(a_o \cdot \frac{P_{age}}{P_{age\,\max}} \right) \tag{3.4}$$

where P_{age} is the plate life, P_{agemax} is the maximum recorded plate lifetime, coefficients A_o, a_o, α, β, χ are obtained via nonlinear regression.

The SNOP can be unfolded in four plots so as to clearly depict the static relationships between motor load, the manipulated inputs and plate age (see Figure 3.6 and Figure 3.7).

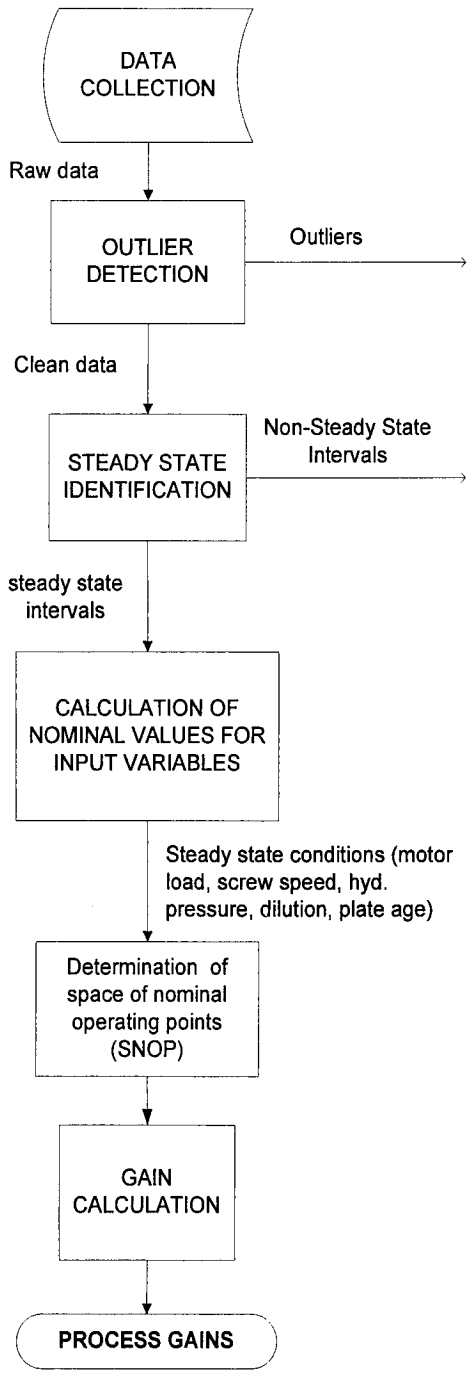

Figure 3.2. Stepwise procedure to determine motor load gains

c. **Gain calculation:** Motor load gains are a function of plate wear (Roche et al., 1996) and the steady state conditions at which the plant operates. In order to obtain the motor load gains (K_{ML}), partial derivatives of the SNOP model in equation (3.1) are taken with respect to each of the manipulated inputs:

$$\begin{aligned}
\frac{\partial ML}{\partial F_c} &= K_{ML-Fc} = A \cdot \alpha \cdot F_c^{\alpha-1} \cdot P_c^{\beta} \cdot F_d^{\gamma} \\
\frac{\partial ML}{\partial P_c} &= K_{ML-Pc} = A \cdot \beta \cdot F_c^{\alpha} \cdot P_c^{\beta-1} \cdot F_d^{\gamma} \\
\frac{\partial ML}{\partial F_d} &= K_{ML-Fd} = A \cdot \gamma \cdot F_c^{\alpha} \cdot P_c^{\beta} \cdot F_d^{\gamma-1}
\end{aligned} \tag{3.5}$$

It has been reported that there is a decrease in the effect of screw speed and hydraulic pressure upon motor load as the plate ages (Roche et al., 1996; McQueen, 1995). Furthermore, Strand and Hartler (Strand and Hartler, 1985) report an increase of hydraulic pressure to compensate for plate aging. We believe that this behaviour may have to do with unbalanced forces affecting the refiner plates. As plates wear grooves lose edge, and thus there is less net space for the steam to escape between the bars[10]. As a result, steam pressure increases and so do the corresponding internal forces acting upon the plates. Since both, the screw speed and the hydraulic pressure entail forces acting from the outside of the refiner, i.e. in opposite direction, their effect upon motor load is most likely to decrease over time. Furthermore, industrial practice indicates that plate wear has a reducing effect on motor load. It is in this context that we have incorporated the factor $\left(\frac{P_{age}}{P_{age\max}}\right)$ in equation (3.4). Thus, ideally –and assuming one-at-a-time setpoint changes- at $P_{age} = P_{agemax}$ the effect on motor load will be the smallest possible. In addition, gains are a function of both the nominal conditions and the plate's

[10] The assumption here is that the bar's depth has been notably reduced because of wearing.

age, and therefore the proposed model assumes a varying rate of change of motor load over time.

3.2.2. Short-term model (G_T)

The procedure to determine the parameters of this (linear) model is summarized in the flow diagram depicted in Figure 3.3. The assumption is that motor load follows a first-order plus delay dynamics in respect to each of the three manipulated inputs.

a. **Uncompressed data collection:** The term "uncompressed data" refers to actual data (as opposed to interpolated data) sampled at a varying rate. Uncompressed operating data for both refiners is collected at periods of time wherein several step changes in any of the three manipulated inputs are observed. Hence, four data series are collected (motor load included) for each refiner.

b. **Time format conversion:** The time recorded during collection is in string format. In addition, time in process information (PI) systems is given in days, hours, minutes and seconds. Hence, conversion of date string data to a numerical format with a unique time scale (seconds) is necessary to perform the calculations.

c. **Homogenizing time ranges and interpolation:** All four ranges are intersected and re-sampled at every second so as to work with a single time structure. At time points where motor load data do not exist a piecewise cubic Hermite interpolation is performed. This type of interpolation preserves the monotonicity and the shape of the data. In the case of the three manipulated inputs a simple linear interpolation is enough as they consist of series of step changes.

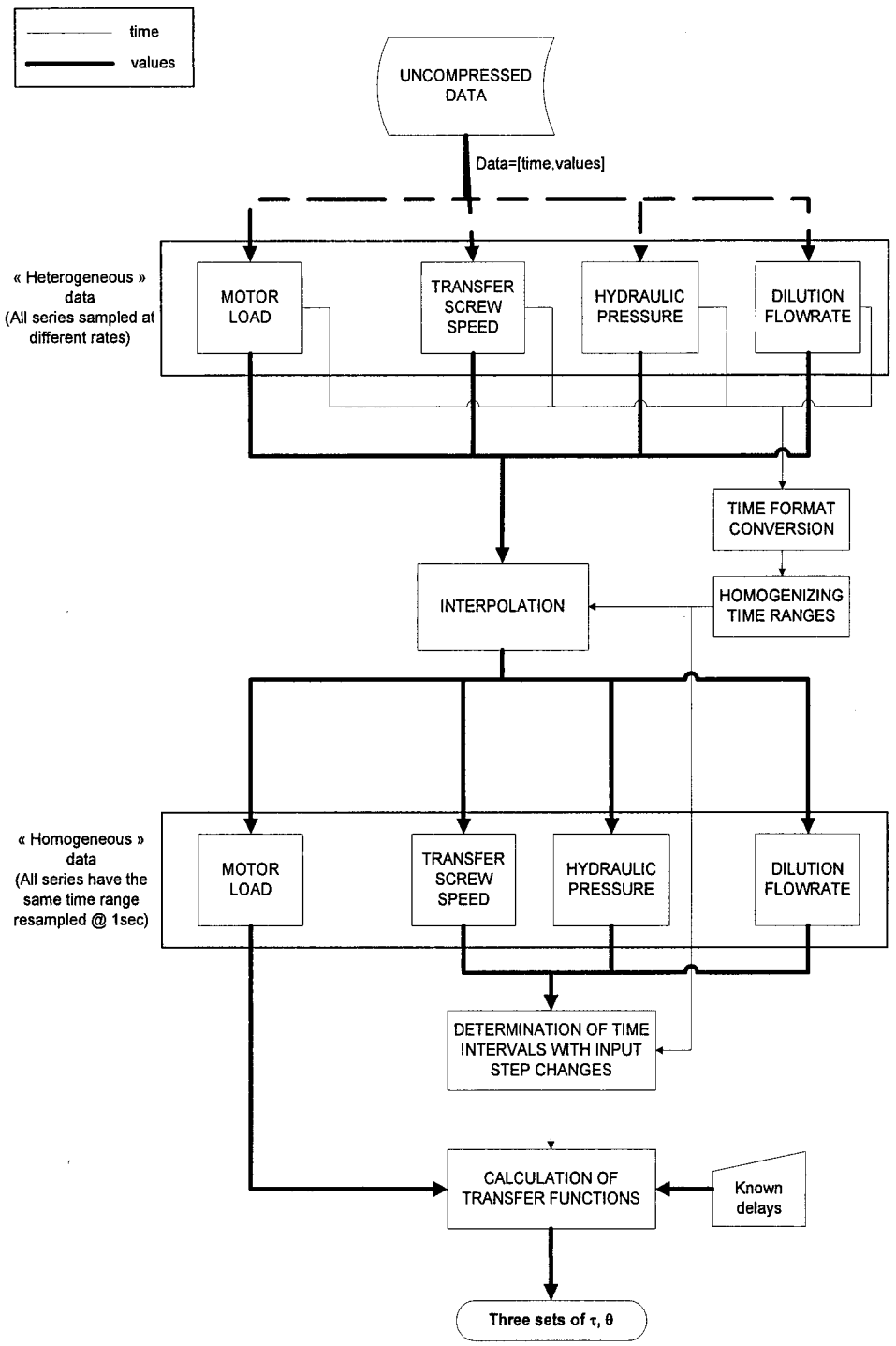

Figure 3.3. Procedure to determine first-order motor load dynamics.

d. **Determination of time intervals (t) with input step changes:** The homogenized time range is divided in as many intervals as step changes occur in any of the three manipulated inputs.

e. **Calculation of the transfer function parameters:** It is important to indicate that the data is gathered in closed-loop conditions. In fact, normally the motor load and/or the freeness control loops set the control objectives for the lower control level i.e., they determine the setpoints for the screw speed, hydraulic pressure and dilution regulatory controls. In this context, the main assumption is that the motor load and freeness control loops have a much bigger closed-loop time constant than that of each regulatory loop. Accordingly, the derivative of the motor load is assumed to be equal to zero (maximum gain) at time t where 98% of their ultimate value is reached. This equals to 3.9 times the corresponding open-loop constant (Ogunnaike and Ray, 1994). Process gains are obtained from section 3.2.1 - equation (3.5) – while time constants (τ_h) are calculated as follows for each time interval h:

$$\tau_h = \frac{t_h - \theta_i}{3.9} \tag{3.6}$$

where θ represents the known delay times -obtained visually from routine data- associated with each regulatory control loop i.

The short-term (linear) model G_T can be factorized in two transfer functions: G_{reg} and G_{ref} representing respectively the regulatory loop (relating a single pair .PV-.SP) and the dynamics inside the refiner:

$$G_T = G_{reg} \cdot G_{ref} \tag{3.7}$$

$$G_{ref} = \frac{K_{ML}}{\tau_{ref} \cdot s + 1} \tag{3.8}$$

$$G_{reg} = \frac{\tau_{ref} \cdot s + 1}{\tau_T \cdot s + 1} e^{-\theta \cdot s} \quad \text{(a)}$$
$$G_{reg} = \frac{1}{\tau_T \cdot s + 1} e^{-\theta \cdot s} \quad \text{(b)} \tag{3.9}$$

Equation (3.9)-(a) represents the dilution and screw speed regulatory loops while equation (3.9)-(b) represents the hydraulic pressure loops. In both equations K_{ML} denotes the gain obtained in section 3.2.1 and τ_{ref} the residence time of the pulp inside the refiner which is calculated as proposed by Miles (Miles, 1991). The time constants of the regulatory loops are denoted by τ_T and are calculated by averaging all the corresponding time constants τ_h.

3.3. Application: Modeling primary and secondary motor loads

3.3.1. Long-term model: Determination of motor load gains

a. **Data collection and outlier detection**: Raw data (motor loads, hydraulic pressures, dilution flowrates and plate age) were collected over a year at hourly averages. All data sets are cleaned using robust filtering (see section 1.4). An example of the application for primary motor load is shown in Figure 3.4.

b. **Motor load steady state identification**: Time intervals wherein highly presumed steady state regimes have been attained are shown in Figure 3.5.

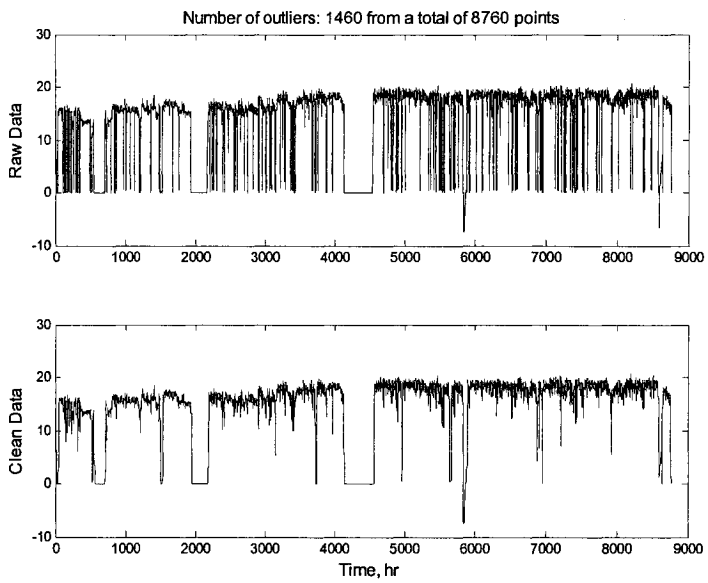

Figure 3.4. Motor Load - Primary refiner. Before and after outlier removal.

c. **Space of nominal operating points (SNOP) – Nonlinear regression**: Due to specific operating strategies imposed to the refiners, several regimes may arise. In fact, motor load, along with screw speed and outlet consistency characterize the major operating drifts in primary refiners. Hence, in our particular study and on a one-year basis, there are two major regimes clearly identifiable by looking at the dilution rate operation (see lower right subplot in Figure 3.6). However, since the current nominal operation is limited by the input constraints given in Table 1.1, only the data inside regime # 2 (crosses) are considered to fit equation (3.1). On the other hand, the secondary refiner only has one regime Figure 3.7. The set of regression coefficients is given in Table 3.1. It should be noted that in spite of not being a manipulated input at the secondary stage, the transfer screw speed has also been considered as part of the corresponding SNOP model since it has a cascade effect upon the secondary motor load.

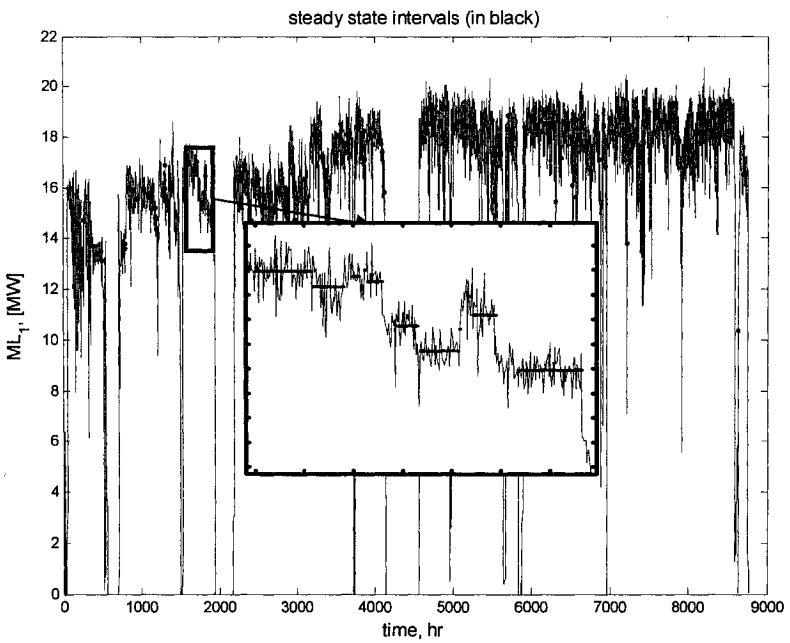

Figure 3.5. Motor load - Primary refiner. Steady state identification.

Table 3.1. Model Parameters

Parameter	Primary Refiner	Secondary Refiner
A_o	0.326	0.138
a_o	-0.014	-0.152
α	0.682	0.497
β	0.179	0.326
γ	-0.297	-0.297

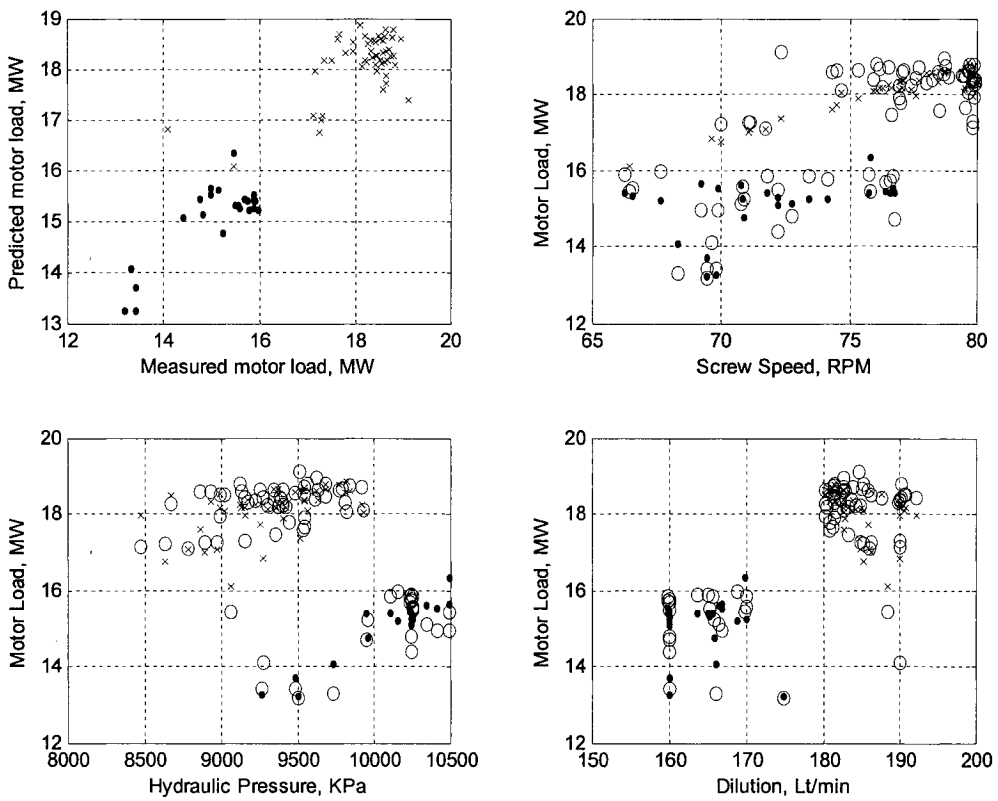

(circles: steady state identification; dots: regime # 1; crosses: regime # 2).

Figure 3.6. Space of nominal operating points (SNOP) - Primary refiner.

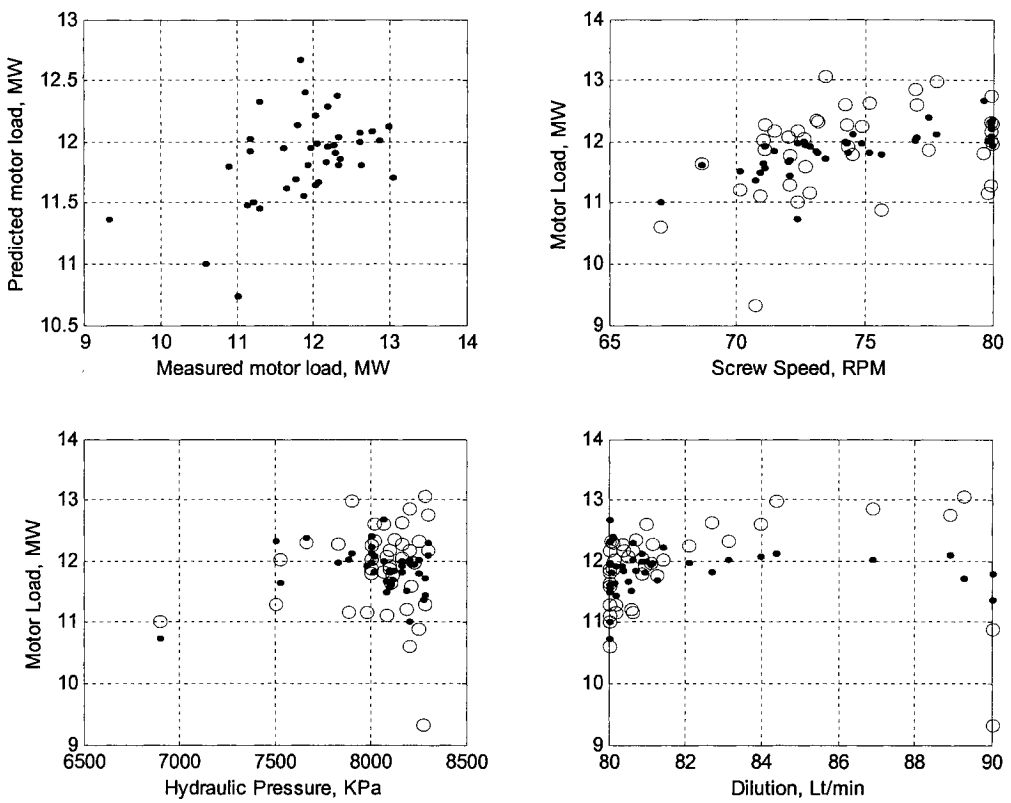

(circles: steady state identification; dots: SNOP model)

Figure 3.7. Space of nominal operating points (SNOP) - Secondary refiner.

As far as modeling is concerned, gain recalculation is necessary every time the nominal operating conditions change, and this evidently includes plate wear. Table 3.2 shows the direction of the change in the motor load gains for a given change in any manipulated input or plate age.

Table 3.2. Effect of operating conditions on motor load gains

Operating conditions	$K_{ML\text{-}Fc}$	$K_{ML\text{-}Pc}$	$K_{ML\text{-}Fd}$
F_c ↑	↓	↑	↑
P_c ↑	↑	↓	↑
F_d ↑	↓	↓	↓
P_{age} ↑	↓	↓	↓

3.3.2. Short-term model, (G_T)

Several data sets have been used to determine average values for the linear model parameters. Table 3.3 shows the parameters for both primary and secondary.

Table 3.3. Dynamics of linear model (in sec.) - Primary and secondary refiners

Motor load with respect to...		Primary Refiner	Secondary Refiner
tss (.SP)	θ	**4**	**12**
	τ_T	**5.04**	**5.04**
P_c (.SP)	θ	**1.7**	**1.7**
	τ_T	**4.39**	**1.48**
F_d (.SP)	θ	**1**	**1**
	τ_T	**2.36**	**1.96**

3.3.3. Model validation

The static relationships between the motor load and the manipulated inputs described in equation (3.1) are validated using two different data sets for each refiner sampled every hour. This *long-term validation* of the model is shown in Figure 3.8. On the other hand, given that the transfer functions G_{reg} dominate the dynamic behaviour of the refiner, the *short-term validation* of the model uses uncompressed data from regulatory loops sampled at a varying rate for about a day. The validation of some of these loops is depicted in Figure 3.9.

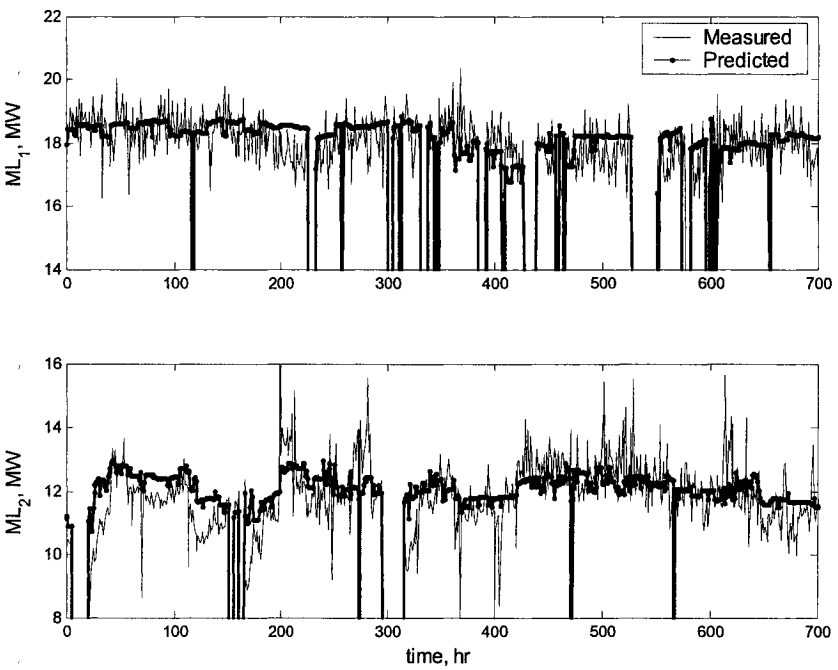

Figure 3.8. Long-term validation – Primary and secondary motor load.

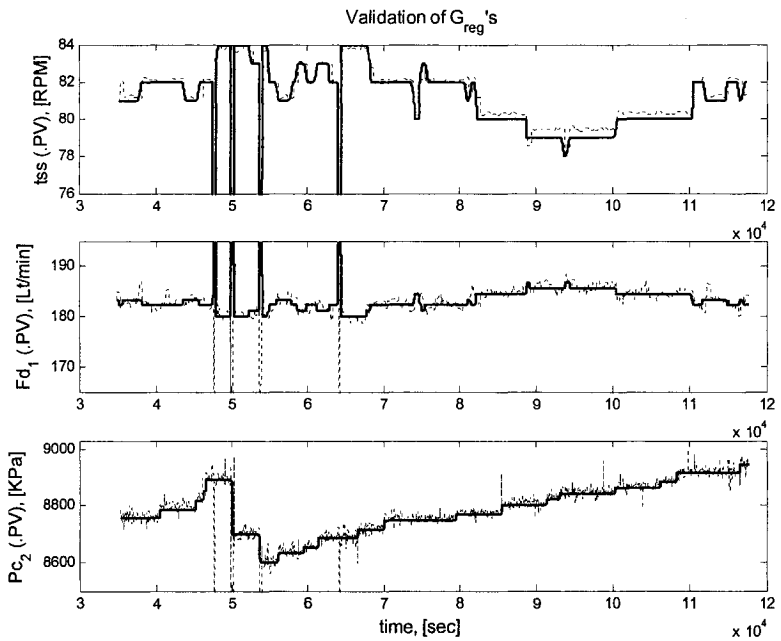

(dotted: measured, solid: predicted).

Figure 3.9. Short-term validation - Some regulatory loops.

3.4. Discussions

This work introduces the use of the space of nominal operating points (SNOP) to analyze the behaviour of motor load with respect to the typical manipulated inputs in a Twin refiner. Incidentally, dilution conditions seem to be a decisive variable in the detection of these operating spaces. In our particular case study and on a one-year basis, two major regimes were clearly detected for the primary stage and one for the secondary stage. Models must be identified within the limits of these operating spaces.

Industrial evidence indicates that linear motor load models vary with plate conditions. Since most of this evidence normally accounts for process gains, the time constants of the linear models presented in equation (3.9) are assumed invariant with respect to plate

age. Although this is not rigorously true, changes in time constants due to plate wear are likely to be negligible since dynamics are mostly dominated by the regulatory loops outside the refiner.

The proposed methodology is primarily intended for Twin refiners. In theory however, the applicability of the procedure can be extended to single and double disc refiners since they also have flat refining zones. Application to conical disc refiners would previously require several experimental trials to identify the direction of motor load gains as plates wear. Current lack of such experimental evidence precludes us from asserting that the model proposed in equation (3.1) will also hold for conical disc refiners.

3.5. Conclusions

A motor load modeling procedure that does not require conventional bump testing has been proposed. This procedure takes full advantage of robust statistical techniques, long-term and short-term data from operations and existing experimental evidence to model motor load as a function of traditional manipulated inputs and plate age. In addition, the proposed procedure allows for extracting refiner dynamics. The proposed procedure can be summarized as follows:

Long-term modeling (Nonlinear)

- Data collection – year basis (sampling: hourly averages).
- Outlier detection.
- Steady state identification.
- Fitting the static nonlinear motor load model (SNOP).
- Motor load gain derivation.

Short-term modeling (Linear)

- Data collection – Uncompressed data (sampling: varying rate).
- Homogenizing time sampling: interpolation and re-sampling at every second.
- Detection of intervals where input step changes occur in any of the manipulated inputs.
- Calculation of regulatory loop's time constants.
- Construction of linear model: gains + time constants.

CHAPTER 4: PULP QUALITY MODELING

"I can't work without a model. I won't say I turn my back on nature ruthlessly in order to turn a study into a picture...but in the matter of form I am too afraid of departing from the possible and the true."
Vincent Van Gogh (1853-1890)

4.1. Introduction

A systematic modeling framework is key in elucidating the effect of internal interactions, plate age and external disturbances on the operation of TMP-refiners such as discussed later on in CHAPTER 5 and CHAPTER 6. Although a great deal of work has been done on the modeling of TMP processes (Strand and Edwards, 1983; Strand and Mokvist, 1989a; Strand, 1989; Di Ruscio, 1993; Allison et al., 1996; Qian, 1997; Horch et al., 1997; Allison et al., 1997), to our knowledge no practical modeling procedures have been proposed to take advantage of the vast amount of data currently available in most pulp mill facilities. In addition, current models do not account for the multivariable effect of plate age on pulp quality. In this chapter, a model of a TMP two-stage Twin refining section of an existing integrated newsprint mill has been developed in MATLAB 6.5 ® to estimate pulp quality. The model relies on available measures of plate age and the prediction of motor load for both refiners made in CHAPTER 1. Pulp quality is estimated via a procedure that uses available laboratory tests, routine and seasonal data, comminution theory (Strand and Edwards, 1983), and other mechanistic correlations (Strand, 1989). In particular, corrective factors are introduced to account for the direct effect of plate age and wood moisture upon freeness and fibre

distribution. The inputs to the model are those given in CHAPTER 1, plus wood moisture and the dilution logics around the latency chest. Although, the model parameters are specific to the mill under study, the modeling methodology proposed here remains sufficiently general so that it can be used as a process analysis tool in most plants operating with Twin refiners.

4.2. Wood density

The wood density model presented here predicts basic wood density (on a dry basis) as a function of the mass proportion of each wood species in the final mix fed to the refiners. As mentioned in section 2.2, the types of wood used regularly along the year are: *Black Spruce*, *Balsam Fir*, *Jack Pine* and hardwood. Accordingly, chips are transferred to a silo with three compartments. Compartment # 1 stores Black Spruce and shavings; Compartment # 2 holds a mix of Jack Pine and Balsam Fir; and Compartment # 3 is filled with hardwood. The nominal densities of all species are given in Table 4.1.

Table 4.1. Density of wood species (oven dry Kg/m^3)

Species	Mean
Black Spruce	423
Balsam Fir	364
Jack Pine	400
Hardwood	525
Mix in Chip Silo	**427**

4.3. Wood moisture

In most TMP facilities, chip moisture is not a variable measured frequently and so, we have taken advantage of its strong correlation with ambient temperature. Wood moisture is represented in this work as a quadratic function of the ambient temperature (see Figure 4.1). Hence, the rate at which moisture is estimated depends on the availability of reliable ambient temperature readings (Figure 4.2). These estimates are to be used later on in the calculation of refining consistency and pulp quality. It should be noted that a more rigorous estimation of wood moisture should also include the wood's basic density, the heartwood and resin content, and the conditions under which chips are procured and stored (Sundholm, 2000).

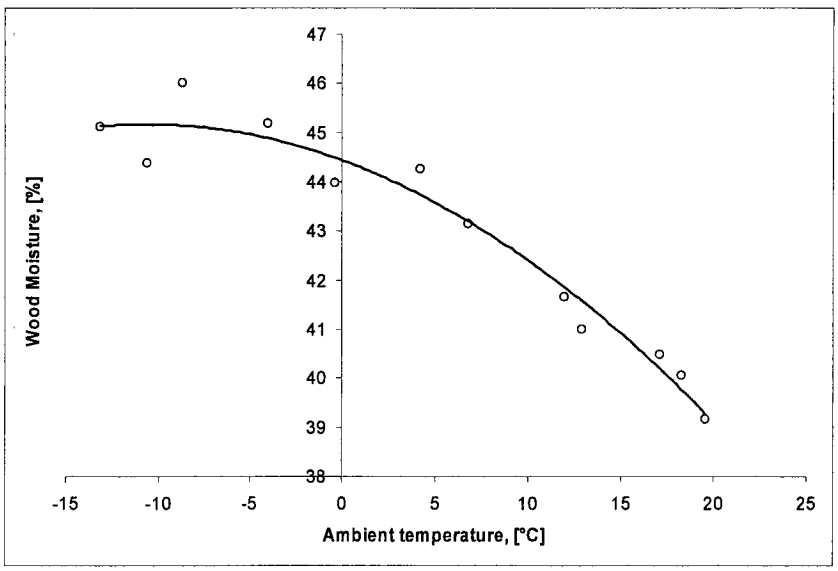

Figure 4.1. Wood moisture estimates based on monthly average ambient temperatures

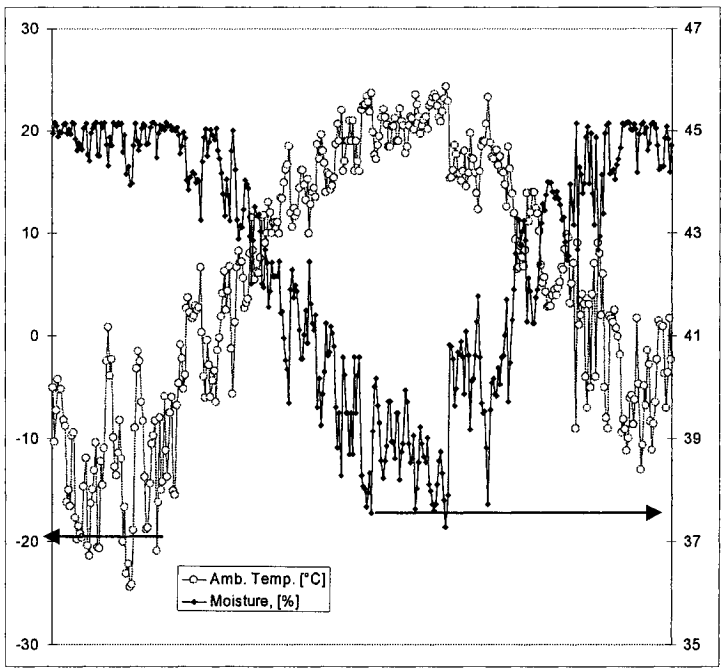

(daily average temperature data provided by Environment Canada)

Figure 4.2. Daily estimates of wood moisture during a year.

4.4. Consistency and steam production

Calculation of inlet and outlet consistencies and the amount of steam produced during refining is based on mass and energy balances. The inlet consistency C_{inlet} is calculated doing a simple mass balance:

$$C_{inlet} = \frac{F_c}{(F_c \cdot \frac{H}{100-H} + F_c + F_{dil} + F_{seal})} \cdot 100 \qquad (4.1)$$

where F_c is the dry production rate [from equation (3.2)], F_{dil} is the dilution mass flowrate, F_{seal} is the seal water mass flowrate, and H is the water content of the pulp

entering the refiner, which incidentally represents wood moisture in case of primary refiners. The amount of steam produced is calculated as follows:

$$W_s = \frac{(1 - e_{loss}) \cdot \eta \cdot ML}{L_e} \tag{4.2}$$

where the efficiency of the motor is represented by η, the heat losses around the refiner by e_{loss}, motor load by ML [equation (3.1)], and the enthalpy of the saturated steam produced during refining is calculated via interpolation from steam tables and denoted by L_e. Finally, the outlet consistency is calculated by:

$$C_{outlet} = \frac{F_c \cdot \frac{(100 - y_{loss})}{100}}{\left[F_c \cdot \frac{H}{100 - H}\right] + F_{dil} + F_{seal} - \left[\frac{(1 - e_{loss}) \cdot \eta \cdot ML}{L_e}\right] + F_c \cdot \frac{(100 - y_{loss})}{100}} \tag{4.3}$$

where y_{loss} denotes yield losses. Calculations leading to equations (4.1), (4.2), and (4.3) are given in APPENDIX A.

4.5. Specific energy and refining intensity

This part of the model relies on the knowledge of the refiner's design characteristics (see Table 4.2), which basically account for the refiner plates' geometry, the friction between pulp and plates, and the rotational speed. The specific energy (SE) is calculated by dividing the motor load by the production rate:

$$SE = \frac{ML}{F_c} \tag{4.4}$$

The efficiency of the refining operation –and therefore the resulting pulp quality- does not only depend on specific energy but also on the intensity of its application. In this work, we express refining intensity as the rate at which energy is transferred. This intensity is called *specific refining power* (*spw*) (Miles, 1990):

$$spw = \frac{SE}{\tau_{ref}} \tag{4.5}$$

For a given motor load, dilution conditions, rotational speed and refiner design, the residence time (τ_{ref}) of the pulp in the refining zone is calculated as proposed by Miles (Miles, 1991):

$$\tau_{ref} = \frac{\mu_r}{\mu_t} \frac{a \cdot SE \cdot C_{inlet} \cdot L_s}{(\omega)^3 \left(L_s \left(r_{ext}^2 - r_{\text{int}}^2\right) + C_{inlet} \cdot SE \cdot r_{\text{int}}^2\right)} \left[\ln\left(\frac{r_{ext}}{r_{\text{int}}}\right) - 0.5 \cdot \ln\left(\frac{L_s - C_{inlet} \cdot SE}{L_s}\right) \right] \tag{4.6}$$

where L_s is the latent heat of steam at a given casing pressure P_{ref}. This value is obtained by interpolation from steam tables. The remaining parameters are given in Table 4.2. The design parameter a is equal to 4 for Twin and Single-disc refiners.

Table 4.2. Refiner design parameters.

Radial friction coefficients between pulp and plates	$\mu_r = 0.25$
Tangential friction coefficients between pulp and plates	$\mu_t = 0.75$
Number of bars per unit length of arc	$n = 83$
Inlet ratio of the refining zone, [m]	$r_{int} = 0.657$
Outlet ratio of the refining zone, [m]	$r_{ext} = 0.787$
Plate's rotational speed, [RPM]	$\omega = 1800$

4.6. Pulp quality

Unlike the well known empirical models of Qian and Tessier (Qian and Tessier, 1995), the pulp quality predicted in this work relies on less empirical and more mechanistic equations. Indeed, our modeling is based on the work done by Kano et al. (Kano et al., 1982) and Strand and coworkers (Strand and Edwards, 1983; Strand and Mokvist, 1989a; Strand and Mokvist, 1989b) regarding the application of Comminution theory to the analysis of refiner performance. One advantage of this approach over purely empirical ones is that defiberization is regarded as a rate process, and thus it relates to the physical phenomena of refining kinetics (Strand and Mokvist, 1989a). In this modeling framework, freeness is not independent of the fibre breakage occurrence as it varies in relation to the amount of long and broken fibre resulting from refining. Furthermore, in the light of the experimental work done by Strand and Mokvist (Strand and Mokvist, 1989a), we incorporate a refining intensity factor in the derivation of the comminution equations. Finally, in order to account for the seasonal and long-term variations in pulp quality, we propose correction factors based on wood moisture and plate age.

4.6.1. Procedure to model pulp quality after refiners

The modeling procedure here proposed allows the prediction of pulp quality characteristics using laboratory and routine operating data. The flow diagram of the procedure is depicted in Figure 4.3.

a. **Bauer McNett – PQM Database**: Several Bauer McNett (Laboratory) tests have been performed on various pulp samples at locations where PQM measurements were available. Hence, a set of fibre distribution data (Bauer McNett – PQM) is obtained to relate laboratory tests and on-line measurements.

b. **Fibre distribution cutting points, λ_1 and λ_2**: In recent years, many plants have replaced the measurement of fibre length fractions via laboratory Bauer-McNett with on-line testing of the amount of "long" (including shives), "medium" and "fine" fibre fractions. In this case, a PQM system is used. Hence, the cutting points λ_1 and λ_2 here proposed serve as conversion parameters to relate laboratory tests and on-line PQM measurements for a particular pulp. For a given set of fibre distribution data, the Bauer-McNett fractions selected for the cutting are R+28 and R+48 as depicted in Figure 4.4. Provided a set of fibre distribution data is available, we can calculate the cutting points λ_1 and λ_2 for any set of data by solving two mass balance equations. Results yielded: $\lambda_1 = 0.75$ and $\lambda_2 = 0.79$.

c. **Data collection**: Due to the lack of on-line data at blowline locations, several laboratory tests for shives content, Bauer McNett fibre distribution and freeness were requested from the mill. Pulp sampling must be done at almost constant operating conditions so as to calculate nominal values for the comminution parameters. In order to relate refiner operation and pulp quality, the values of transfer screw speed, motor load, and dilution flowrates were also registered at the moment of sampling.

d. **Calculation of nominal comminution parameters:** Comminution of shives (SV) and the corresponding development of long fibres [+28] (LF_{28}) can be expressed in terms of selection (S_{SV} and S_{LF}) and breakage (B_1) parameters (Strand and Mokvist, 1989a):

$$SV = SV_o \cdot e^{-S_{SV} \cdot SE} \tag{4.7}$$

$$LF_{28} = \frac{SV_o \cdot S_{SV} \cdot B_1 \cdot e^{-S_{SV} \cdot SE}}{S_{LF} - S_{SV}} + \frac{LF_o \cdot (S_{LF} - S_{SV}) - SV_o \cdot B_1 \cdot S_{SV}}{S_{LF} - S_{SV}} \cdot e^{-S_{LF} \cdot SE} \tag{4.8}$$

where SV_o and LF_o are respectively, the corresponding contents of shives and long fibre [+28] at the refiner's inlet. As mentioned earlier, provided quality measurements are available at quasi-stable conditions the nominal comminution parameters, namely S_{SV}, S_{LF} and B_1 can be obtained using the least-square Gauss-Newton Method. Results for the primary refiner were: $S_{SV} = 2.57$, $S_{LF} = 0.64$, and $B_1 = 0.89$, while for the secondary refiner were: $S_{SV} = 1.05$, $S_{LF} = 0.33$, and $B_1 = 0.86$.

e. **Incorporation of the refining intensity factor, f_i, in the comminution parameters:** Work by Miles (Miles, 1990) and Qian (Qian, 1997) has shown that shive and long fibre content also depend on the specific refining power, *spw*, which is a measurement of the refining intensity at a given specific energy. Provided nearly constant operating conditions are achieved at the time of sampling, a nominal (average) specific refining power, spw_o, can be calculated from the data gathered in (c) using equation (4.6). Hence, the selection parameters can be expressed as a function of factor $f_i = \frac{spw}{spw_o}$:

$$S_{SV} = S_{SVo} \cdot f_i \quad \text{and} \quad S_{LF} = S_{LFo} \cdot f_i \tag{4.9}$$

where S_{SVo} and S_{LFo} are the selection parameters obtained in (d), i.e. when $f_i = 1$. As for the breakage parameter B_1, the assumption is that its value remains relatively constant in spite of changes in wood species or operating conditions (Strand and Mokvist, 1989a).

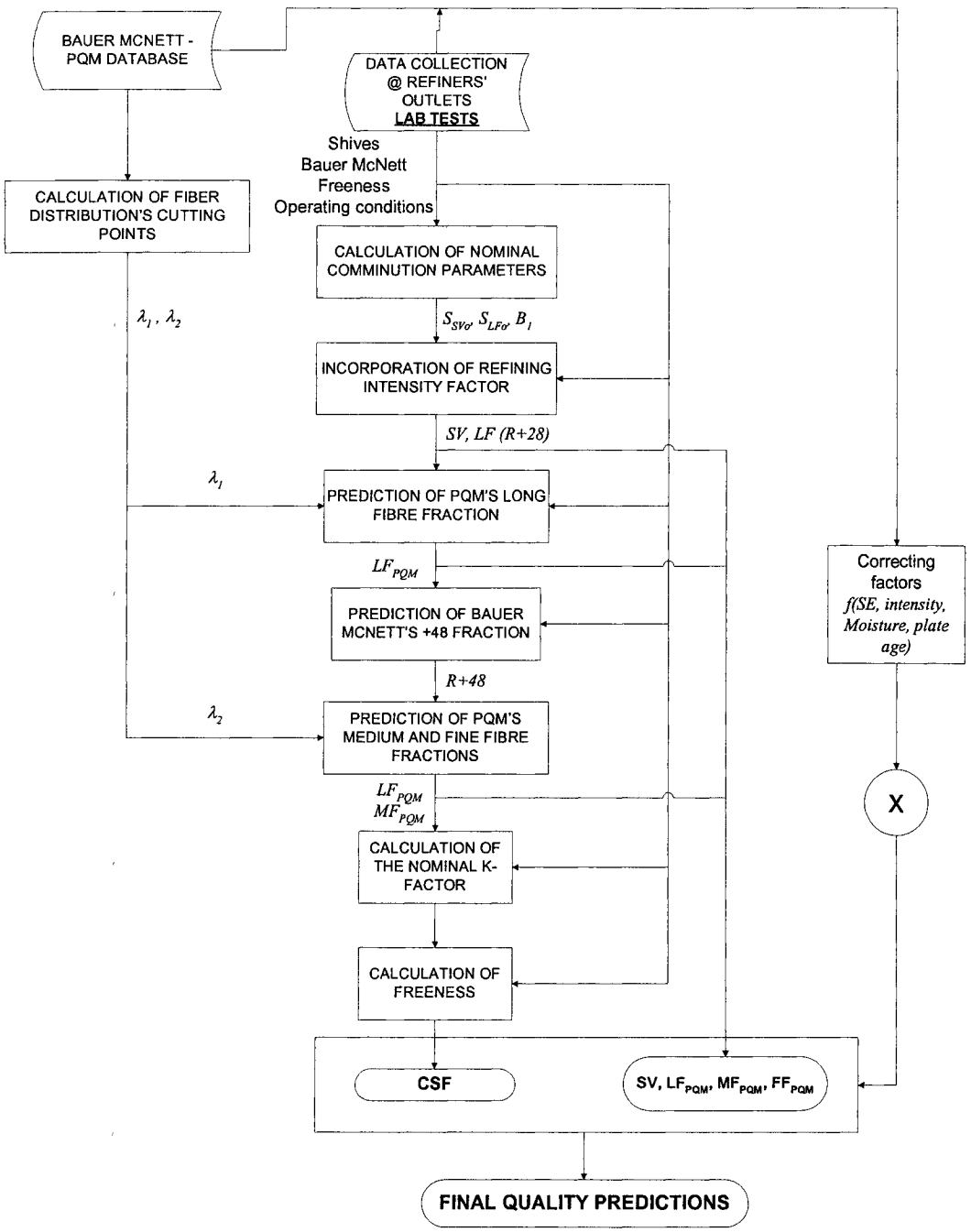

Figure 4.3. Procedure to develop a pulp quality model.

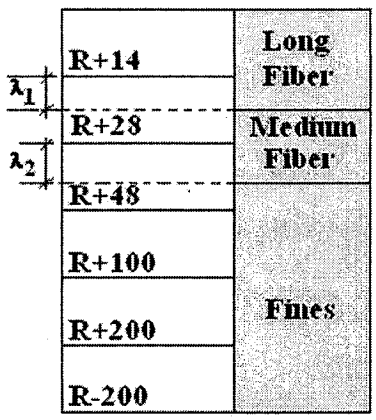

Cutting points λ_1 and λ_2 vary between 0 and 1.

Figure 4.4. Relationship between Bauer-McNett and PQM fibre classification.

f. Prediction of the PQM's long fibre, LF_{PQM} : From the Bauer McNett data gathered in (c) (fractions +14 and +28) and using the fibre distribution cutting point λ_1 obtained in (b), the long fibre fraction that a PQM system would yield is calculated as follows:

$$LF_{PQM} = (SV + LF_{28}) \cdot \chi \tag{4.10}$$

Where χ is the long fibre PQM cutting point: $\chi = \dfrac{(R14 + R28 \cdot \lambda_1)}{R14 + R28}$

For both the primary and secondary refiners χ resulted in 0.83.

g. Prediction of Bauer McNett fraction +48, R_{48}: Work by Strand and Edwards (Strand and Edwards, 1983) indicates that the remaining fibre size distribution, namely fractions R+48, R+100, R+200 and R-200 follow a Rosin-Rammler

distribution function with respect to the cumulative weighted average fibre length[11]. Thus, the correlation predicting the Bauer McNett fraction +28/48, R_{48} can be written as:

$$R_{48} = 1 - e^{-g \cdot L_{48}^{z}} - SV - LF_{28} \tag{4.11}$$

where L_{48} is the cumulative weighted average fibre length at fraction +48 and g and z are regression coefficients. Regressions yielded L_{48} = 1.82, g = 32.3, z = -5.16 for the primary refiner, and L_{48} = 1.84, g = 17.5, z = -4.54 for the secondary refiner.

h. Prediction of the PQM's medium fibre, MF_{PQM}, and fines FF_{PQM}: Using the fibre distribution cutting point λ_2 obtained in (b), the Bauer McNett fraction +48 predicted in (g), and the PQM's long fibre fraction predicted in (f), the PQM's medium and fine fibre fractions can be calculated as:

$$MF_{PQM} = \left[(SV + LF_{28}) \cdot (1 - \chi) + R_{48} \cdot \lambda_2\right] \tag{4.12}$$

$$FF_{PQM} = 1 - LF_{PQM} - MF_{PQM} \tag{4.13}$$

i. Calculation of the nominal K-factor: Freeness is closely related to the amount of fibre development, which accounts for the bonding phenomena as a consequence of refining. Strand (Strand, 1989) introduced the *K*-factor (K_f) to quantify the degree of surface development in the pulp. Accordingly, he assumed that the contribution to surface development of each individual fraction was additive, and thus derived –

[11] Data for the average fibre length of each Bauer McNett fraction is given in (Tasman, 1972).

using data from previous experimental work such as (Forgacs, 1963)- the following equation to predict the total specific surface area of the pulp, A_{TOT} :

$$A_{TOT} = 0.6 + K_f \cdot \left[\frac{LF_{PQM}}{L^2_{LF_{PQM}}} + \frac{MF_{PQM}}{L^2_{MF_{PQM}}} + \frac{FF_{PQM}}{L^2_{FF_{PQM}}} \right] \tag{4.14}$$

where $L_{LF_{PQM}}$, $L_{MF_{PQM}}$, and $L_{FF_{PQM}}$ are the weighted average fibre length for the long fibre, medium fraction and fine fraction, respectively. They are calculated from data collected in (a) and the values tabulated in (Tasman, 1972). Parameters are found to be $L_{LF_{PQM}} = 2.15$, $L_{MF_{PQM}} = 1.4$, and $L_{FF_{PQM}} = 0.66$ mm for the primary refiner, and $L_{LF_{PQM}} = 2.2$, $L_{MF_{PQM}} = 1.4$, and $L_{FF_{PQM}} = 0.45$ mm for the secondary refiner. Parameter K_f is calculated differently for the primary and the secondary refiners as proposed by Strand and Edwards (Strand and Edwards, 1983):

$$\text{For the primary refiner: } K_{f1} = 1.54 \cdot e^{SE_1 \cdot x_1 \cdot (0.123 - 0.0237 \cdot C_{inlet1})} \tag{4.15}$$

where C_{inlet1} is the inlet consistency [fractional], SE_1 is the specific energy given (in MWh/TN), and x_1 is a tuning parameter specific for the plant under study. For the secondary refiner:

$$K_{f2} = K_{f1} \cdot e^{\left[SE_2 \cdot \left(-0.598 + x_2 \frac{0.088 \cdot SE_2}{K_{f1}} - 4.99 \cdot K_{f1} \cdot C_{inlet2} \right) \right]} \tag{4.16}$$

where C_{inlet2} is the inlet consistency to the secondary refiner, SE_2 the corresponding specific energy, and x_2 a tuning parameter specific for the plant under study.

j. Calculation of Canadian Freeness Standard (CSF_{ref}): Freeness is calculated using the empirical relationship found in (Strand and Edwards, 1983):

$$CSF_{ref} = e^{\frac{21.263 - A_{TOT}}{3.3032}} \tag{4.17}$$

4.6.2. Procedure to model pulp quality after latency chest

In our model we have included the drop in freeness as a result of latency removal (Mohlin, 1980). The latency chest is modeled as a perfectly mixed tank. As shown in Figure 2.4, there are two dilution points: the first dilution flowrate goes directly into the latency chest while the second one is much smaller and serves to keep the outlet consistency at about 4-6%. The fibre distribution after this small dilution point is represented by: long fibre content (LF_3), medium fibre content (MF_3) or fine content (FF_3). Likewise, CSF_3 is the freeness at the same location.

We have mentioned earlier that chip moisture has an important effect on pulp strength, yet none of the relationships describing long and medium fibre contents include the direct effect of moisture. In addition, refining intensity as described in equation (4.5) does not explicitly account for the effect of plate age that in practice - and at constant specific energy - has proved to increase the intensity of refining. It is in this context that we propose the introduction of corrective factors (f_{CSF}, f_{LF}, f_{MF}) to account for the direct effect of plate age and wood moisture on the final pulp quality under given conditions of total specific energy, production rate and dilution:

$$\begin{aligned} CSF &= f_{CSF} \cdot CSF_3 \\ LF &= f_{LF} \cdot LF_3 \\ MF &= f_{MF} \cdot MF_3 \\ FF &= 100 - LF - MF \end{aligned} \tag{4.18}$$

Corrective factors are written as a linear combination of important operating conditions:

$$
\begin{aligned}
f_{CSF} &= a_1 + a_2 \cdot LF + a_3 \cdot SE_{TOT} + a_4 \cdot P_{age1} \cdot spw_1 + a_5 \cdot P_{age2} \cdot spw_2 \\
f_{LF} &= b_1 + b_2 \cdot H + b_3 \cdot SE_{TOT} + b_4 \cdot P_{age1} \cdot spw_1 + b_5 \cdot P_{age2} \cdot spw_2 \\
f_{MF} &= c_1 + c_2 \cdot LF + c_3 \cdot SE_{TOT} + c_4 \cdot P_{age1} \cdot spw_1 + c_5 \cdot P_{age2} \cdot spw_2
\end{aligned}
\qquad (4.19)
$$

where SE_{TOT} is the total specific energy (for both refiners) as calculated by equation (4.4), *spw* is the specific refining power (intensity) as calculated by equation (4.5), and the final estimations of freeness, long fibre content, medium fibre content and fine content are denoted by *CSF, LF, MF, FF*, respectively. It should be noted that coefficients a_i = [2.19, 7.45e-3, -1.79e-4, -8.48e-10, -1.93e-8], b_i = [1.75, -1.66e-2, -1.88e-5, -2.69e-9, -2.53e-9] and c_i = [1.07, -7.83e-3, 1.71e-5, 6.96e-9, 3.78e-9] have been calculated empirically using hourly average data from the mill. The corresponding regression plots are shown in Figure 4.5.

4.7. Results and discussion

The model has been developed in MATLAB ® using hourly averaged data for 8760 hrs (1 year) under the operating conditions shown in Figure 4.6. Accordingly, the model takes into account plate age, hydraulic pressure, production and dilution rates, and the dilution conditions at the latency chest. In terms of pulp quality predictions, we believe some remarks are necessary regarding the methodology proposed in section 4.6.1:

- We placed our cutting points λ_1 and λ_2 at fractions R+28 and R+48 as a result of a trial-and-error calculation. This selection of fractions depends entirely on the quality of the wood furnish and the pulp produced at a given plant.

- Pulp sampling can only be performed when quasi-stable operating conditions have been attained. As suggested in section 1.4.1, motor load is a good indicator of steady state regimes given its critical impact on specific energy, refining intensity, and therefore pulp quality.

- Both tuning parameters x_1 and x_2 in equations (4.15) and (4.16) compensate for our choice of using inlet consistencies instead of outlet consistencies as originally proposed by Strand and Edwards (Strand and Edwards, 1983). Indeed, if outlet consistencies are not measured in the plant the use of inlet consistencies introduces less uncertainty in the calculations. Furthermore, by including inlet consistencies we have implicitly considered refining intensity in the determination of K_f factors.

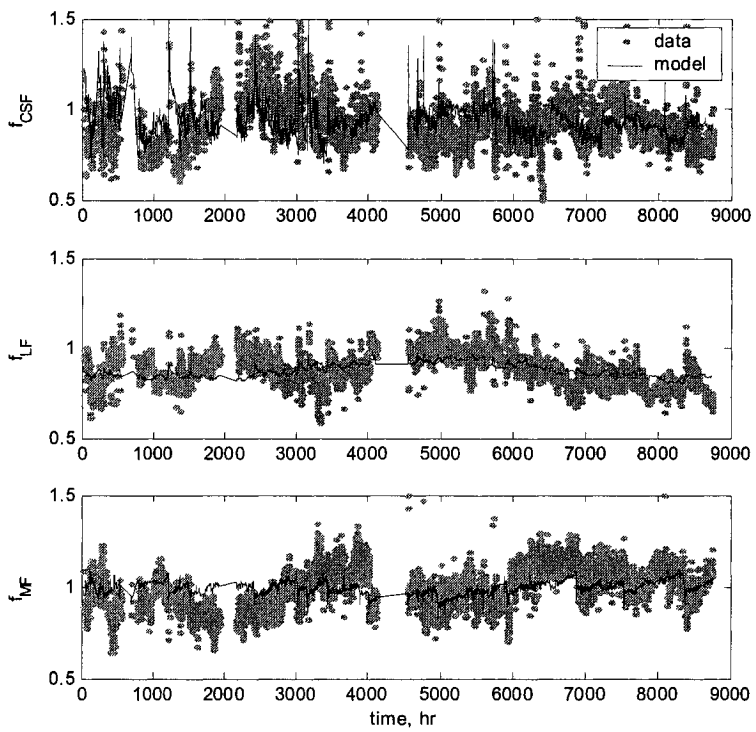

Figure 4.5. Estimation of corrective factors for pulp quality.

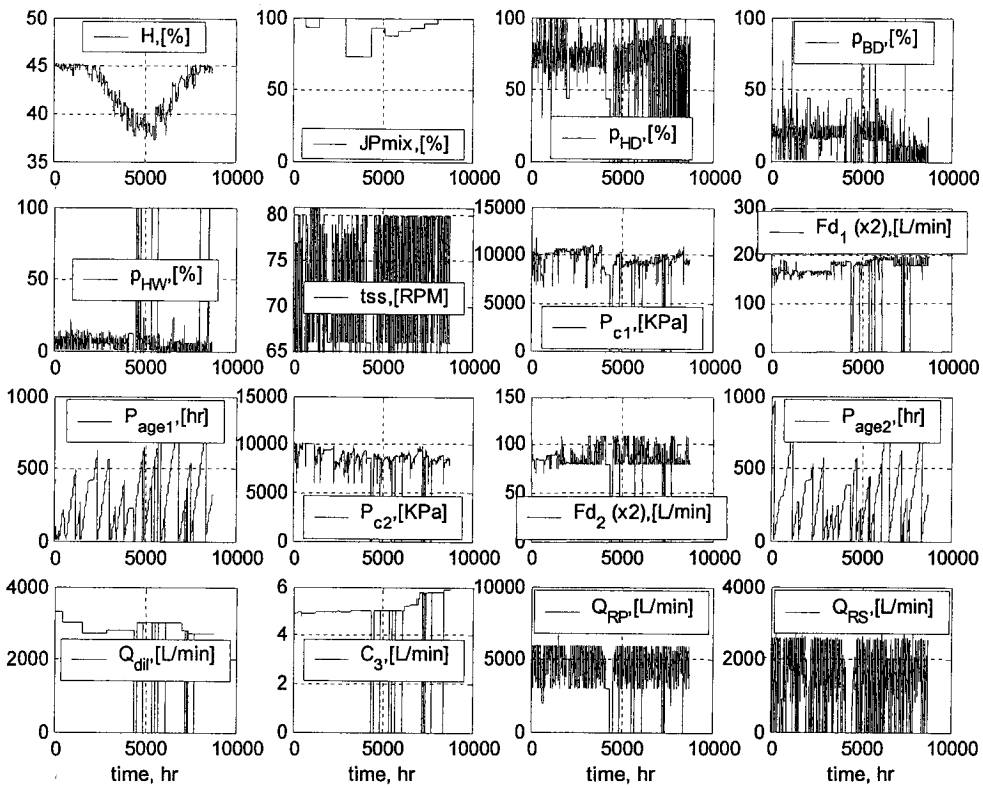

Figure 4.6. Input operating conditions for model validation

Results for the most important outputs (measured quality) are depicted as a function of time in Figure 4.7 and as operating windows in Figure 4.8. Predictions follow fairly well real long-term trends and shifts. In particular note in Figure 4.8 that the average operation has been appropriately captured by the model. It is important to underline that the model requires more information on wood quality to account for the long variability that has not been captured.

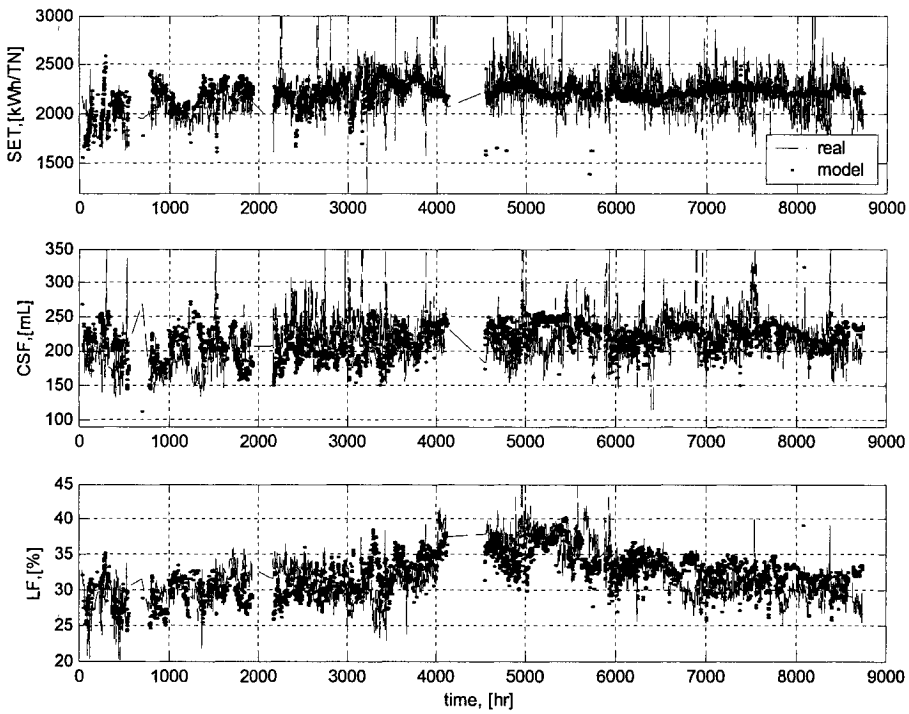

(Pulp quality is measured out of the latency chest)

Figure 4.7. Estimation of total specific energy, freeness, and long fibre content for one year of operation.

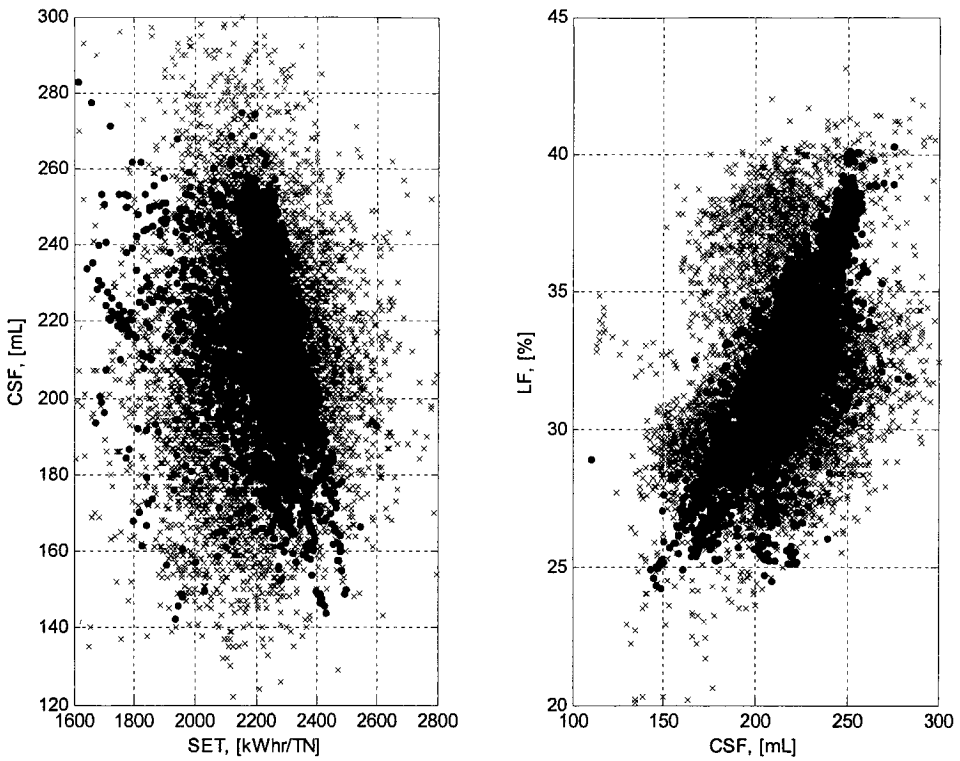

(crosses: real, dots: model). Pulp quality is measured out of the latency chest.

Figure 4.8. Operating windows.

The proposed methodology is primarily intended for twin refiners. As mentioned earlier in CHAPTER 3, the applicability of the procedure can be extended to single and double disc refiners since they also have flat refining zones. Application to conical disc refiners would previously require several experimental trials to elucidate the effect of plate age on motor load and pulp quality.

4.8. Conclusions

A modeling procedure has been proposed to predict pulp quality. The model relies on available measures of plate age and the prediction of motor load for both primary and secondary refiners (see CHAPTER 3). In order to account for most variations in pulp quality, corrective factors based on chip moisture, specific energy, refining intensity and plate age are introduced. The model puts in evidence how important wood characteristics and species proportions are in order to reliably predict pulp quality. The proposed procedure can be summarized as follows:

Modeling operating targets:

- Consistency and steam production.
- Specific energy and refining intensity.

Modeling quality:

- Data collection – PQM system and Laboratory tests.
- Estimation of fibre fractions and freeness using comminution theory and specific surface area calculations (Strand and Edwards, 1983).
- Correction of pulp quality estimations with respect to plate age and refining intensity.

Special attention has been paid to the structure and configuration of the process so that the model and procedures remain sufficiently general to be used as a process analysis tool in most TMP refining plants that operate with Twin refiners. Finally, the prediction of fibre fractions after both refiners in terms of PQM values allows the evaluation of the entire operation –latency chest included- using a single fibre distribution standard.

CHAPTER 5: ANALYZING THE DIRECTIONALITY OF TMP-REFINING INTERACTIONS

"There is nothing wrong with change, if it is in the right direction."
Winston Churchill (1874-1965)

5.1. Introduction

The inherently interactive nature of TMP-Refining processes is one of the most important sources of variability in pulp quality. Hence, an analysis of the directionality of these internal interactions is critical to determine controllable ways to operate chip refiners. A vast amount of experimental work has been done on the operation of TMP-refiners. Miles and coworkers (Miles, 1990; Miles and May, 1990; Miles et al., 1991; Stationwala et al., 1993; Alami et al., 1997) extensively studied the effect of refining intensity on pulp quality. Strand and Hartler (Strand and Hartler, 1985) studied the effects of specific energy, residence time, plate age and vibrational energy on the pulp quality-energy relationships. Stationwala (Stationwala et al., 1994) and Strand (Strand et al., 1993) have looked at the effect of production rate on refining. Roche et al. (Roche et al., 1996) elucidated the important relationships and variables to take into account to properly control TMP refiners. McQueen et al. (McQueen et al., 1999) studied the effect of production rate, hydraulic pressure and dilution flowrate on motor load and consistency at different plate conditions. Model-based analyses include the work of Qian (Qian, 1997) and Du (Du, 1998) who simulated different TMP-refining conditions to demonstrate process interactions, nonlinearity and input-output quantitative relationships. Eriksson et al. (Eriksson et al., 2002) have used a linear

model to analyze the impact of production rate, hydraulic pressure and dilution upon consistency, refining temperatures and casing pressures in a two-stage refining line. Berg and Karlstrom (Berg andKarlstrom, 2004) studied these interactions but with the purpose of decoupling the system. More recently, Lama et al. (Lama et al., 2004) have investigated the effect of internal interactions on operating targets and pulp quality by applying controllability indices to a two-stage refining model.

As far as modeling is concerned, the motor load relationships used to perform most of the aforementioned analyses are linear and do not explicitly consider plate age in their formulations[12]. Moreover, the only quality models used in simulation-based analyses (Qian, 1997; Du, 1998) are purely empirical and do not take into account the proven physical connections between fibre distribution and freeness.

In this chapter, the nonlinear model presented in CHAPTER 3 and CHAPTER 4 is used to study the directionality of the internal interactions affecting TMP refining. The analysis includes the effect of plate age on operating targets and the quality of the refined pulp.

5.2. Effect of refining conditions on pulp quality

Refining conditions refer to the way in which the screw speed (*tss*), the hydraulic pressures (Pc_1, Pc_2) and the dilution flowrates (Fd_1, Fd_2) are manipulated in both refiners under given conditions of plate age (P_{age1}, P_{age2}) and wood quality. The proportions in which wood species are fed to the plant are assumed constant and so are the corresponding densities. *Operating targets* such as primary motor load (ML_1), the total specific energy (SET)[13] and the power split ($splitPR$)[14] between the two refining

[12] Even though the work by Strand and Hartler (Strand and Hartler, 1985) takes into account the effect of two different plate conditions, the relationship between motor load and plate age are not explicitly addressed.
[13] Total specific energy is the sum of the specific energies (SE_1 and SE_2) applied to both refiners.
[14] With respect to the primary refiner.

stages are associated with a higher control level in the plant, and therefore relate directly to pulp quality. Finally, pulp quality is expressed in terms of freeness (*CSF*) and long fibre content (*LF*). It should be noted that in order to account for as many refining conditions as possible, we had to run our model under a constant transfer screw speed and a wide range of hydraulic pressures in both refiners[15].

5.2.1. Effect of plate age on motor load

Motor load gains change with plate age and operating conditions. It has been reported that there is a decrease in the effect of screw speed (production rate) and hydraulic pressure upon motor load as plates age (Roche et al., 1996; McQueen, 1995). Furthermore, Strand and Hartler (Strand and Hartler, 1985) report an increase of hydraulic pressure to compensate for plate aging. As mentioned in CHAPTER 3, the physical phenomena underlying those changes in direction may have to do with unbalanced forces affecting the refiner plates. Finally, industrial practice indicates that plate wear has a reducing effect on motor load.

Using the model proposed in CHAPTER 3, we have plotted several nonlinear operating windows that relate motor load to different conditions of plate age, transfer screw speed, hydraulic pressure and dilution rates (Figure 5.1). We observe that at constant operating conditions the attainable motor load decreases as plates get older. This is congruent with industrial evidence which indicates that as plates wear the refining operation demands more motor load to hold on to a given pulp strength. Large dilutions will also result in lower motor loads at relatively constant plate conditions. These results show that operation with new plates at low dilution rates should yield the largest attainable motor loads. Incidentally, motor load increases with hydraulic pressure and screw speed. Similar results can be obtained for the secondary motor load.

---

[15] Pc_1: [6500 – 10500 kPa]; Pc_2: [5000 – 10000 kPa].

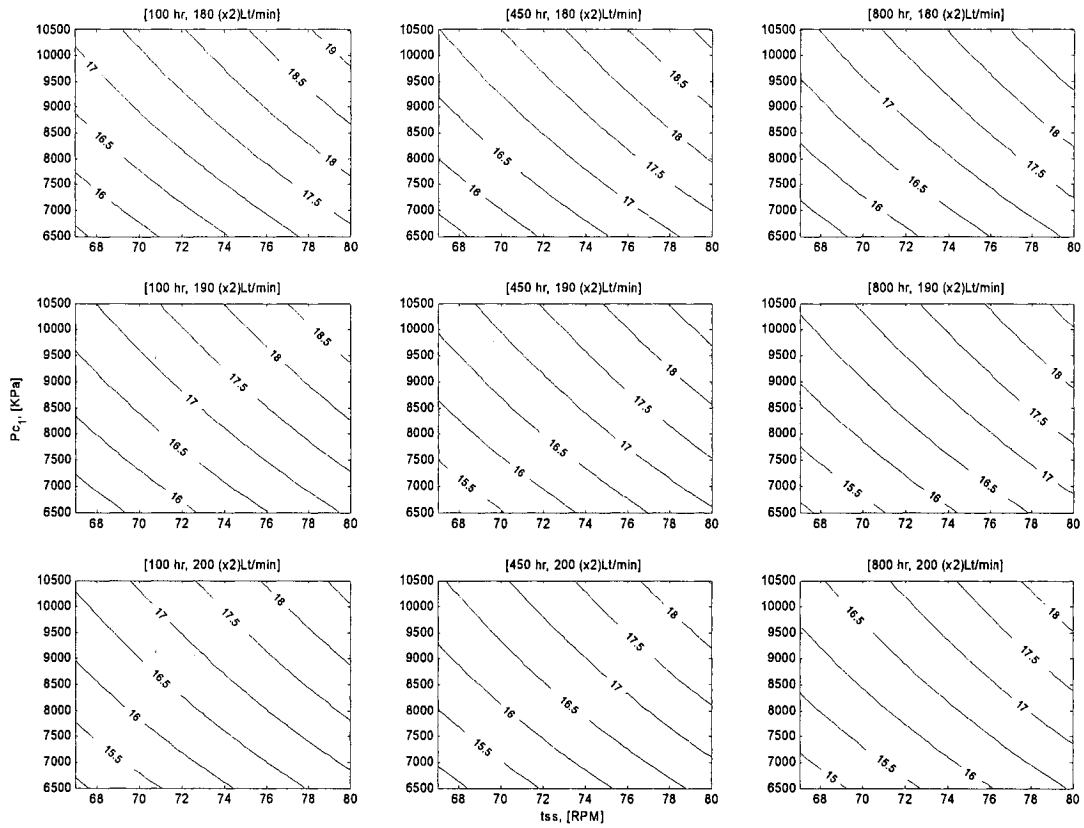

Figure 5.1. Primary refiner motor load (ML_1). Each plot corresponds to a different condition of plate age and dilution.

5.2.2. Effect of total specific energy and power split ratio on pulp quality

As depicted in Figure 5.2, the nominal operation can be moved to different zones within the pulp quality window only by changing the total specific energy and the energy split between refining stages. Accordingly, under constant dilution conditions, production rate and plate age, long fibre content and freeness can be increased if the operation moves toward lower specific energy levels and higher power split ratios

(Figure 5.2b). It can also be observed that for a given freeness we can obtain higher long fibre content (Figure 5.2d) by for instance increasing the specific energy –or the motor load provided production rate is constant- in the primary refiner. Conversely, at constant freeness we may produce less long fibre if the primary specific energy decreases (Figure 5.2a). Increasing the total specific energy by mounting the motor load in the secondary refiner may result not only in shorter fibres, but also lower freeness (Figure 5.2c).

5.2.3. Effect of plate age on pulp quality

Plate age has a long term effect upon pulp quality. The direction in which the pulp quality window shifts over time depends on the plate conditions in each refiner (Figure 5.3). Our results indicate that older plates in the primary refiner will mostly reduce long fibre content (Figure 5.3b), whereas plate conditions in the secondary refiner will predominantly affect freeness, reducing it as time goes on (Figure 5.3c). These results make physical sense given that the primary refiner's objective is to separate –i.e. "create"- fibres from the chip's bulk, while the secondary refiner is mostly in charge of developing the specific surface area of the pulp. Moreover, this also implies that in the primary refiner there is a loss of long fibre fractions in favour of more medium fractions, whereas in the secondary refiner fines increase their proportion at the expense of medium fractions. Hence, if both refiners start operation with new plates, as time elapses, the attainable quality window will gradually move toward lower freeness and long fibre contents (Figure 5.3a). In any case, the reduction in either parameter of quality is likely due to the increase in refining intensity as plates get older. Indeed, when plates are worn there is less space between bars, and therefore the residence time of the pulp within the bars decreases.

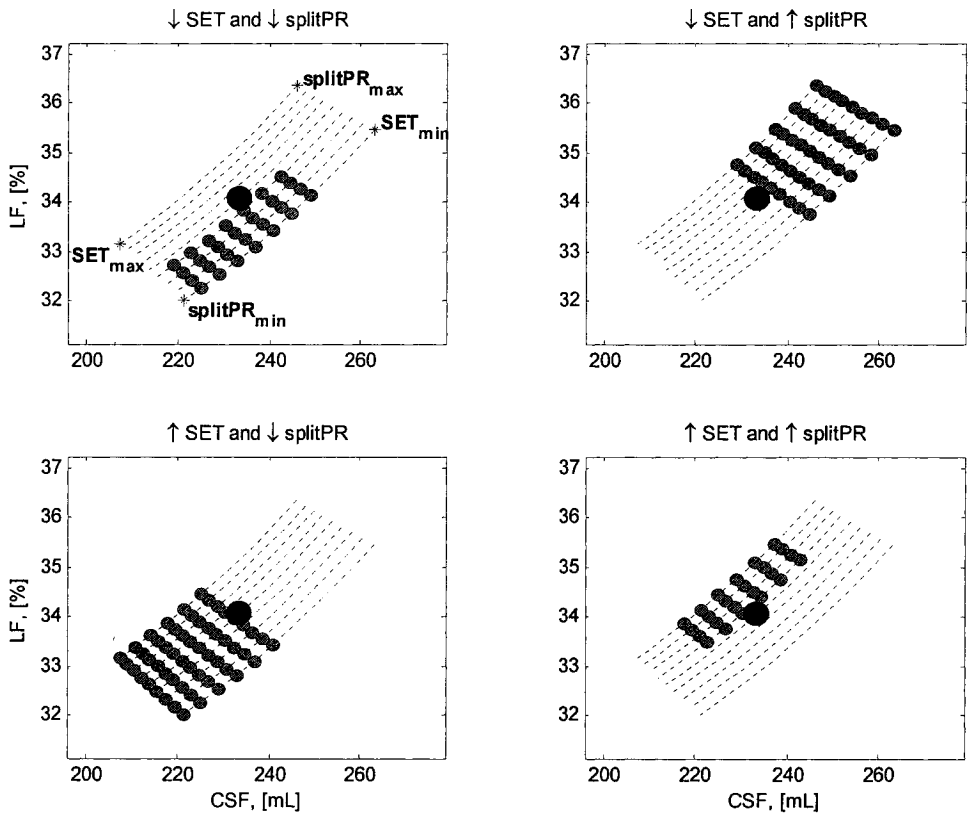

Nominal conditions (centre dot): tss = 74 RPM, Fd_1 = 190, Fd_2 = 90 L/min, $P_{age1} = P_{age2}$ = 450 hrs.

Figure 5.2. Effect of total specific energy (SET) and power split (splitPR) on pulp quality.

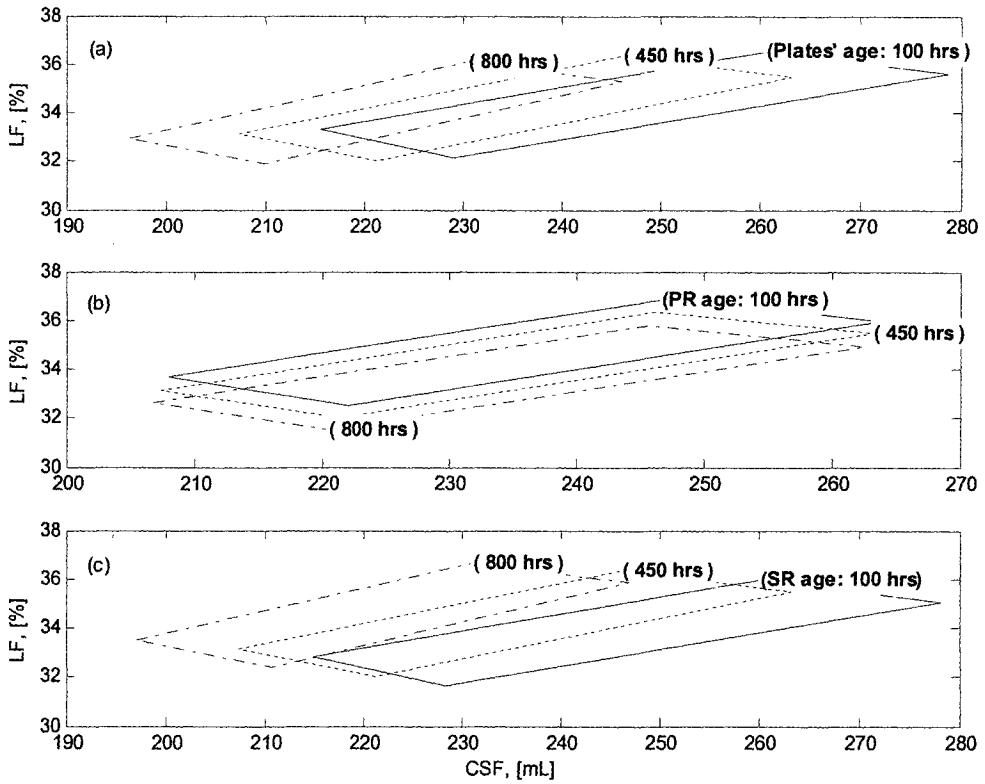

Nominal conditions: tss = 74 RPM, Fd_1 = 190 L/min, Fd_2 = 90 L/min. (a): Both refiners with plates of same age; (b): Different plate ages in primary refiner (P_{age2} = 450 hrs); (c): Different plate ages in secondary refiner (P_{age1} = 450 hrs).

Figure 5.3. Effect of plate age on pulp quality.

5.2.4. Effect of dilution flowrates on pulp quality

As illustrated in Figure 5.4, long fibre content decreases as dilution is increased in either the primary or the secondary refiner. Indeed, more water (more mass) entails higher centrifugal forces acting on the fibre which translates into a smaller residence time of the pulp inside the refiner, and thus a higher intensity operation (Miles and

May, 1990; Sundholm, 2000). On the other hand, freeness only decreases when the first-stage dilution is increased (Figure 5.4a). When higher dilutions are applied to the secondary refiner (at constant first-stage dilution) the attainable quality window moves somewhat toward higher freeness (Figure 5.4b). This behaviour is most likely due to the reduction in the attainable total specific energy which outweighs the rise in refining intensity at the secondary-stage. Indeed, increasing dilution results in lower motor loads (see Figure 5.1), and thus lower specific energy levels.

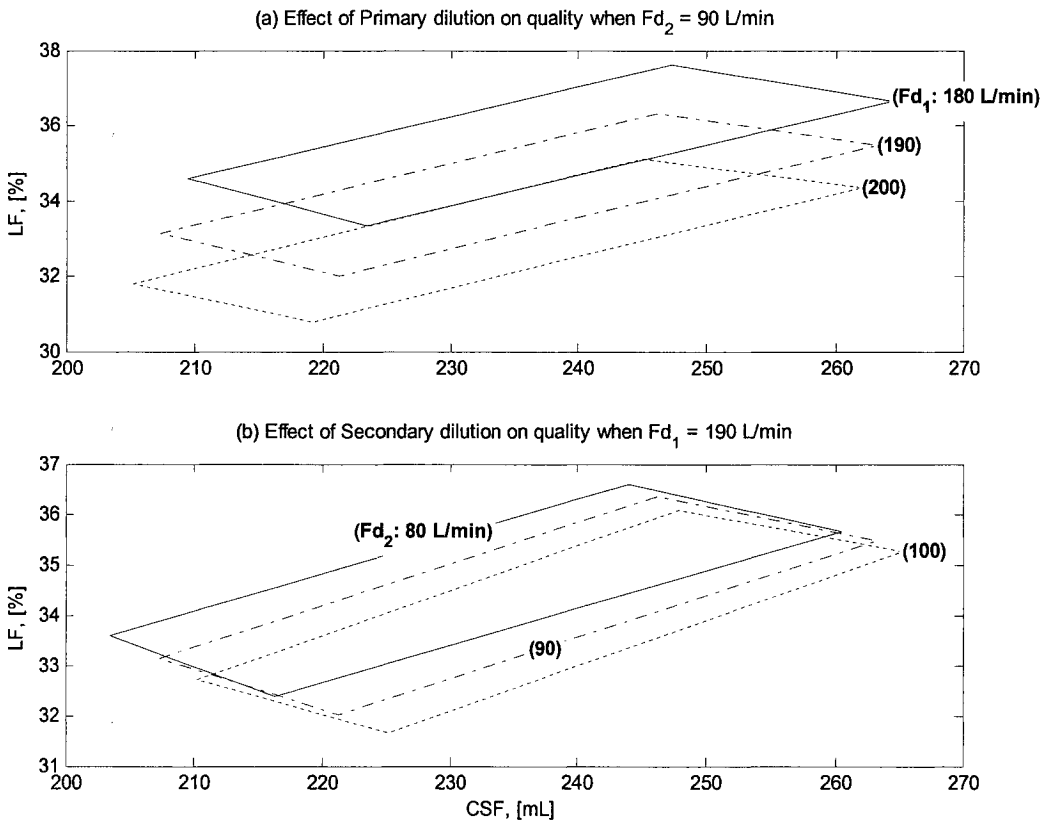

Nominal conditions: *tss* = 74 RPM, $P_{age1} = P_{age2} = 450$ hrs.

Figure 5.4. Effect of dilution on pulp quality.

5.2.5. Effect of chip moisture on pulp quality

The effect of chip moisture on the attainable quality window is depicted in Figure 5.5. Under constant dilution conditions, production rate and plate age, long fibre content and freeness decrease as chip moisture increases. This reduction in freeness and long fibre content is the consequence of a more intense operation at higher chip moisture. Indeed, the higher the moisture the lower the refining consistency, and thus the higher the intensity. In particular, Figure 5.5 illustrates how long fibre content seems to be more affected than freeness. This relationship between moisture and pulp quality is confirmed elsewhere (Qian and Tessier, 1995).

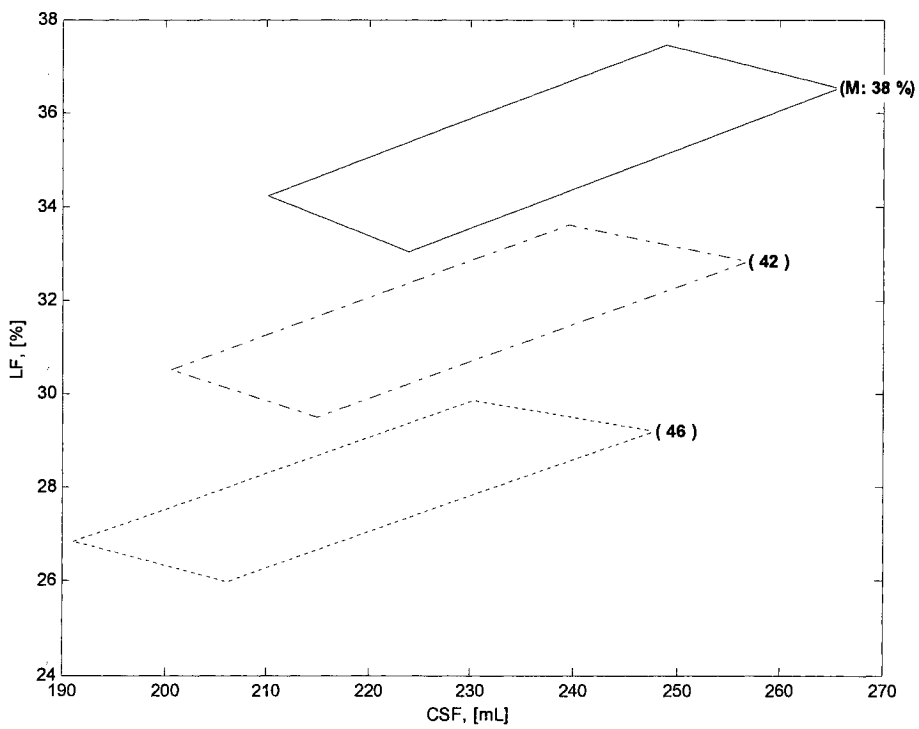

Nominal conditions: tss = 74 RPM, Fd_1 = 190, Fd_2 = 90 L/min, $P_{age1} = P_{age2}$ = 450 hrs.

Figure 5.5. Effect of wood moisture on pulp quality.

5.3. Directionality between manipulated inputs, plate age, operating targets and pulp quality

Although the analysis made above provides some answers in terms of tendencies and trends in addition to depict multiple steady state conditions at once, it does not capture the direction of the effect of each manipulated input on the entire operation. Indeed, directionality is strongly affected by the interactions taking place –both in parallel and in series- as plates wear. In this section, we depict the independent effect of each of the usual five manipulated inputs on the quality of the pulp leaving the latency chest. In order to do so, several step changes –of different magnitude and direction- were independently applied to each manipulated input. Results are depicted in Figure 5.6.

5.3.1. Effect of production rate (transfer screw speed)

Production rate (or transfer screw speed) is aligned in the same direction as motor loads, both consistencies, power split, long fibre content and freeness. For instance, if production rate decreases all the above mentioned outputs will tend do so as well. On the other hand, total specific energy and both refining intensities will tend to move in the opposite direction.

Cascade effects due to changing production rate

If production rate is reduced, both the primary and the secondary motor loads will decrease. Depending on the magnitude of this reduction, the total specific energy in each refiner will either increase or decrease. In our specific case, a decrease in production rate outweighs the drop in motor load (resulting from the throughput reduction), and therefore total specific energy increases. In the meantime, both outlet consistencies drop since: (a) there is less fibre mass entering the refiner and (b) less steam is produced at lower motor loads. Lower consistency in turn involves a smaller

residence time, and thus a more intense operation. In terms of quality, freeness and long fibre content decrease since both the specific energy and the refining intensity increase.

5.3.2. Effect of primary hydraulic pressure

The primary hydraulic pressure is aligned in the same direction as the primary motor load, the consistency in the primary refiner, total specific energy, power split and long fibre content. On the other hand, refining intensities and freeness will tend to move in the opposite direction.

Cascade effects due to changing the primary hydraulic pressure

If the hydraulic pressure to the primary refiner is reduced, the primary motor load decreases. As a result, the total specific energy decreases. In the meantime, both outlet consistencies drop accordingly as less steam is produced. This in turn results in smaller residence times, and therefore a more intense operation in both refiners. The effect of operating at higher intensity prevails over the reduction in total specific energy, and therefore the long fibre content decreases. On the other hand, freeness seems to be more affected by the reduction in total specific energy, and thus its value increases.

5.3.3. Effect of primary dilution flowrate

The primary dilution flowrate is only aligned in the same direction with refining intensities. Hence, primary motor load, both consistencies, total specific energy, power split and both quality parameters will tend to move in the opposite direction.

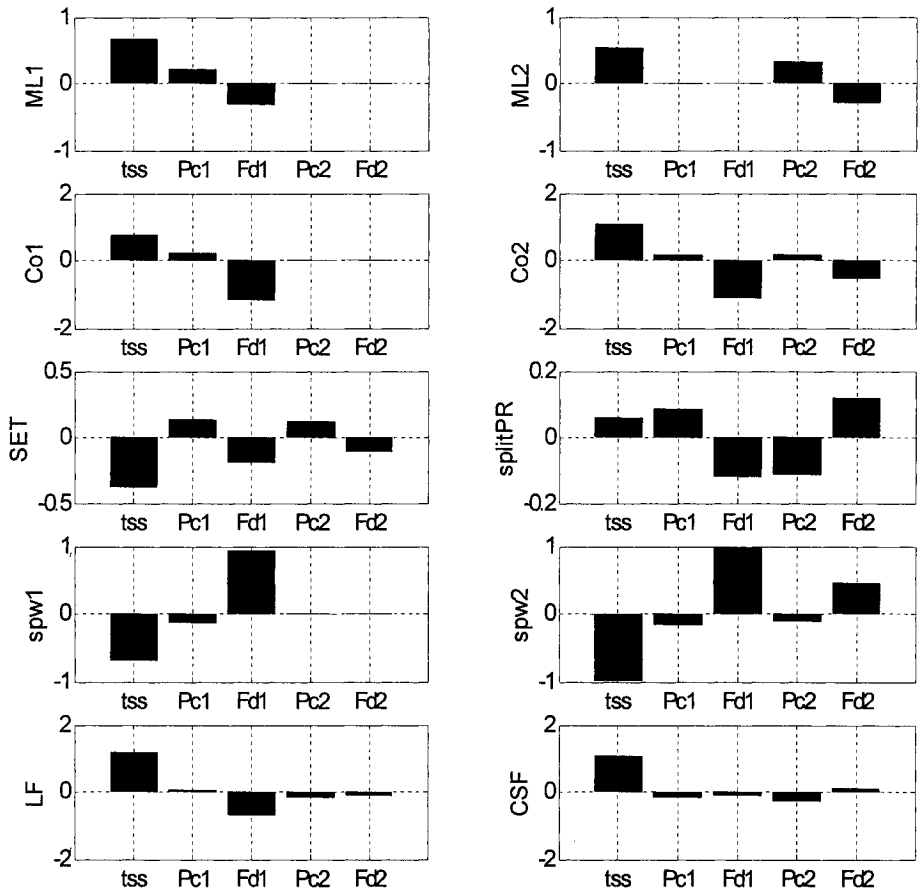

Results given in terms of relative gains with respect to a given initial condition (% output change / % input change).

Figure 5.6. Directionality of manipulated inputs.

Cascade effects due to changing the primary dilution flowrate

If the dilution flowrate to the primary refiner is increased, the primary motor load decreases. As a result, total specific energy decreases. In the meantime, both outlet

consistencies drop due to higher dilution and less steam produced. This of course involves a more intense operation in both refiners. Finally, the effect of refining intensity prevails over the reduction in specific energy, and therefore both freeness and long fibre content decrease.

5.3.4. Effect of secondary hydraulic pressure

The secondary hydraulic pressure is aligned in the same direction as secondary motor load, the consistency in the secondary refiner, and total specific energy. Conversely, power split, secondary refining intensity and both quality parameters will tend to move in the opposite direction.

Cascade effects due to changing the secondary hydraulic pressure

If the hydraulic pressure to the secondary refiner is reduced, the secondary motor load decreases along with total specific energy. In the meantime, the secondary consistency drops accordingly as less steam is produced at a lower secondary motor load. Evidently, this entails a more intense operation. Finally, both freeness and long fibre content increase since the effect of operating at lower specific energy outweighs the higher intensity operation in the secondary refiner.

5.3.5. Effect of secondary dilution flowrate

The secondary dilution flowrate is aligned in the same direction as power split, the secondary refining intensity and freeness. On the other hand, the secondary motor load, the corresponding consistency, total specific energy, and long fibre content will tend to move in the opposite direction.

Cascade effects due to changing the secondary dilution flowrate

If the dilution flowrate to the secondary refiner is decreased, the secondary motor load increases along with total specific energy. In the meantime, the secondary consistency grows given that more steam is produced and less water is entered in the refiner. In terms of quality, freeness again seems to be more affected by the increase in specific energy than by the reduction in refining intensity, and thus its value decreases. In contrast, long fibre content seems to respond more to refining intensity changes, and thus its value increases.

5.3.6. Effect of plate age on process gains

Assuming both refiners start to operate simultaneously, plate age is aligned in the same direction as both refining intensities, and power split (Figure 5.7). This means that as plates wear the operation becomes increasingly intense. On the other hand, plate age reduces the attainable total specific energy.

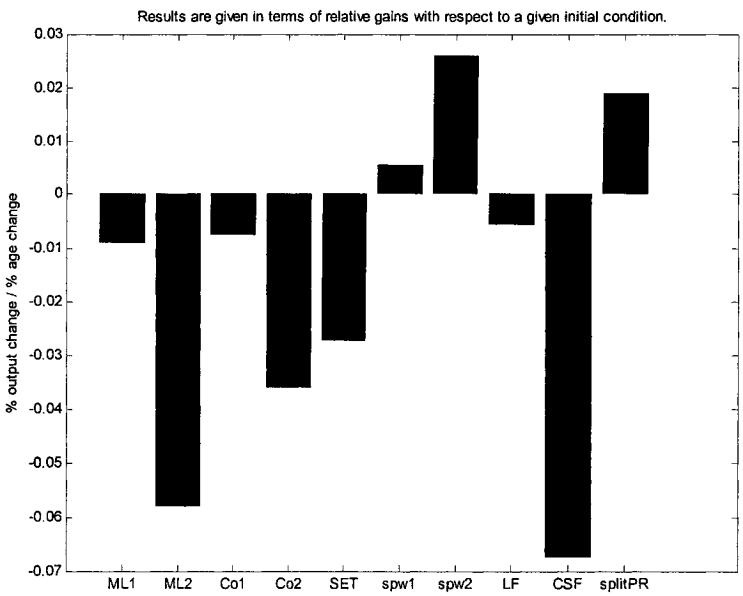

Figure 5.7. Effect of plate age on process outputs.

5.4. Illustrating directionality

The TMP-refining process is a highly interactive system (Roche et al., 1996; Lama et al., 2004). Understanding these interactions is crucial as they will affect the control performance of the refining plant. The schematic shown in Figure 5.8 is a result of exhaustive model simulations and summarizes, in a qualitative manner, the direction and cascade effect of each external disturbance and manipulated variable upon the entire refining operation and pulp quality. It is clear that interactions affect the operation in more than one direction, and therefore pulp quality is ultimately a function of the control structure imposed on the plant and the magnitude of the associated control action.

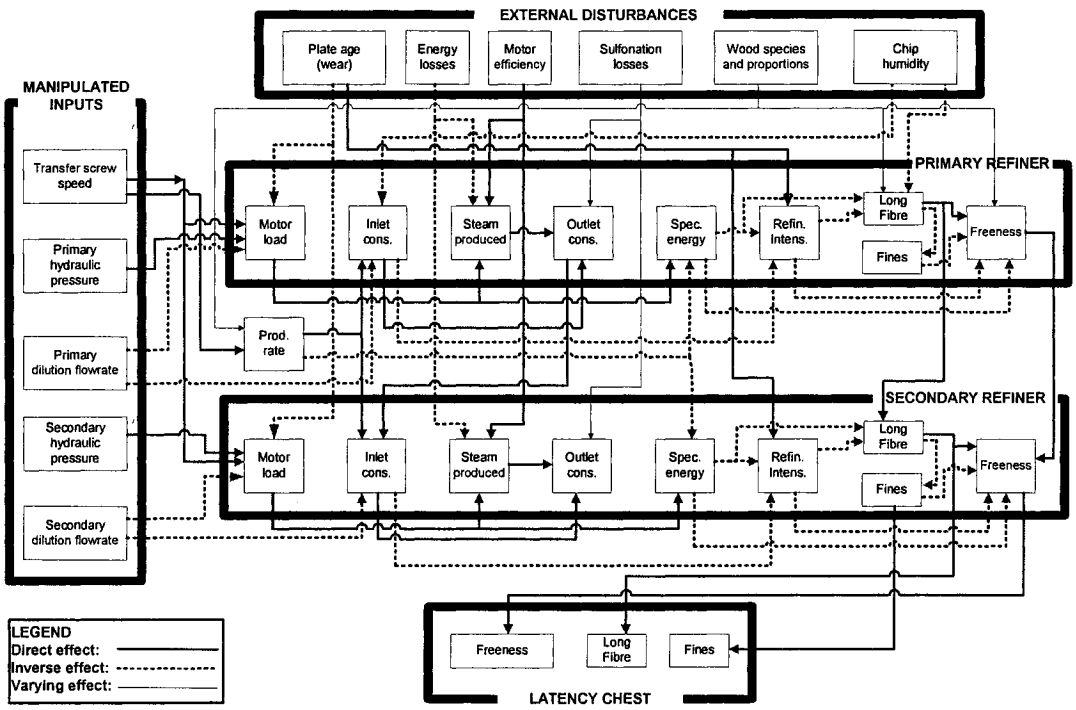

Figure 5.8. Directionality of internal interactions

5.5. Conclusions

In this chapter, a model has been used to elucidate the directionality of the internal interactions affecting TMP refining. This information is useful for proposing optimal ways to operate chip refiners as plates wear, as it will be shown in CHAPTER 6.

We can conclude that for given conditions of plate age, dilution and production rate, the highest values of long fibre content and freeness are attained at high power split ratios and low (total) specific energy levels. This is most likely a result of charging less energy to the secondary refiner.

According to the results depicted in Figure 5.7, as plates get older refiners cannot keep applying the same amount of energy to the pulp, especially in the secondary refiner since in our case power split increases with plate age. In addition, Figure 5.7 also indicates that plate wear entails higher intensity conditions in both refiners. Hence, the quality window shifts towards either lower fibre contents or lower freeness depending on the conditions of the plates in each refiner and the attainable total specific energy.

As to wood moisture and dilution conditions, they predominantly move the quality window towards lower long fibre contents. All these observations are synthesized in Figure 5.9.

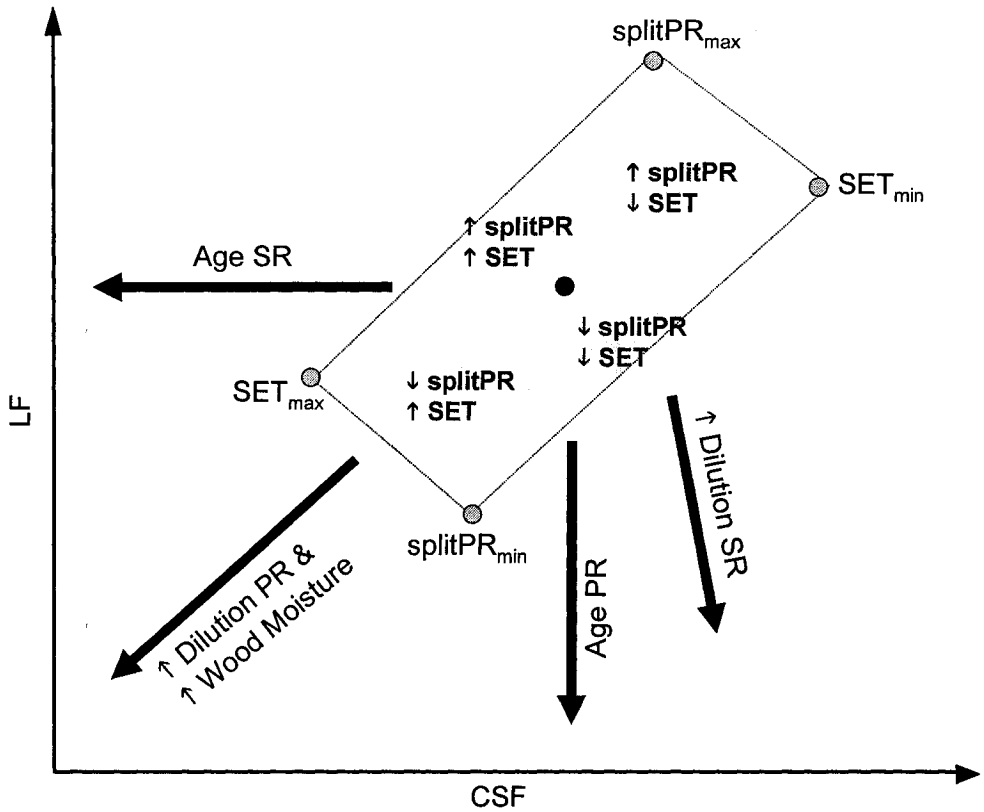

Arrows indicate direction of change of the pulp quality window. The dot in the center of the window represents a nominal operating point at a given age, production rate and dilution conditions. (PR: Primary refiner; SR: Secondary refiner)

Figure 5.9. Effect of refining conditions on pulp quality.

CHAPTER 6: EFFECT OF REFINER PLATE AGE ON THE OPTIMAL OPERATION OF TMP REFINERS

"Nature uses as little as possible of anything."
Johannes Kepler (1571-1630)

6.1. Introduction

The use of steam in TMP processes involves the application of large amounts of energy. In fact, the amount of energy needed in refining represents about 70-75% of the total energy requirements of a modern Canadian integrated newsprint mill (Francis et al., 2002). Hence, any effort to minimize the energy consumption in TMP refining while constraining the quality of the pulp within acceptable limits should translate into a better economic performance of the entire newsprint process.

The physical phenomena underlying the refining process are very complex, and thus uncertain in many respects. Indeed, the varying composition of the wood matter, the level of uncertainty in process measurements, the presence of multiple physical phases, and the highly interactive nature of the process - as shown in CHAPTER 5 - makes a purely mechanistic model-based optimization an unrealistic task. This is why early work on optimization of TMP refiners made use of both empirical and first principle models. Strand and co-workers (Strand and Edwards, 1983; Strand and Hartler, 1985; Strand et al., 1991) used both mechanistic and factorial models to optimize the operation of different types of refiners. Cluett et al. (Cluett et al., 1995) presented an approach to empirical optimization –pulp strength maximization- based on factorial experimental design methods. Broderick et al. (Broderick et al., 1995) proposed the

application of genetic algorithms to fuzzy models to investigate different operating strategies in high-yield chemi-mechanical pulping. Miles and coworkers (Miles, 1990; Miles and May, 1990; Miles et al., 1991; Stationwala et al., 1993; Alami et al., 1997) investigated the relationship between refining intensity on pulp quality in the context of reducing energy consumption. Qian et al. (Qian et al., 1997) used fuzzy relational models to study the optimal operation of an industrial two stage refining process.

Most of the recent work on optimization of TMP processes is focused on using hierarchical model-based control to improve the efficiency of the operation and the quality of the pulp. Strand et al. (Strand et al., 2000) used off-line multivariate analysis, modular simulation, pulp quality soft-sensors and multivariable predictive control to minimize energy consumption, reduce pulp quality variability and increase long fibre content at a given freeness. More recently, Sidhu et al. (Sidhu et al., 2004; Sidhu et al., 2005) proposed a two-level control strategy based on empirical linear models and model predictive range control with a global optimizer on top to take care of the interactions between control layers.

One major aspect yet to be directly addressed is the long-term effect of plate age on the optimal operation of TMP refiners. Indeed, the gains between the operating targets and the manipulated inputs change over time, i.e. as plates wear (Strand and Hartler, 1985). In addition, the intensity of refining increases with older plates thereby reducing freeness and long fibre content (McQueen, 1995; Roche et al., 1996) (see also Figure 5.7, p.93). As for wood quality, major drifts in chip moisture and density cause changes in specific energy and refining consistency during defiberization which in turn leads to impaired pulp strength and freeness (Sundholm, 2000). This chapter presents a model-based optimization approach to operate TMP refiners in the face of plate wear and seasonal changes in wood quality. Specifically, the focus is to minimize energy consumption while keeping pulp quality under constraints. Finally, the sensitivity of the optimal operation to the most critical process constraints is also underlined.

6.2. Formulation of the optimization problem

The operating policy of any TMP-Refining plant must satisfy constraints on pulp quality, in particular, long fibre content (*LF*) and freeness (*CSF*) as these two properties affect the strength of the pulp, and ultimately the runnability of the paper machine. Evidently, the operation is constrained in terms of the plant's throughput capacity (i.e. the transfer screw speed, *tss*), the hydraulic pressures applied in each refiner to transfer the energy from the plates into the pulp (Pc_1, Pc_2), and the corresponding dilution flowrates that limit the intensity at which this energy is applied (Fd_1, Fd_2). In addition, refining must be performed in such a way as to appropriately balance the power load (*splitPR*) between the two stages. Outlet consistencies (Co_1, Co_2) also need to be constrained in order to avoid either inefficient energy application (low consistencies) or excessive fibre cutting (high consistencies) (Strand, 1998). Finally, since TMP-Refining is an energy intensive process, we have assumed that an optimal operation is dictated by the amount of total specific energy (*SET*) applied to both refiners. Thus given, the problem presented here seeks to find the operation that minimizes –for a given wood quality- the consumption of total specific energy throughout the plate lifetime in both refiners.

The dynamics involved in the entire refining process -from the transfer screw feeder to the outlet of the latency chest- range from seconds to minutes, and thus are very small compared to plate wear dynamics (hours to days), and the seasonal drifts in wood quality (days to weeks). Hence, by using a relatively long optimization time step, we gain two major advantages: (a) the effect of long-term disturbances on the optimal operation becomes more perceptible, and (b) the computational effort is considerably smaller since the refining dynamics can be neglected. The last aspect is especially important considering the optimizer has to calculate optimal values for five decision variables (*tss*, Pc_1, Pc_2, Fd_1, Fd_2) along the entire plate lifetime which in practice normally lasts between 700 to 800 hours.

In this work, the length of each time step k was chosen to be 50 hours which is about 100 times the longest process time constant. The initial time t_i for both refiners is set equal to 50 hours since start-up dynamics are not considered in this work. The final time t_f is equal to 700 hrs which is in average an acceptable plate lifetime. The solution methodology consists of performing $N = (t_f - t_i)/50$ static optimizations using sequential quadratic programming at each time step k. As a result, the optimal profiles are obtained by piecewise concatenation of static optimal solutions. The values of outputs $y(k)$ used to check up on the objective function and the constraints are all averages for the interval k so as to allow for a robust solution searching. Mathematically, we can formulate the problem as follows:

$$\min_{u(k)\ldots u(N)} J = \overline{SET(k)}$$

$$\begin{aligned}
&s.t.\\
&y(k) = f(u(k)) \qquad \rightarrow \text{Nonlinear model}\\
&u(k) = \left[tss(k), Pc_1(k), Fd_1(k), Pc_2(k), Fd_2(k)\right]\\
&u_{lower} \le u(k) \le u_{upper}\\
&y_{lower} \le \left[\overline{ML_1(k)}, \overline{Co_1(k)}, \overline{Co_2(k)}, \overline{splitPR(k)}, \overline{LF(k)}, \overline{CSF(k)}\right] \le y_{upper}
\end{aligned} \tag{6.1}$$

Note: the symbol $\bar{}$ denotes average values for interval k.

6.3. Optimal operating policies

6.3.1. Base Case: Optimal operation during winter

The corresponding wood moisture is about 44% and the specific gravity of the major wood component in the feed is 423 kg/m^3. Process constraints are the same given in Table 1.1. Optimal operation for the above conditions is illustrated in Figure 6.1.

During the first 200 hours, the energy share (power split) in the primary refiner increases progressively since the optimal solution at constant throughput involves the minimization of both motor loads, especially in the secondary refiner. Accordingly, the primary motor load lies on its lower constraint throughout the entire optimal operation. Once the power split hits its upper bound, dilution flowrates move very little and the two hydraulic pressures increase so as to avoid reductions in motor loads and pulp quality because of plate wear.

The trajectories shown in Figure 6.1 also indicate that optimal operation applies as much dilution as possible to the first-stage while it tends to minimize dilution to the secondary refiner as plates wear. In other words, in order to minimize the total specific energy, the primary refiner must be operated at high intensity levels (i.e. at high dilution) followed by a low-intensity (i.e. low dilution) secondary stage. This operating strategy has also been reported by Miles and coworkers (Miles et al., 1991; Alami et al., 1997; Stationwala et al., 1993).

For a given level of total specific energy, increasing refining intensity normally results in lower long fibre content and sometimes lower freeness (Miles et al., 1991; Stationwala et al., 1993; Alami et al., 1997; Strand, 1998). Since the increase in refining intensity due to plate wear is inherently unavoidable (see Figure 5.7, p.93), freeness and long fibre content start dropping so long as the total specific energy is held constant (which is the case from $t = 200$ hrs onward). Incidentally, this last behaviour is confirmed by previous work on the effect of plate age upon pulp quality (Strand, 1989; Qian et al., 1997).

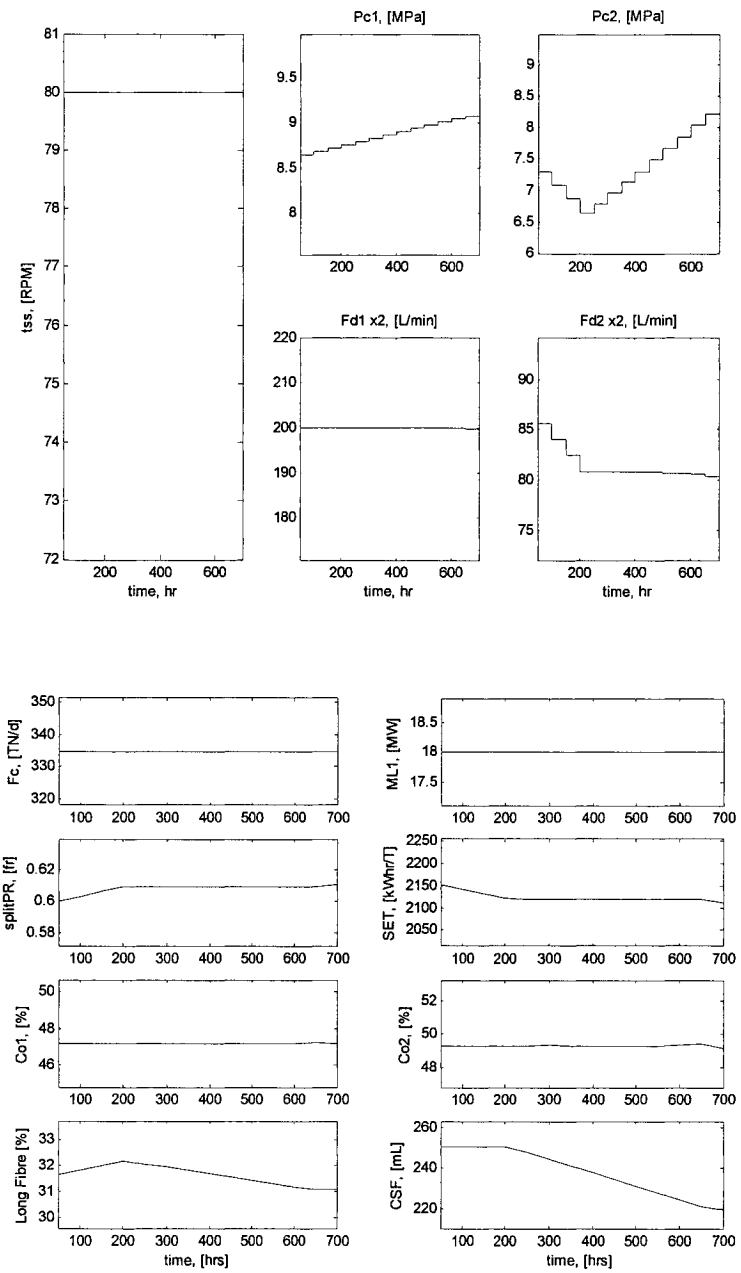

Figure 6.1. Optimal operation: Base Case.

6.3.2. Case 1: Effect of seasonal wood moisture changes

The optimal operation during winter (base case, moisture = 44%) was compared with that of summer (moisture = 41%). During this time of the year, wood chips have less water content due to –among other handling factors- the higher ambient temperatures. The seasonal drift simulated by the optimizer is shown in Figure 6.2.

At low moisture levels, the optimizer starts applying a higher dilution flowrate and hydraulic pressure to the secondary refiner so as to avoid violating pulp quality constraints, particularly that of long fibre content which is directly affected by moisture. Unfortunately, this also involves an increase in the initial total specific energy due to the significant initial pressure in the secondary refiner.

Because plate age has a reducing effect on long fibre content and motor load, the operation does not need to stay at high intensity conditions, and so the optimizer progressively –and carefully- decreases the secondary dilution flowrate provided the long fibre content remains within bounds. Since the objective is to minimize the total energy consumption, the optimal rates at which dilution and pressure change are such that they do not completely counteract the effect of plate age on the secondary motor load. As a result, the energy share in the secondary refiner gradually decreases along with the total specific energy. Towards the end of the horizon, the minimal total specific energy is almost the same for both moisture conditions. In comparison, for a given freeness (see $t \sim 380$ hrs, Figure 6.2) the operation is capable of saving more energy when moisture conditions are higher.

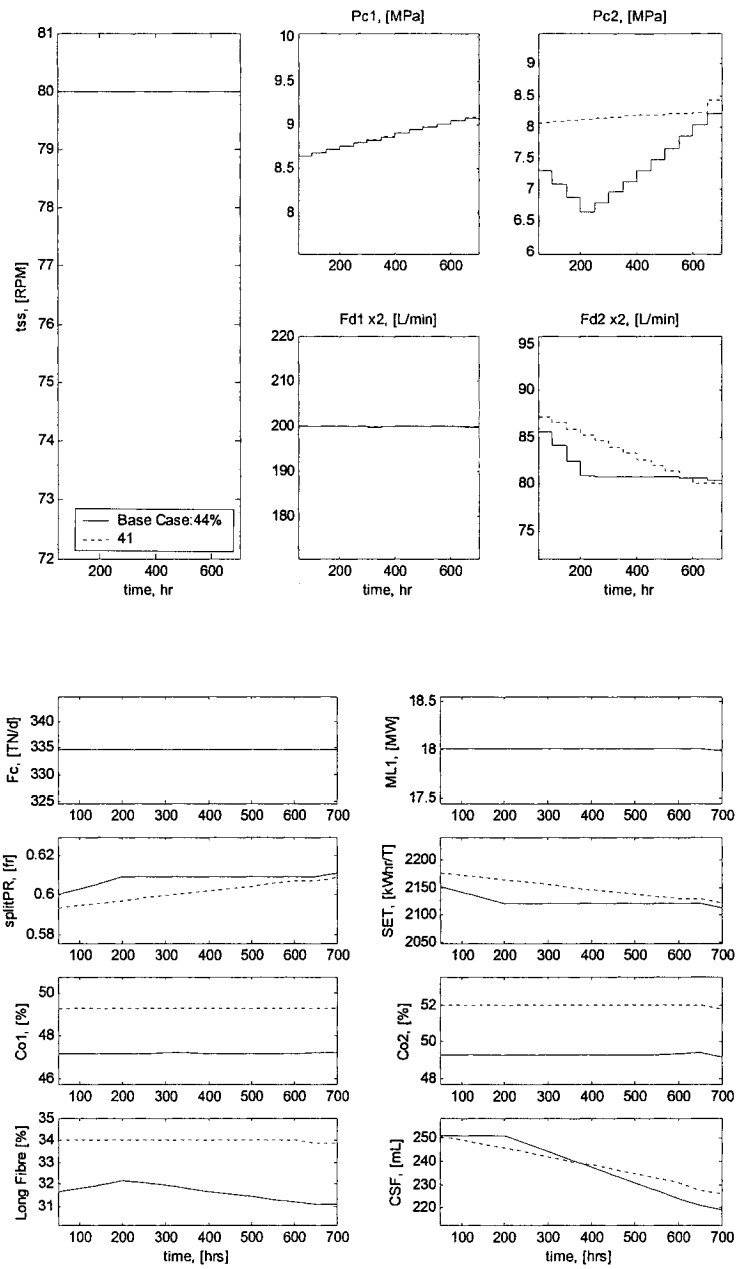

Figure 6.2. Optimal operation: Effect of seasonal wood moisture changes.

6.3.3. Case 2: Effect of major drifts in wood density

A major drift in wood density can profoundly affect motor load, specific energy and pulp quality. In Figure 6.3, two different basic density values of the major wood component in the feed are considered. Unlike moisture, a drift in wood density directly affects production rate, and thus it influences in more ways the refining operation.

At high wood density, in order to minimize the initial energy consumption the optimizer (1) starts applying high dilution flowrates and hydraulic pressures to the secondary refining stage, (2) keeps the transfer screw speed at its maximum, and (3) specifies low hydraulic pressures to the primary refiner. In this regard, it is apparent from the graph that when the wood is less dense more hydraulic pressure is needed in the primary refiner and less in the secondary one, at least at first. During the first 400 hours and at high density conditions, the optimizer decreases dilution and hydraulic pressure in the secondary stage. This results in a gradually lower energy share in the secondary refiner, and consequently a lower total specific energy as plates wear. Freeness remains almost constant during this period since the effect of specific energy and that of plate wear cancel each other out. On the other hand, long fibre content increases its value because both dilution flowrates and the total specific energy drop significantly thereby outweighing the effect of plate wear.

The remaining 200-300 hours involve lower secondary hydraulic pressures to refine wood of higher density. Furthermore, during this time the effect of plate wear on quality is obvious as both freeness and long fibre decrease regardless of the otherwise steady operating conditions. Finally, results indicate that at constant freeness levels (see first 200 hrs in Figure 6.3) high density wood favours energy savings at relatively higher intensity levels in the secondary stage. In addition, optimal refining of high density wood yields pulp of higher attainable freeness and long fibre content especially when plates get old (see t = 300 hrs onward). Some of these results, particularly those

involving the relationship between specific energy, long fibre, density and wood species are in agreement with several experimental studies (Sundholm, 2000).

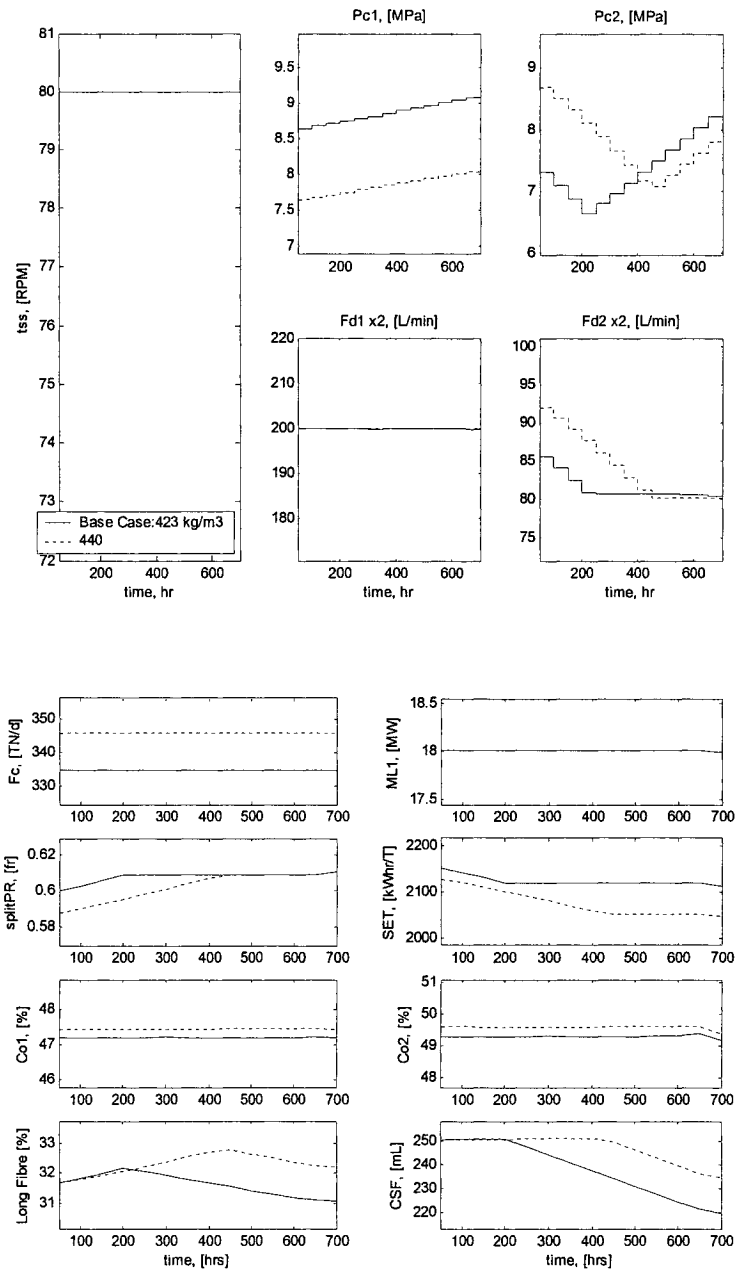

Figure 6.3. Optimal operation: Effect of changes in wood density.

6.3.4. Case 3: Effect of process constraints

In optimization, Lagrange multipliers represent the sensitivity of the objective function to changes in the inequality (or equality) constraints. In particular, our results yield non-null –i.e. sensitive- Lagrange multipliers only for the lower constraint on the primary motor load and the upper constraint on freeness.

Sensitivity to changes in primary motor load's lower constraint

The primary motor load (ML_1) is one of the most critical operating targets in TMP refining because it specifies –along with power split- the attainable total specific energy. In addition to the base case, Figure 6.4 shows two different lower constraints for primary motor load: "High" and "Low". Aside the first 200 hrs, the "High" bound requires more hydraulic pressures in both refiners and if set too high, it could entail violation of the power split's upper constraint when the plates get too old. For a given freeness (see first and last 100 hrs, i.e. new and old plates), tightening the motor load constraints ("High" bound) involves less energy savings but higher long fibre content – along the entire plate's lifetime- since refining intensity at the secondary stage is relatively lower. On the other hand, optimal operation with relaxed motor load constraints ("Low" bound) entails not only energy savings but also higher attainable values of freeness especially, when plates start getting old.

Sensitivity to changes in objective freeness' upper constraint

Most TMP facilities rely –almost solely- on the measurement of freeness (CSF) as the basis for quality control. In Figure 6.5, different upper bounds for freeness are considered. From the graph, it is clear that changing freeness' upper objective only affects the operation of the secondary refiner. Thus, initially a tighter freeness window (bound @ 240 mL) results in higher hydraulic pressures and dilution flowrates.

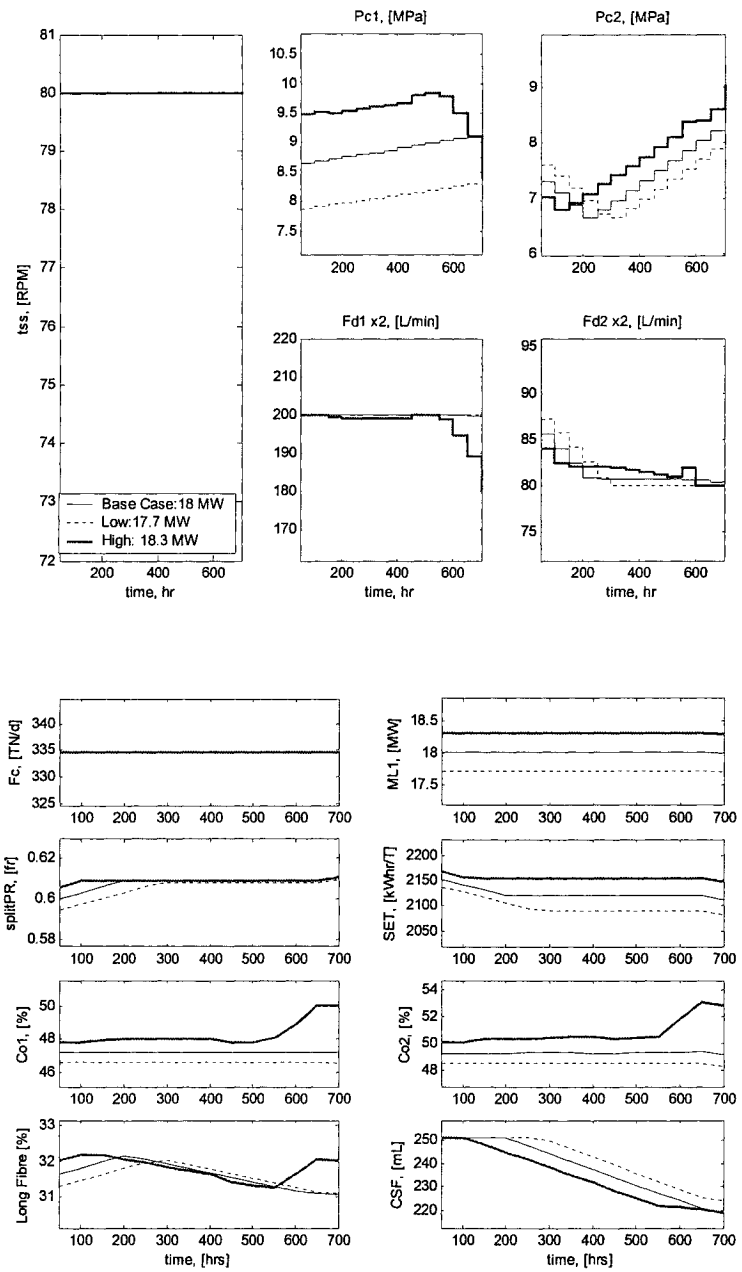

Figure 6.4. Optimal operation: Effect of different ML_1 lower constraints.

During the first 350 hours, this operation leads to a gradually lower total specific energy consumption as well as lower energy share in the secondary refiner. The profiles described by the long fibre content depend on the combined effect of dilution, plate wear, specific energy, power split and the freeness' upper bound. The last 350 hours depict the same optimal operation regardless of where the upper bound is placed. Finally, results indicate that a more relaxed freeness window (bound @ 260 mL) requires less specific energy while at the same time yields higher long fibre contents, particularly when plates are relatively new.

6.4. Discussions

For simplicity's sake it has been assumed that both refining stages start operation at the same time and under the same conditions of plate wear. However, it must be noted that the structure of the model allows for simulating different plate age conditions in each refiner.

Another major conceptual assumption in this work is that plate wear is equivalent to plate age. This is not rigorously true, and thus further research must be done to elucidate the actual relationship between these two variables if optimal control is to be implemented.

All the optimal operating policies here presented have in common that in order to minimize total specific energy the operation should decrease – as plates wear- the energy load in the secondary refiner. Furthermore, the primary refiner must be operated at high dilution flowrates – i.e. at high intensity levels - whereas the secondary refining stage must operate at relatively lower intensity conditions. This comes in agreement with previous experimental studies by Miles and coworkers (Miles et al., 1991). Additionally, since the objective is to minimize total specific energy, the transfer screw

speed –and thus, production rate- is unsurprisingly pushed as close as possible to its upper constraint.

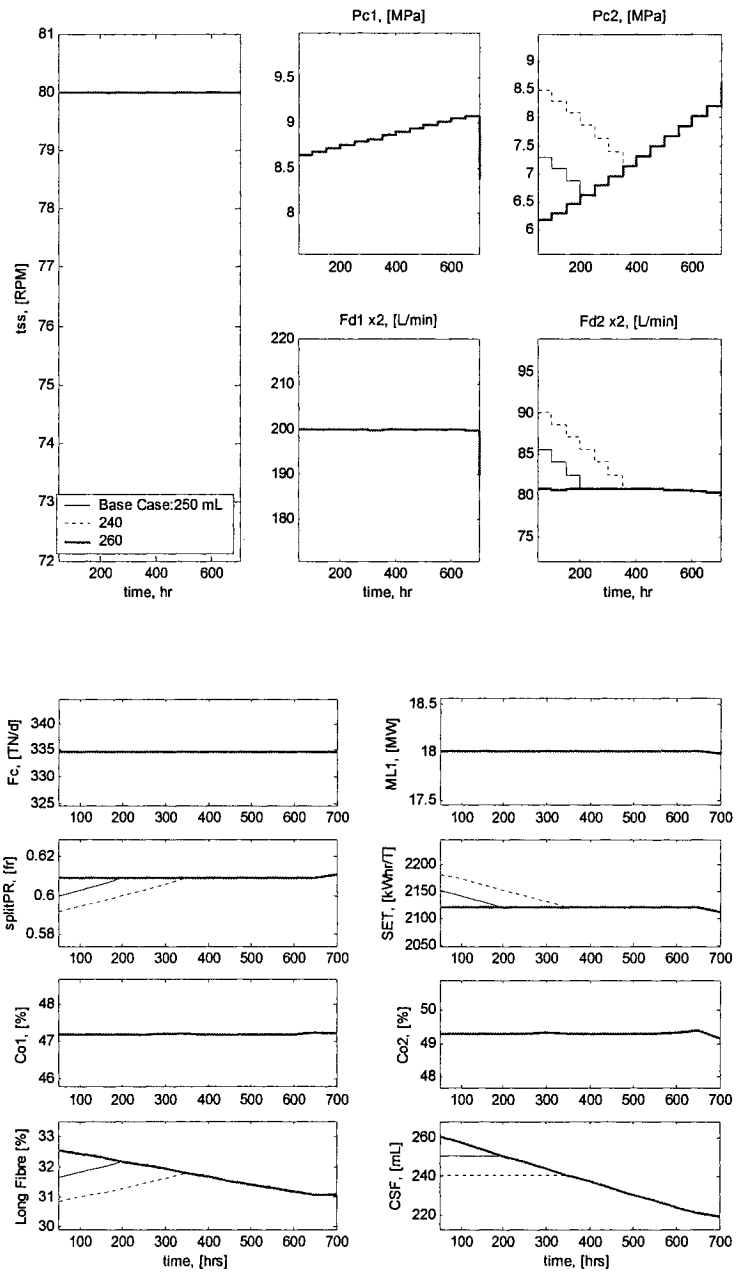

Figure 6.5. Optimal operation: Effect of different CSF upper constraints.

The level of moisture in the chips is regarded here as a seasonal attribute of wood quality. Accordingly, optimization results indicate that for the same freeness objective the operation saves more energy during the winter than during the summer but also yields pulp of lower long fibre content.

When wood is less dense and plates are relatively new, more hydraulic pressures are required in the primary refiner and less in the secondary one, provided primary dilution and screw speed conditions remain the same. On the other hand, it was found that at constant freeness, high density wood favours energy savings at relatively higher intensity levels in the secondary stage. Furthermore, as plates get older optimal refining of high-density wood yields pulp of higher attainable freeness and long fibre content. The validity of these optimization results is supported by previous experimental work reported elsewhere.

It was found in all simulations that total specific energy is highly sensitive to changes in the primary motor load's lower constraint and the freeness' upper constraint. For a given freeness, a more relaxed motor load window –from below- entails considerably less total energy consumption and higher secondary refining intensity than an operation with tighter bounds. Moreover, as plates get older a more relaxed motor load window allows for higher attainable values of freeness. On the other hand, if long fibre content wants to be maximized along the plate's lifetime a more tightened motor load window is required. As for the freeness' upper constraint, results indicate that a more relaxed freeness window –from above- involves more energy savings and higher long fibre contents, particularly when plates are relatively new.

6.5. Conclusions

This chapter has presented a model-based approach to optimize the operation of a two-stage TMP-Refining plant. This framework was used to elucidate the effect of major

drifts in wood quality and some process constraints on the optimal operation of TMP-Refiners. As formulated, the optimization problem takes into account the long-term effect of plate wear on refining to minimize total energy consumption while maintaining pulp quality, primary motor load, power split and refining consistencies within desired constraints. Using this approach, different sub-optimal scenarios can be considered. Indeed, searching for optimal operating points a bit away from the feasible boundaries will significantly improve the controllability characteristics of the operation as the actual constraints will not be violated. In practice, this can be achieved by setting tighter fictitious constraints (back-off) when solving the optimization problem. Given the inherent trade-off between optimality and controllability, it is clear that additional specific energy is involved in better controlling the process in the face of simultaneous and random short-term variations in wood quality. In this context, this optimization framework is used in CHAPTER 7 and CHAPTER 8 to determine inherent potential for energy reduction and variability attenuation under different scenarios of plate condition and back-off.

CHAPTER 7: DETECTING THE INHERENT POTENTIAL FOR ENERGY REDUCTION IN TMP-REFINING OPERATIONS

"Why does the eye see a thing more clearly in dreams than the imagination when awake?"
Leonardo Da Vinci (1452-1519)

7.1. Introduction

In this chapter, a methodology is proposed for the first time to determine the inherent potential of a TMP-refining plant as to reducing energy consumption. The methodology relies on routine data from operations, a steady state detection technique, and a model-based optimization. The optimization problem is solved using basically the same formulation given in CHAPTER 6 (section 6.2) only this time, the solution is an optimal operating point as opposed to an optimal profile. Indeed, unlike CHAPTER 6 the optimizations performed in the present chapter do not aim at characterizing the long-term effect of plate wear dynamics, but instead involve the calculation of an alternative (optimal) operating point with acceptable controllability properties (use of *back-offs*). This optimal point is compared to the current one to assess potential for energy reduction. Results indicate that this potential strongly depends on refiner plate conditions.

7.2. Methodology

The methodology is divided into two major steps: (a) extracting low-variability (LV) operating conditions, and (b) proposing alternative operating conditions for lower energy consumption.

7.2.1. Extracting LV operating conditions

The procedure for detecting LV operating conditions is depicted in Figure 7.1. It starts by detecting long steady state intervals (SSI), and then within each SSI, LV conditions that can be acceptably represented by the model.

7.2.1.1. Data collection

As mentioned in section 1.4, hourly average operating data for the entire TMP-refining process are collected over a year. The process variables involved in data collection are given in Table 7.1. Data for all process inputs are obtained from setpoints signals (.SP) whereas process outputs come from process variable signals (.PV). The longest time constant of the process fluctuates between 35 and 45 minutes (latency chest), while the fastest dynamics vary from fractions of a second to a few seconds (each refiner). Hence, it is clear that most of the high-frequency variability originated at the refiners will eventually be filtered out by passing through the latency chest. Furthermore, pulp quality out of the latency chest can only be sampled every 50 minutes, and thus averaging at a 1-hour rate was a limitation rather than a choice. On the other hand, this sampling rate permits tackling the remaining problem of low-frequency variability later in CHAPTER 8 (section 8.3.1) as well as capturing a wide range of seasonal and operating conditions, including the slow effect of plate aging.

7.2.1.2. Data pre-treatment and identification of steady state intervals (*SSI*)

Performed such as explained in section 1.4 (step 1) and section 1.4.1.

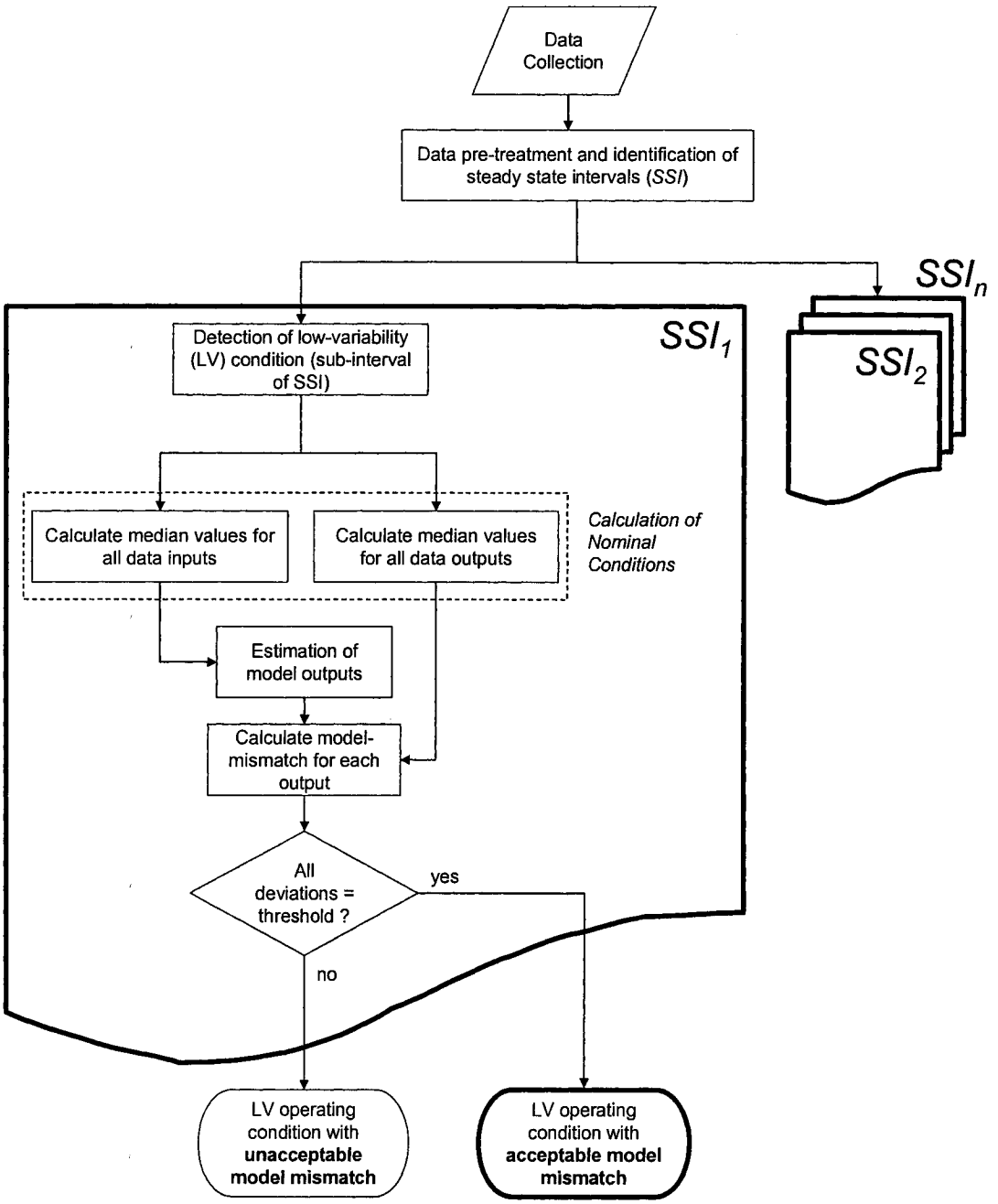

Figure 7.1. Procedure for extracting LV operating conditions.

Table 7.1. Variables involved in the extraction of LV conditions.

Variables	Unit operations				
	Primary ref.		Secondary ref.		Latency chest
	Input	Output	Input	Output	Output
Transfer screw speed	x				
Hydraulic pressure	x		x		
Dilution flowrate	x		x		
Wood furnish composition	x				
Plate age	x		x		
Humidity	x				
Motor load		x		x	
Refining consistency		x		x	
Long fibre content					x
Freeness					x
Total specific energy				x	

As mentioned in section 1.4.1, the primary motor load has been chosen to be the *key steady state indicator* as it substantially affects refining intensity, applied specific energy, and therefore pulp quality.

Since some of the detected intervals may be too short to be considered at steady state, a security filter is implemented in the algorithm so as to take into account only steady state intervals lasting 24 hours or more. Results yielded 38 SSI, ranging from 25 to 142 hours.

7.2.1.3. Detection of LV conditions

The SSI identified in section 7.2.1.2 represent long-term steady operating conditions lasting from 1 to almost 6 days. Since a too long SSI may not represent anymore the operation at a certain plate age, it is only reasonable to think of selecting a smaller interval within each SSI. Thus, a fixed-length moving-window (FLMW) is selected to search for LV conditions within each SSI. As in section 7.2.1.2, the (outlier-clean) primary motor load data is used to detect low-variability conditions for the entire refining operation. In particular, the FLMW searches for the sub-interval of smallest variability within each SSI. In order to neglect possible outliers, variability is here calculated as follows:

$$Variability = \frac{median\left(\left|x_j - median(x_{FLMW})\right|\right)}{median(x_{FLMW})} \tag{7.1}$$

where x_j is an element j of the (primary motor load) data set within FLMW, x_{FLMW}. The FLMW is set equal to 80% of the smallest SSI to facilitate moving freedom during the search. Since the smallest SSI lasts at least 24 hours then the length of each of the 38 FLMW's is 19 hours. Remark: The degree of variability around each FLMW depends on the minimum length of the SSI chosen by the user in section 7.2.1.2.

The *plate age operating space* is introduced in Figure 7.3 as a way to depict plate age conditions where LV is detected.

7.2.1.4. Calculation of nominal operating points

The median of each input and measured output is calculated for each LV condition (Figure 7.2). Again, the use of the median as opposed to the mean compensates for any outlier that may still exist within each LV condition. The nominal plate age – in both

refiners - is the one detected at the onset of each LV condition. Figure 7.2 also confirms the validity of selecting the primary motor load as a suitable steady state-LV indicator.

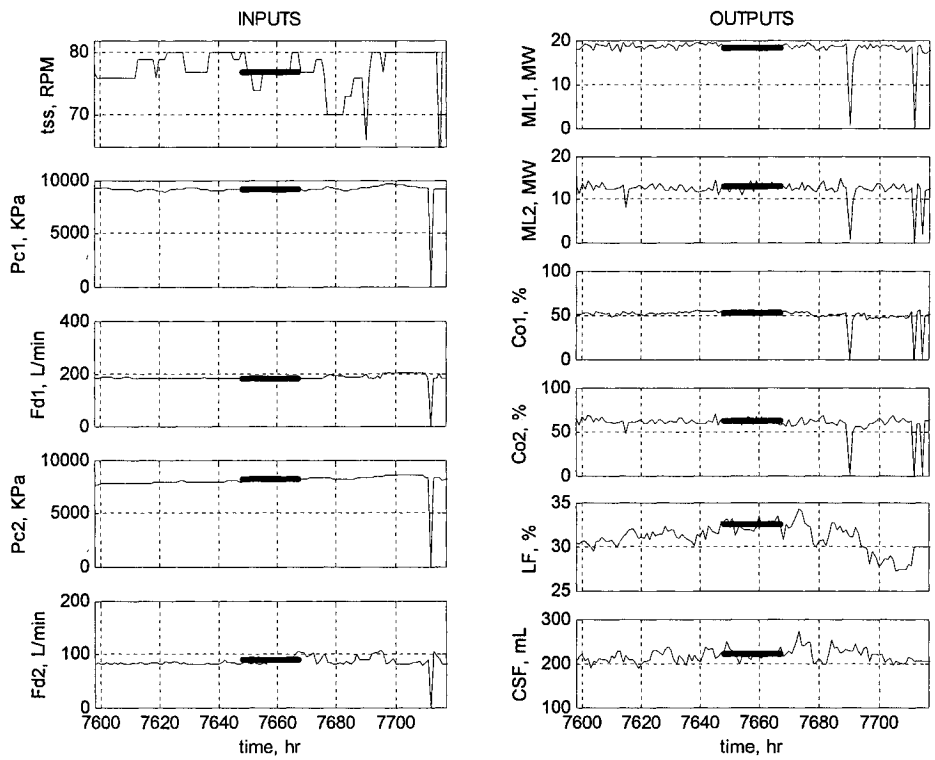

Thick line indicates LV sub-interval.

Figure 7.2. LV conditions. Plate age conditions: Primary = 119 hrs, Secondary = 119 hrs.

7.2.1.5. Estimation of model outputs for each LV condition

Process outputs are estimated by solving the TMP-refining model for the process inputs calculated in section 7.2.1.4.

7.2.1.6. Selection of LV conditions with acceptable model mismatch

For each LV condition, output estimations are compared to the corresponding median-based real outputs. If the model-mismatch (= | (estimate – real) | / real · 100%) is larger than a given threshold then the LV condition is not considered a valid operating point for further analysis. Thresholds are user-defined and set the accuracy in detecting LV conditions. A model-mismatch threshold of 8% is used for all process outputs that are physically measured i.e. primary and secondary motor loads, long fibre content and freeness. It is advisable to also consider seasonal characteristics. Seasonal conditions can be represented to some extent by the average moisture content in the wood. In this work, only wood moisture levels between 43 and 45% are considered.

As shown in Figure 7.3, results yielded 8 LV conditions with acceptable model-mismatch during the winter months. The corresponding model-mismatches for each of the measured outputs are given in Table 7.2.

Table 7.2. Model-mismatch. Wood moisture between 43%-45%

Variables	| (estimate – real) | / real · 100%		
	Minimum	Mean	Maximum
Primary motor load	0.9	**2.6**	6.0
Secondary motor load	0.08	**3.7**	7.9
Long fibre content	0.1	**3.0**	7.4
Freeness	1.0	**3.1**	7.4

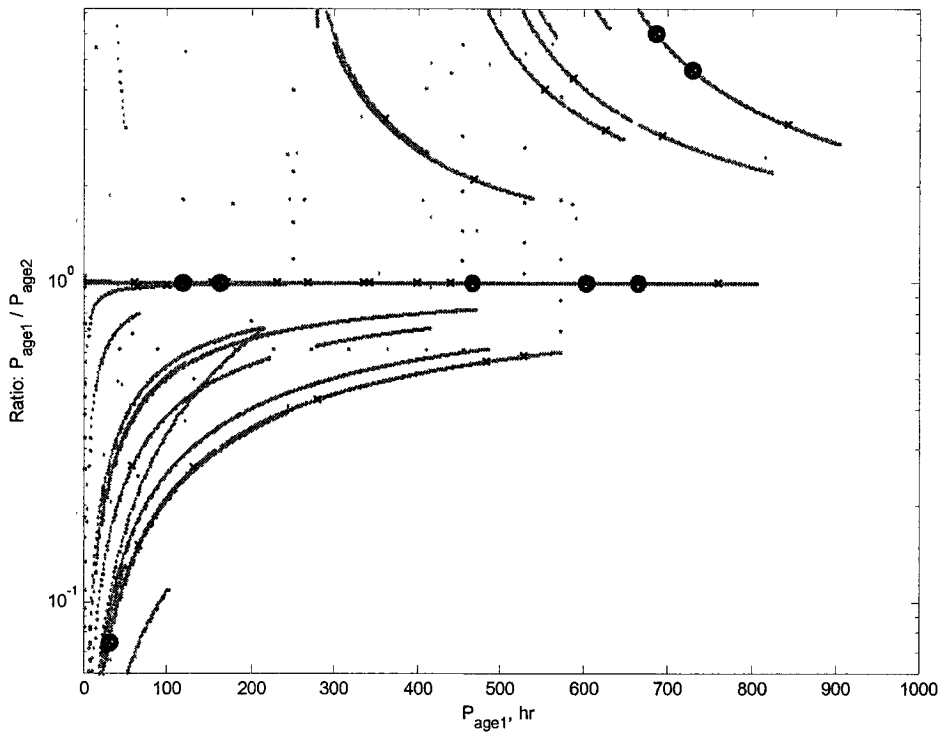

Curves represent plate age in both refiners for a year of operation. Detected LV conditions denoted by (x); Selected LV conditions (circles).

Figure 7.3. Plate age operating space.

7.2.2. Alternative operating conditions for lower energy consumption

Since TMP-Refining is an energy intensive process, the search for alternative operating conditions is determined by the *minimization of the total specific energy (SET)* applied to both refiners. Hence, in terms of objective function and process constraints the formulation of this optimization problem is identical to that shown in section 6.2 except this time the solution is not a profile, but instead an operating point corresponding to a single plate age condition.

7.2.2.1. Optimization

The TMP-refining model is used to perform optimizations around each of the LV conditions extracted in section 7.2.1.6. These conditions are divided by plate age into four scenarios:

(a) Both refiners operating with new plates (less than 400 hours)
(b) Both refiners operating with old plates (more than 400 hours)
(c) Primary refiner operating with new plates and secondary refiner with old plates
(d) Secondary refiner operating with new plates and primary refiner with old plates

Figure 7.3 and Table 7.3 show that there are two LV conditions that correspond to scenario (a), three to scenario (b), one to scenario (c), and two to scenario (d). In order to facilitate comparison, only one LV condition per plate age scenario is considered. Selection is based on model-mismatch. Accordingly, as shown in Table 7.3, LV conditions P119-S119, P602-S602, P31-S413 and P685-P114 are the ones considered for optimization and henceforth called *benchmark operating conditions*. Another interesting outcome from Table 7.3 is that overall variability (OV) tends to increase in the system as secondary plates get older. Overall variability (OV) is here expressed as the sum of the following process outputs' variability: ML_1, ML_2, Co_1, Co_2, *LF*, *CSF*, and *SET*. APPENDIX B shows the model estimates for *LF*, *CSF* and *SET*.

Because each of the benchmark operating conditions represents a nominal operation, no dynamics are included in the calculation of *alternative operating conditions*. In order to obtain several alternatives to each benchmark condition, the optimization is carried out under different scenarios of *back-off* and quality constraint relaxation. As mentioned in section 2.6.1, back-off accounts for the effect the expected disturbances on plant operation, i.e. it involves the reduction of the feasibility region by setting tighter "fictitious" constraints when solving the optimization problem. On the other hand, high

back-off's can also lead to unfeasible scenarios, and consequently some constraints need to be relaxed to restore feasibility. Here, pulp quality constraints were chosen to open up the solution space. APPENDIX C shows how back-off and constraint relaxation have been applied.

Table 7.3. LV conditions by plate age scenario

LV-condition ID(*)	Wood Moist. (%)	Plate age scenario	OV(**) Σv (%)	Model mismatch (%)			
				ML_1	ML_2	LF	CSF
P119-S119	**43.4**	a	**16.3**	1.43	7.32	**1.00**	**5.71**
P162-S162	44.0		23.3	2.01	0.08	4.48	7.38
P466-S446	44.7	b	32.2	5.95	7.85	7.39	1.73
P602-S602	**45.0**		**31.6**	0.93	3.87	**1.48**	**1.81**
P665-S665	45.0		29.9	2.75	4.19	5.69	1.42
P31-S413	**43.7**	c	**32.2**	1.59	1.34	**1.11**	**2.92**
P685-S114	**43.0**	d	**14.7**	1.85	2.11	**0.13**	**2.07**
P729-S157	43.0		14.5	4.35	2.97	3.10	1.71

(*) e.g. P119-S119 means: plate age equal to 119 hrs in both refiners.

(**) max Σv = 700 % (seven outputs are considered), min Σv = 0 %.

7.2.2.2. Final selection

Some feasible alternatives shown in Table- C.1 may be unacceptable if compared to their corresponding benchmarks. In order to be accepted as a valid nominal point for further analysis, each feasible alternative must be evaluated in terms of pulp quality specifications. Thus, with respect to a benchmark condition, an "ideal" alternative operation would yield pulp within specifications (such as those given in Table 1.1),

with higher long fibre content while applying less specific energy. Even in cases where the benchmark condition produces pulp outside the current quality constraints, several alternatives better than the benchmark can be obtained. It could also occur that the alternative operation produces pulp within specification and with more long fibre content than the benchmark operation even though more energy is required. This alternative may be "worth to consider" depending on how much additional energy is involved.

From the above, it is clear that any feasible alternative operation can be categorized qualitatively with respect to the corresponding benchmark. Accordingly, Figure 7.4 depicts the logics behind the qualitative classification of feasible alternatives. In this work, only feasible alternatives deemed as "ideal", "excellent", "very good", "good", or "satisfactory" are considered candidates.

Finally, for each plate age scenario, the ultimate alternative is selected firstly from the candidates that have the highest feasible back-off, and then from those with the lowest total specific energy. In case these criteria are fulfilled by two or more alternatives, the one with the highest long fibre content is chosen. Resulting alternative operating conditions - for each plate age scenario - are given in Table 7.4. An important observation is that the potential for reducing energy consumption increases as plates in the secondary refiner get older (P602-S602 and P31-S413). This potential is even more noticeable if the primary refiner operates with new plates (P31-S413) in which case achievable freeness and long fibre content increase dramatically. However, when both refiners have old plates (P602-S602) complying with quality specifications becomes harder, particularly in terms of freeness. Finally, when the secondary refiner operates with new plates (P119-S119 and P685-S114) and especially when both refiners have new plates (P119-S119), the current operation (benchmark) is very close to the optimal one (alternative).

Table 7.4. Results benchmark operation vs. alternative operation

Variables	Plate age category			
	P119-S119	P602-S602	P31-S413	P685-S114
H (%)	43.4	45.0	43.7	43.0
p_{HD} (%)	88.2	88.2	82.5	87.7
p_{LD} (%)	11.8	11.8	11.2	12.3
p_{HW} (%)	0.0	0.0	6.3	0.0
Quality (see Figure 7.4):	Alternative is "Ideal"	Alternative is "Satisfactory"	Alternative is "Ideal"	Alternative is "Excellent"
	Manipulated Inputs			
	Bench. / Altern.	Bench. / Altern.	Bench. / Altern.	Bench. / Altern.
tss (RPM)	77 / **78.2**	79.5 / **79.4**	75 / **78.2**	80 / **78.8**
Pc_1 (kPa)	9165 / **9316**	9970 / **8701**	9510 / **8858**	9420 / **9592**
Fd_1 (L/min)	182.5 / **187**	181.9 / **184.7**	186.3 / **187.6**	190 / **189.8**
Pc_2 (kPa)	8135 / **8033**	8600 / **8725**	9500 / **9152**	8138 / **7494**
Fd_2 (L/min)	88.4 / **83**	80.4 / **81.0**	83.5 / **83.7**	81.2 / **82.8**
	Process Outputs			
ML_1 (MW)	18.0 / **18.2**	18.6 / **18.1**	17.9 / **18.2**	18.2 / **18.1**
ML_2 (MW)	11.9 / **12.1**	11.7 / **11.7**	12.0 / **12.1**	12.4 / **11.9**
Co_1 (%)	51.3 / **50.6**	51.5 / **49.5**	49.6 / **50.1**	50.4 / **50.0**
Co_2 (%)	52.9 / **54.2**	54.5 / **52.2**	52.7 / **53.4**	55.1 / **53.0**
LF (%)	32.1 / **32.4**	31.4 / **30.7**	30.6 / **32.0**	32.2 / **32.0**
CSF (mL)	232.0 / **233.2**	213.8 / **215.2**	205.9 / **221.0**	235.0 / **237.9**
SET (kWh/TN)	2258 / **2252**	2215 / **2180**	2292 / **2223**	2227 / **2216**

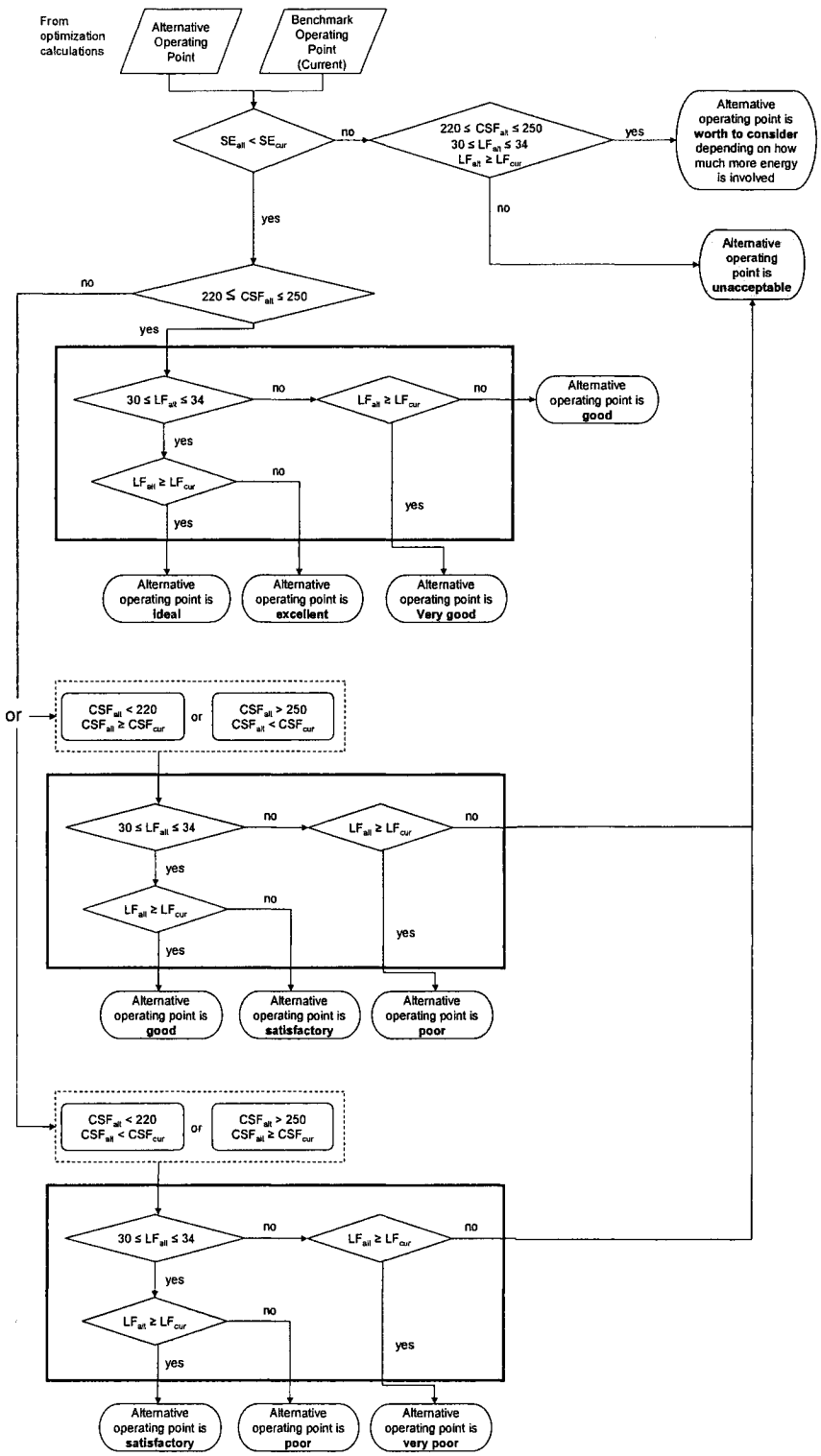

Figure 7.4. Qualitative classification of alternative operating points

7.3. Conclusions

A methodology has been proposed to first, calculate an alternative to the current nominal TMP-Refining operation, and then determine its inherent potential for energy reduction. In particular, the methodology detects operating windows of low variability (*benchmarks*) and then verifies – through model-based optimizations - whether an improved operating condition (*alternatives*) can be found. Process constraints and plate age are all integrated in the problem formulation. Optimization results indicate that having old plates - particularly in the secondary refiner - leads to unfeasible operation at high back-offs. On the other hand, the potential for energy reduction – compared to benchmark conditions - increases as plates get older in the secondary refiner. In the next chapter, we discuss the potential for variability attenuation around the alternative operating points obtained here.

CHAPTER 8: POTENTIAL FOR VARIABILITY ATTENUATION IN TMP-REFINING OPERATIONS

"The more you understand what is wrong with a figure, the more valuable that figure becomes."
Lord Kelvin (1824-1907)

8.1. Introduction

The quality of TMP depends on several factors whose multivariable effects are difficult to quantify. On the other hand, it is clear that any effort to reduce pulp quality variability in TMP-refining should translate into a better economic performance of the entire papermaking operation. This however is not an easy task given the complexity of the physical phenomena underlying wood refining processes. Indeed, the varying composition of wood matter, the degree of plate wear, the limits in design and nominal operating conditions, and the inherently interactive nature of the system all contribute to pulp quality variability. Most of these issues have to do with the process' inherent performance limitations, and thus they cannot be overcome by even the most advanced control system. In this chapter, we build on the results from CHAPTER 7 and propose a methodology to determine the inherent potential of a TMP-refining plant for variability attenuation. The methodology is independent of the control configuration and uses a linearized version of the model described in CHAPTER 3 and CHAPTER 4 to calculate necessary conditions for variability attenuation. Results are given for different plate age conditions and for all possible variations in wood moisture and wood density.

8.2. Linear model

As mentioned earlier, the inherently interactive nature of TMP-Refining processes is one of the most important sources of variability in pulp quality. The model described in CHAPTER 3 and CHAPTER 4 is here linearized around both the benchmark and the alternative conditions detected in CHAPTER 7. The two disturbances taken into consideration are wood moisture and wood density which, aside species proportions, are the only wood quality measurements available with certain frequency.

The linear model used throughout this chapter has the form given in equation (2.1) (p. 23), i.e. they are represented by transfer function matrices. The model reproduces the cascade effect of manipulated inputs and disturbances throughout the three unit operations of the TMP-refining process under consideration, namely the two refiners and the latency chest. The basic transfer function has a first-order-plus-delay form:

$$TF(s) = \frac{K}{\tau \cdot s + 1} \cdot e^{-\theta \cdot s} \tag{8.1}$$

where TF denotes the transfer function (e.g. an element in matrix G or G_d), K the process gain, τ the time constant, and θ the time delay. Gains represent a ratio between output and input deviations from steady state. They vary with nominal conditions and plate age and are generated by perturbing each model input one by one, and then recording the resulting changes in each of the output variables. In particular, 500 random perturbations are carried out per each model input. Perturbations are limited by the constraints given in Table 1.1. Final gains for each input-output pair are calculated by taking the median of all 500 recorded results.

Excluding the power split (*splitPR*) which is replaced by the secondary motor load (ML_2), all manipulated inputs u and process outputs y are the ones used in the formulation of the optimization problem (section 6.2, equation (6.1)).

As mentioned above, the two external disturbances considered are wood moisture (H) and wood density (ρ)[16]. Refiner dynamics are given in CHAPTER 3 (section 3.3.2), while those of the latency chest are simply a linear approximation of a perfectly mixed tank (see Table 8.1). Lack of information on the actual volume used for mixing precluded us from modeling the latency chest as a perfectly mixed tank followed by a plug flow region such as suggested by (Qian and Tessier, 2000).

In terms of scaling (see section 2.6.2), the maximum allowed deviations in each manipulated input and process output are extracted for both the benchmark and the alternative operating conditions. Results are shown in Table 8.2 and Table 8.3 for different plate age scenarios. In the case of outputs, deviations result from multiplying variability (in %) by the corresponding nominal value. For each output, variability (in %) is extracted from the LV conditions detected in CHAPTER 7 (section 7.2.1.6). Although this variability corresponds to benchmark operating conditions, here it is also applied to alternative conditions since the objective is to compare the potentials for variability attenuation. As for the inputs, deviations are calculated with respect to their corresponding constraints (see Table 1.1).

Proper scaling of both disturbances is critical because low-variability conditions strongly depend on wood quality variations. However, in most mill facilities wood disturbances are not measured with the necessary frequency to assess their true impact on refining. For the plant under study, it is only known that the expected daily deviation in wood moisture (ΔH_{max}) does not exceed 4 % its nominal value. The same

[16] Because of its large proportion in the wood furnish (> 80%), the wood density assumed here is that of Black Spruce, i.e. $\rho = \rho_{BS}$.

upper bound is assumed for the maximum expected deviation in wood density ($\Delta\rho_{max}$). In any case, these limits are only referential as both disturbances may vary in magnitude and direction during the 19 hour-operation (length of FLMW obtained in section 7.2.1.3). Hence, in this work disturbance scaling is carried out using different magnitudes of ΔH_{max} and $\Delta\rho_{max}$ so as to depict the potential for variability attenuation in terms of all possible variations in wood moisture and wood density.

Table 8.1. Linear dynamics of a TMP-Refining process*

Outputs after:	Manipulated input variables, u				
	tss	Pc_1	Fd_1	Pc_2	Fd_2
Prim. Refiner	$\frac{1}{5.04\cdot s+1}\cdot e^{-4\cdot s}$	$\frac{1}{4.39\cdot s+1}\cdot e^{-1.7\cdot s}$	$\frac{1}{2.36\cdot s+1}\cdot e^{-1\cdot s}$	-	-
Sec. Refiner		$e^{-8\cdot s}$		$\frac{1}{1.48\cdot s+1}\cdot e^{-1.7\cdot s}$	$\frac{1}{1.96\cdot s+1}\cdot e^{-1\cdot s}$
Latency Chest			$\frac{1}{\left(\frac{V}{Q_{out}}\right)\cdot s+1}\cdot e^{-5\cdot s}$		
	Load disturbances, d (H, ρ)				
Prim. Refiner			$\frac{1}{\tau_{ref1}\cdot s+1}\cdot e^{-4\cdot s}$		
Sec. Refiner			$\frac{1}{\tau_{ref1}\cdot s+1}\cdot e^{-4\cdot s}\cdot\frac{1}{\tau_{ref2}\cdot s+1}\cdot e^{-8\cdot s}$		
Latency Chest			$\frac{1}{\tau_{ref1}\cdot s+1}\cdot e^{-4\cdot s}\cdot\frac{1}{\tau_{ref2}\cdot s+1}\cdot e^{-8\cdot s}\cdot\frac{1}{\left(\frac{V}{Q_{out}}\right)\cdot s+1}\cdot e^{-5\cdot s}$		

* The residence time of the pulp inside the refiners (τ_{ref1} and τ_{ref2}) is calculated as proposed by Miles (Miles, 1991). Parameters V and Q_{out} are respectively, the useful volume and the outlet flowrate of the latency chest.

Table 8.2. Variable deviations used in model scaling – Benchmark case

Variables	Plate age scenario			
	P119-S119	P602-S602	P31-S413	P685-S114
	Manipulated Inputs, Δu_{max}			
tss (RPM)	3.0	0.5	5.0	0.0
Pc_1 (KPa)	1335	530	990	1080
Fd_1 (L/min)	2.50	1.88	6.25	10.0
Pc_2 (KPa)	1865	1400	500	1863
Fd_2 (L/min)	8.44	0.44	3.52	1.19
	Process Outputs, Δy_{max}			
ML_1 (MW)	0.27	0.41	0.21	0.30
ML_2 (MW)	0.37	1.17	0.83	0.38
Co_1 (%)	0.49	1.58	1.56	0.71
Co_2 (%)	2.18	2.99	1.46	0.73
LF (%)	0.40	0.61	0.99	0.70
CSF (mL)	4.23	12.7	17.5	7.34

Table 8.3. Variable deviations used in model scaling – Alternative case

Variables	Plate age scenario			
	P119-S119	P602-S602	P31-S413	P685-S114
	Manipulated Inputs, Δu_{max}			
tss (RPM)	1.8	0.6	1.8	1.2
Pc_1 (KPa)	1184	1799	1643	909
Fd_1 (L/min)	7.01	4.74	7.6	9.83
Pc_2 (KPa)	1967	1275	848	2494
Fd_2 (L/min)	3.03	1.02	3.68	2.80
	Process Outputs, Δy_{max}			
ML_1 (MW)	0.27	0.39	0.22	0.30
ML_2 (MW)	0.38	1.18	0.83	0.36
Co_1 (%)	0.48	1.52	1.57	0.71
Co_2 (%)	2.24	2.86	1.48	0.70
LF (%)	0.40	0.60	1.03	0.70
CSF (mL)	4.25	12.8	18.8	7.43

8.3. Minimum manipulated effort as a measure of variability attenuation

In this section, variability attenuation is regarded from the acceptable control perspective such as described in section 2.6.2.2 (offset $\|e\|_\infty \leq 1$), and therefore results presented here provide only necessary conditions for variability attenuation in TMP-Refining processes.

8.3.1. Potential for long-term variability attenuation

Steady state linear models (gain matrices) are used to determine the inherent potential for long-term variability attenuation.

8.3.1.1. Exact solution

The max-min optimization in equation (2.13) is solved for one disturbance direction d at a time. Accordingly, the following four disturbance directions are considered: $[1, 1]^T$, $[0, 1]^T$, $[1, 0]^T$ and $[-1, 1]^T$. It is clear that the worst disturbance direction d will be the one that yields the highest $\|U_{\min}\|_\infty$.

If indeed acceptable control is possible then one can say that there is potential for variability attenuation (PVA) for all conditions where $0 < \|U_{\min}\|_\infty < 1$. In other words, *this potential could be expressed as the input effort still available for variability attenuation* under certain conditions of ΔH_{max} and $\Delta\rho_{max}$:

$$PVA = \left[1 - \|U_{\min}\|_\infty\right]_{\Delta H_{\max}, \Delta\rho_{\max}} \tag{8.2}$$

From equation (8.2), if $\|U_{\min}\|_\infty \rightarrow 0$ the potential for variability attenuation increases, whereas cases where $\|U_{\min}\|_\infty > 1$ (PVA < 0) involve input constraint violation to keep $\|e\|_\infty = 1$, i.e. no further attenuation is possible. In particular, PVA = 1 (i.e. $\|U_{\min}\|_\infty = 0$) entails a self-regulated system where theoretically no control is needed to keep $\|e\|_\infty < 1$. However, given that only two disturbances are considered in this work, PVA = 1 has a less conservative connotation in practice, and thus represents conditions for which control may not be needed. This analysis is done for different plate age scenarios and for both benchmark and alternative conditions. Solutions are mapped into the *wood variability space* (ΔH_{max} vs. $\Delta\rho_{max}$) (see Figure 8.1 and Figure 8.2).

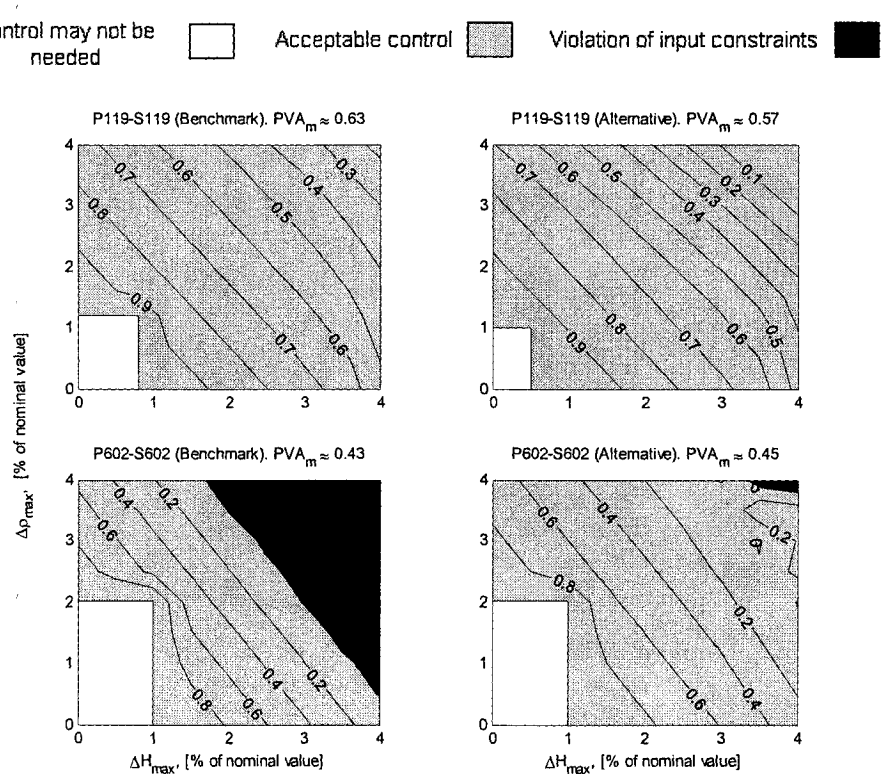

(PVA$_m$: mean of all 0<PVA's <1)

Figure 8.1. PVA (Steady state): Optimal solution. Scenario: Same plate age in both refiners.

When plates in both refiners have the same age, results indicate – for both benchmark and alternative conditions - that it is harder to attenuate high variations in wood moisture and wood density when plates are old (Figure 8.1). In addition, the space where control may not be needed extends to zones of higher variation in wood density when both refiners operate with old plates (up to $\Delta\rho_{max} = 2$ % for both the benchmark and the alternative case). On the other hand, Figure 8.2 shows that for different plate conditions in each refiner, variability attenuation is easier when there are new plates in the primary refiner and old plates in the secondary refiner. Furthermore, in this case the system can, theoretically, absorb more variations in wood moisture and wood density without control (up to 2 % for both the benchmark and the alternative case).

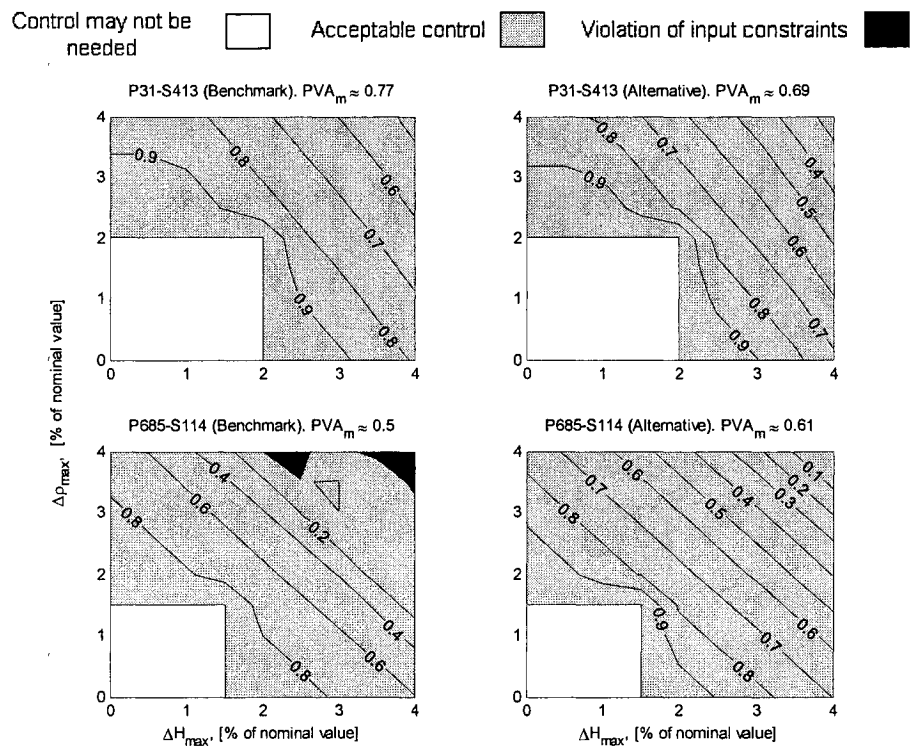

(PVA$_m$: mean of all 0<PVA's <1).

Figure 8.2. PVA (Steady state): Optimal solution. Scenario: Different plate age in each refiner.

As to whether there is an increase in the potential for variability attenuation by operating around alternative conditions, results show a contrasting difference especially in the case of refiners operating with old plates (bottom plots in Figure 8.1). Indeed, for this case operating around alternative conditions involves better control for almost any possible variation in wood moisture and density. Although not as remarkable, a similar improvement is obtained for high variations in wood moisture and density when the primary refiner has older plates than the secondary one (bottom plots in Figure 8.2).

8.3.1.2. Approximate solution

Results are plotted in Figure 8.3 and Figure 8.4.

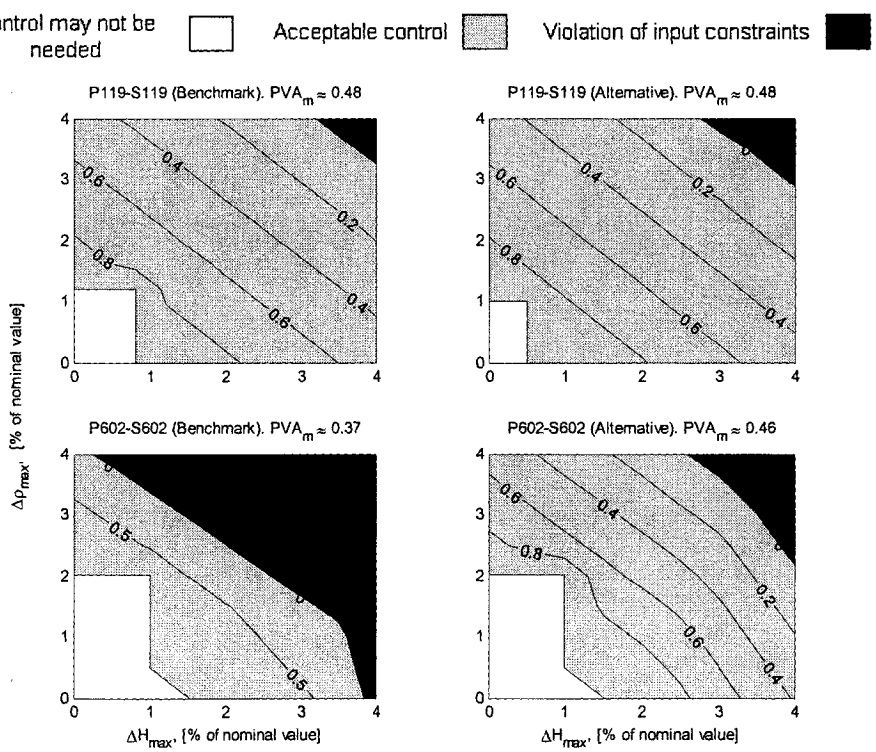

(PVA$_m$: mean of all 0<PVA's <1).

Figure 8.3. PVA (Steady state): Approximate solution. Scenario: Same plate age in both refiners.

It is clear that compared to optimal results, approximate ones tend to be more conservative, i.e. in general they show a lower potential for variability attenuation. This, in addition to the fact that solving equation (2.14) requires considerably less computational effort than that needed to solve equation (2.13), makes of the approximate method a more suitable – and conservative - tool for computing PVA as a function of frequency in section 8.3.2.

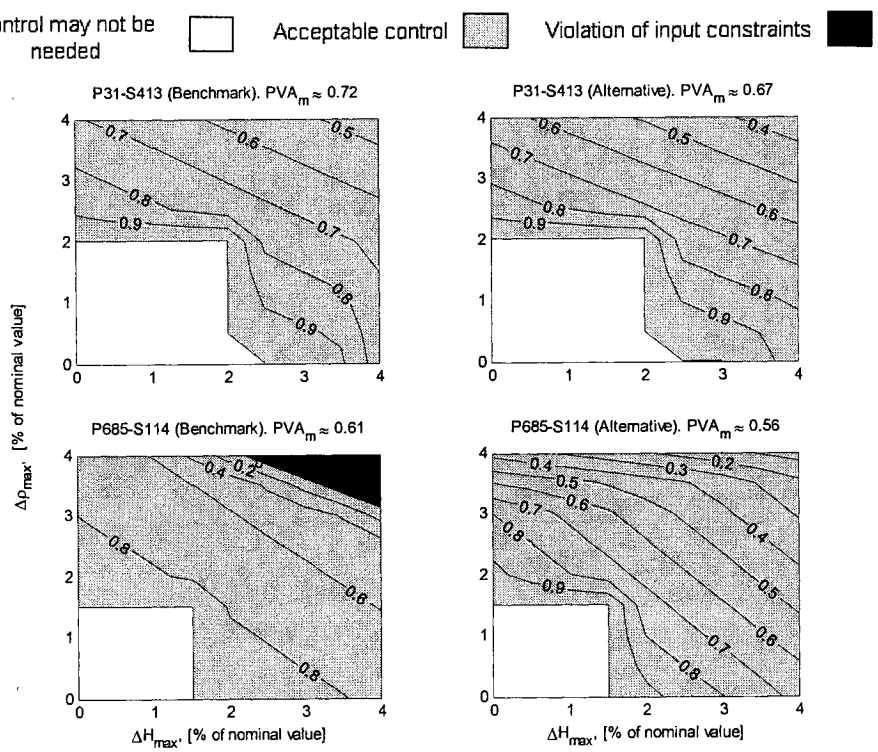

(PVA$_m$: mean of all 0<PVA's<1).

Figure 8.4. PVA (Steady state): Approximate solution. Scenario: Different plate age in each refiner.

8.3.1.3. Worst disturbance direction

Results in sections 8.3.1.1 and 8.3.1.2 correspond to the worst disturbance direction entering the system for different magnitudes of ΔH_{max} and $\Delta\rho_{max}$. Such a direction requires a large manipulated effort from the part of the system to keep the outputs under control ($\|e\|_\infty \leq 1$). Plots in Figure 8.5 are obtained by solving equation (2.13) for different plate age scenarios and the following specific disturbance directions: Same direction ($d = [1\ 1]^T$), opposite direction ($d = [1\ -1]^T$), only wood density ($d = [0\ 1]^T$), and only wood moisture ($d = [1\ 0]^T$).

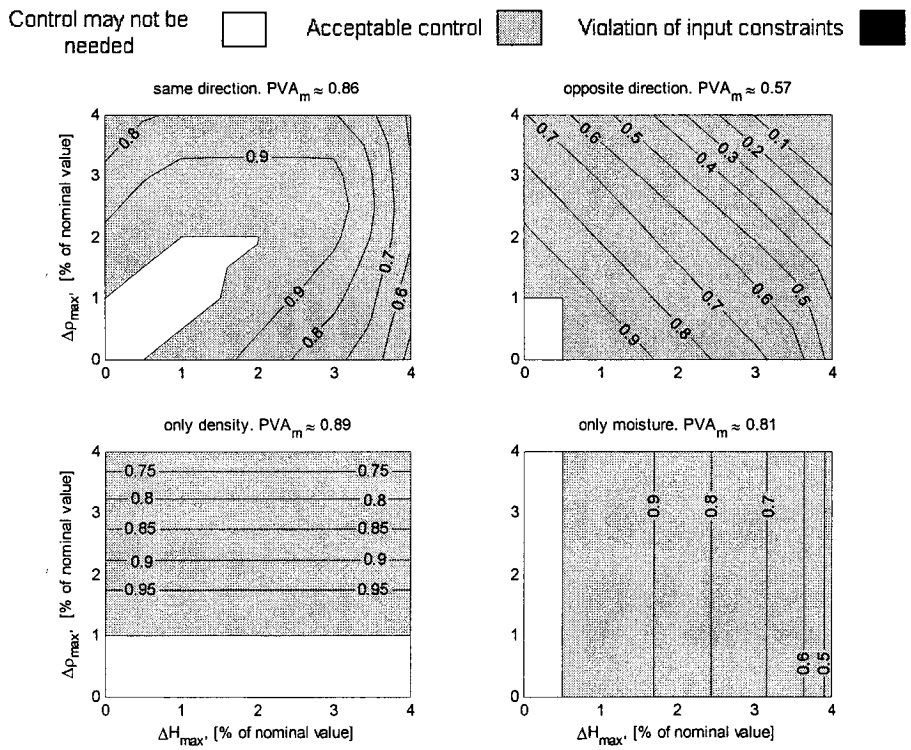

(PVA$_m$: mean of all 0<PVA's <1).

Figure 8.5. PVA (Steady state): Optimal solution. Scenario: P119-S119. Alternative operation

Results are independent of the sophistication and configuration of the controller and indicate that the worst disturbance is that entering the system in opposite directions, i.e. $d = [1\ -1]^T$ (e.g. an increase in wood moisture along with a decrease in wood density). The same calculations were performed for different plate age scenarios (see Table 8.4) and in all cases the opposite direction ended up being the most problematic.

Table 8.4. PVA as a function of disturbance directions – Alternative Operation

Plate age scenario	PVA_m (mean of all $0 < PVA's < 1$)			
	$d = [1\ 1]^T$	$d = [1\ -1]^T$	$d = [0\ 1]^T$	$d = [1\ 0]^T$
P119-S119	0.86	**0.57**	0.89	0.81
P602-S602	0.89	**0.45**	0.89	0.71
P31-S413	0.92	**0.69**	0.93	0.91
P685-S114	0.93	**0.61**	0.91	0.88

8.3.2. Potential for variability attenuation as a function of frequency

As mentioned earlier, the PVA can be computed in the frequency domain using the approximate method described in section 2.6.2.2.2. As in the steady state case, the dynamic potential for variability attenuation also depends on plate age. In order to isolate the impact of plate age from the individual effect of each refining stage, only scenarios having the same plate conditions in both refiners are considered. Since solution of equation (2.14) is obtained frequency-by-frequency, the issue of causality (output dependency on past inputs) is neglected (Skogestad and Postlethwaite, 1996). This means that the dynamic PVA depicted in Figure 8.8 to Figure 8.11 reflects only necessary conditions for achieving $0 < PVA < 1$ under the worst disturbance direction.

Before computing the dynamic *PVA*, it is necessary to check whether control is definitely needed. Indeed, variability attenuation via control is definitely required if $|G_d|_{\max}$ is larger than 1, i.e. when variations in wood moisture and density are such that they make the outputs go beyond their acceptable deviations ($\|e\|_\infty \geq 1$). When plates are new (see Figure 8.6) control up to 14.6 rad/s is definitely required to attenuate the effect of the highest possible variation in wood moisture and density in the worst direction. Control is less needed (light zone) if the maximum variation in wood density is smaller than 1% and that in wood moisture does not go past 0.5 %.

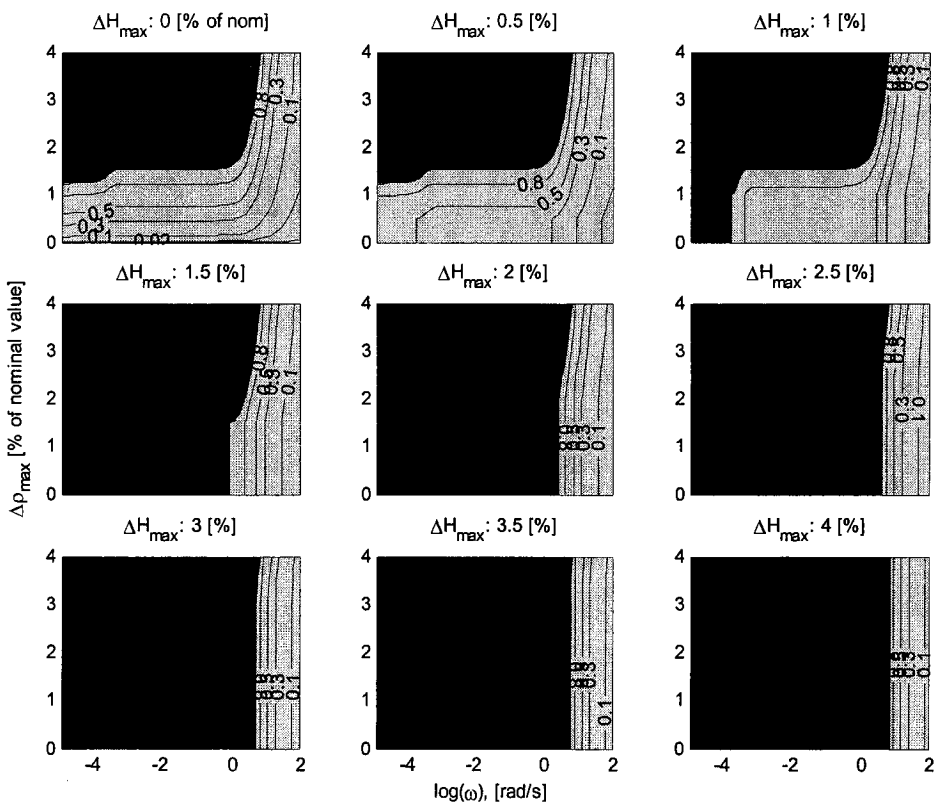

Figure 8.6. Wood variability conditions where control is definitely needed $|G_d|_{\max} > 1$ (dark areas). Plate age scenario: P119-S119.

On the other hand, when plates are old (see Figure 8.7) control is definitely needed at lower frequencies (up to 4 rad/s). For instance, if variations in wood density and moisture are as high as 3% and 2 % respectively, the frequency up to which control is definitely required can drop from 5 rad/s (new plates) down to 0.0006 rad/s (old plates). Moreover, at equal frequencies the system with old plates can absorb – theoretically without control - higher wood variations than the system with new plates since plate wear reduces the effect of disturbances on the outputs (smaller disturbance gains).

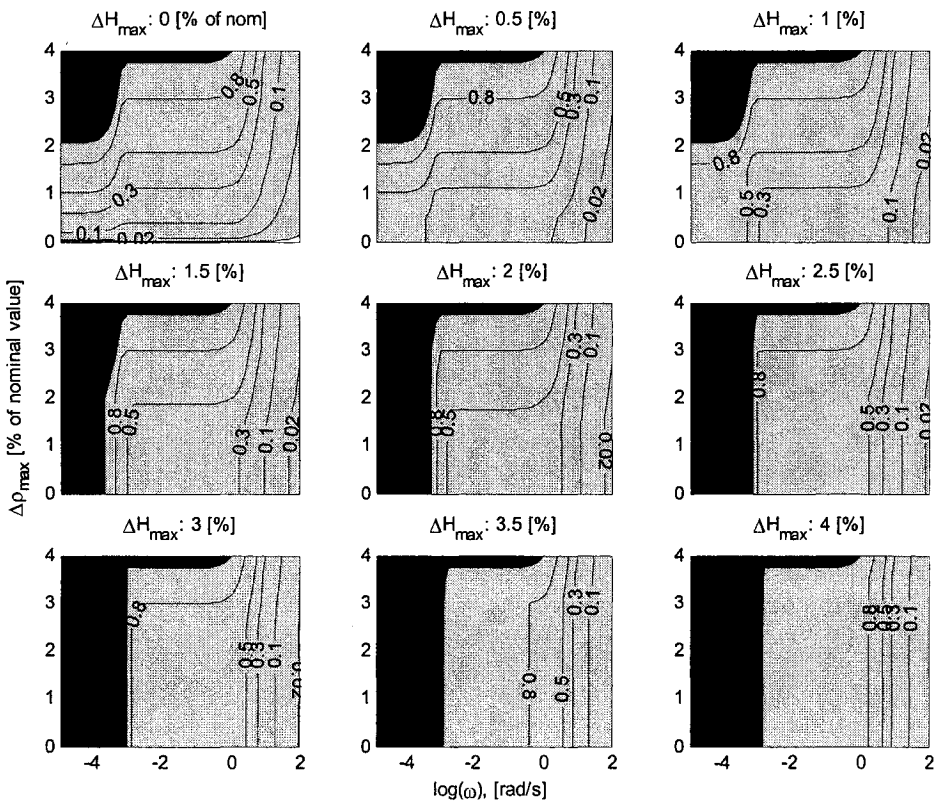

Figure 8.7. Wood variability conditions where control is definitely needed $|G_d|_{max} > 1$ (dark areas). Plate age scenario: P602-S602.

Nonetheless, plate wear also reduces process gains i.e. the sensitivity of the outputs to changes in the manipulated inputs. This means that although theoretically the need for control is less than that required when plates are new, at frequencies where control is actually required the manipulated effort may involve constraint violation. The dynamic PVA for the case where both refiners operate with new plates around benchmark conditions is shown in Figure 8.8.

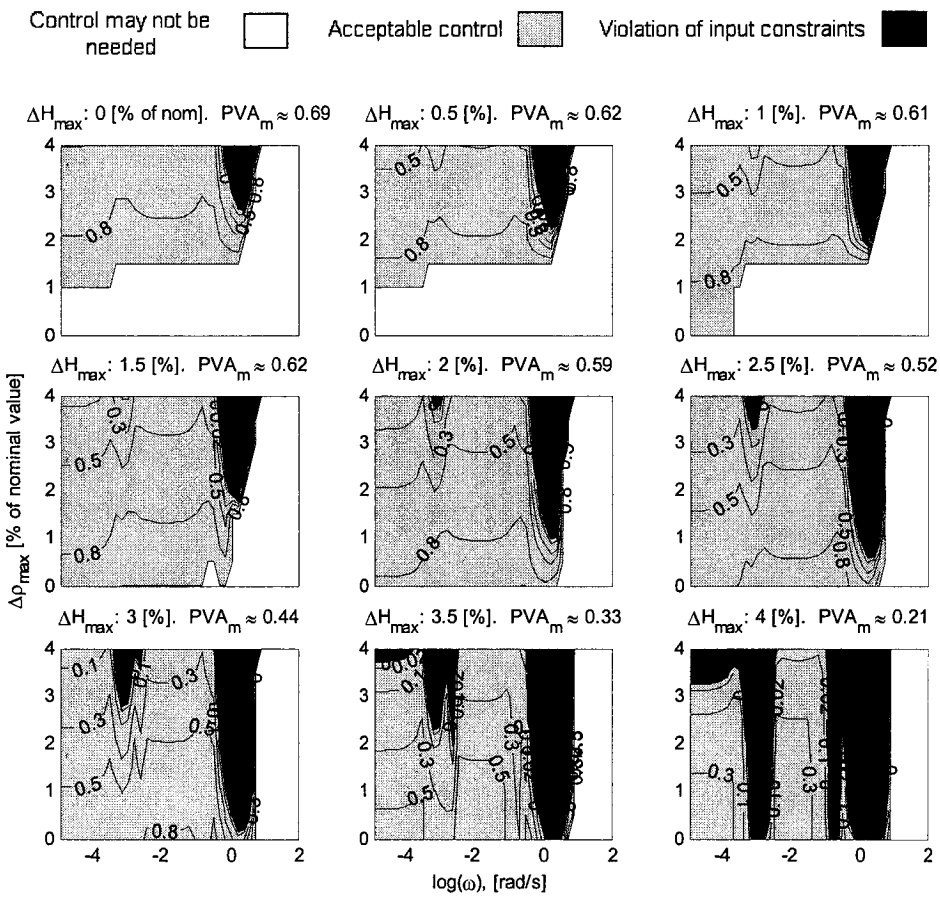

Figure 8.8. Dynamic PVA: Benchmark operating condition. Plate age scenario: P119-S119.

From the plots, two major dynamics can be identified for wood moisture variations higher than 2%. One is associated with both refiners (high frequency range: ~ 0.1 – 10 rad/s), and the other with the latency chest (low frequency range: ~ 0.0003-0.003 rad/s). Results also indicate that attenuation of pulp quality variations, i.e. control of latency chest dynamics, is not a problem at any frequency or density variation as long as maximum variations in wood moisture do not exceed 2 %. On the other hand, at this variability limit in wood moisture, attenuation of motor loads and refiner consistencies, i.e. control of refiner dynamics, will not be a problem at any frequency so long as maximum variations in wood density do not go over 1%.

As to the dynamic PVA when plates are old, plots in Figure 8.9 show that at benchmark operating conditions variability attenuation at low frequencies is much more difficult. Indeed, at these frequencies operating with old plates may saturate the inputs (constraint violation) whereas use of new plates – under the same wood variability conditions – involves acceptable control.

Finally, the dynamic PVA for the alternative operating conditions is depicted in Figure 8.10 (new plates) and Figure 8.11 (old plates). Although in both scenarios, alternative operating conditions allow for a more resilient operation at all frequencies (less dark zones) –especially if wood variability is low- the improvement is more dramatic and noticeable when refiners have old plates. In this case, variations in wood moisture up to 2.5% and in wood density up to 4% can be attenuated without input saturation, which was not possible when operating around benchmark conditions. Furthermore, for the highest variation in wood moisture (4%), variability attenuation is possible at any frequency provided wood density variations do not exceed 1%. For the same wood variability conditions, the benchmark case did not allow for control without input saturation at steady state (see Figure 8.9).

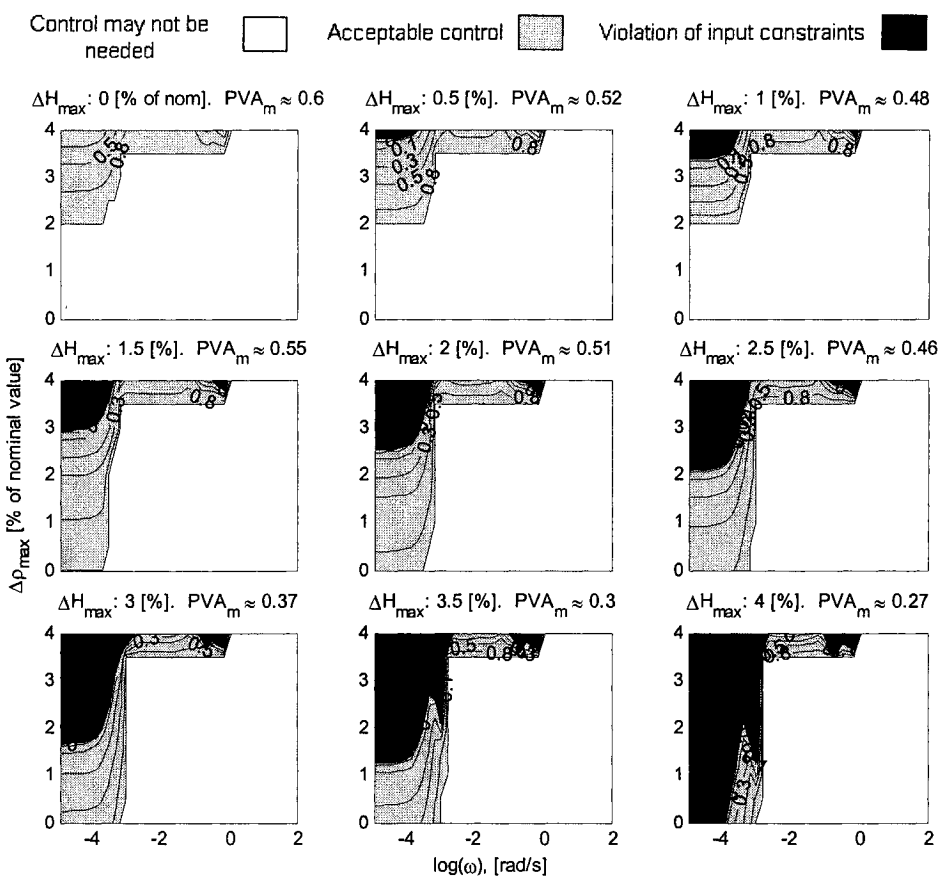

Figure 8.9. Dynamic PVA: Benchmark operating condition. Plate age scenario: P602-S602.

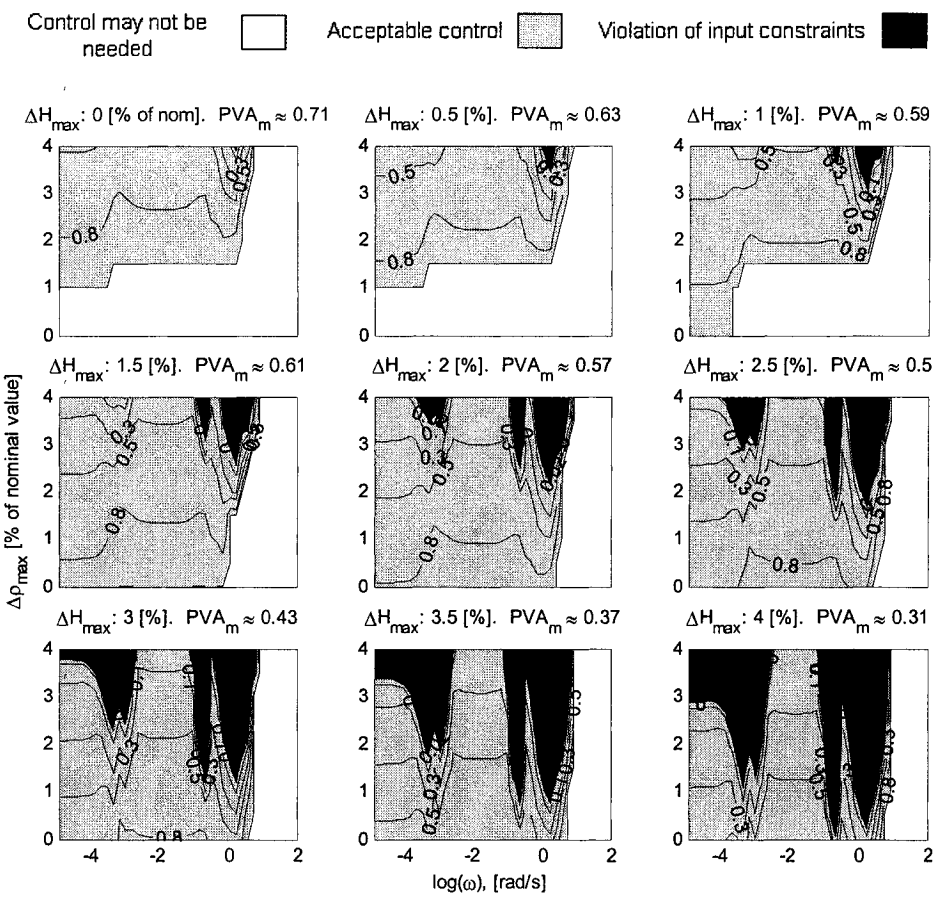

Figure 8.10. Dynamic PVA: Alternative operating condition. Plate age scenario: P119-S119.

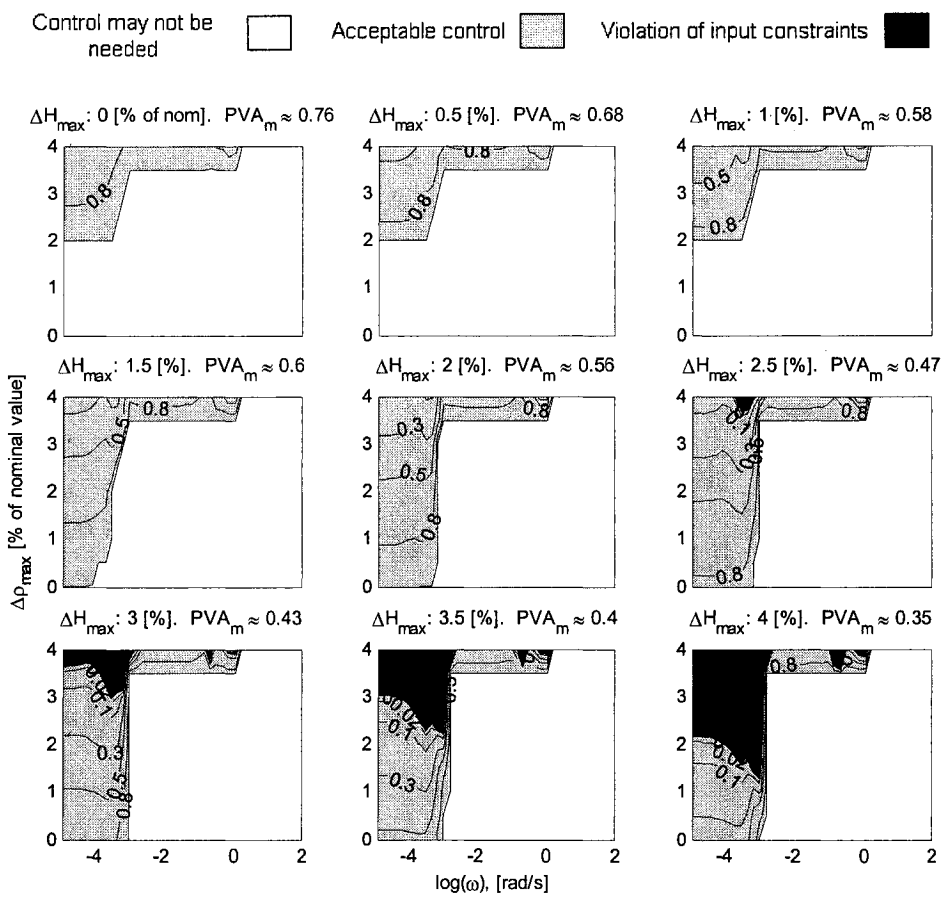

Figure 8.11. Dynamic PVA: Alternative operating condition. Plate age scenario: P602-S602.

8.4. Conclusions

A methodology has been proposed to determine the inherent potential of TMP-refining plants as to attenuating process variability. Given the conditions upon which the analysis is made results should not be regarded as specific limits for variability reduction. Instead, they are a depiction of the inherent potential of a TMP-refining process to attenuate - at a given plate condition - the effect of important wood quality variations. Furthermore, results provide only with necessary conditions for variability attenuation. Process constraints, fundamental internal interactions, plate age, and wood variations in moisture and density are all integrated in the problem formulation.

Solutions are independent of the control configuration currently in place and are analyzed from both steady state and dynamic standpoints. In particular, the graphical way by which PVA is represented allows for identifying the level of maximum wood variability (in terms of density and moisture) the system would be able to handle under control.

Variability attenuation at steady state

When plates in both refiners have the same age results indicate that it is harder to attenuate the effect of wood moisture and density variations when plates are old. On the other hand, when plate conditions are different in each refiner, variability attenuation is easier when the primary refiner has new plates and the secondary old ones.

Variability attenuation as a function of frequency

Plate age reduces the effect of disturbances on process outputs and consequently refining may not require control at certain frequencies and wood quality conditions. On the other hand, age also reduces the sensitivity of the process to changes in the

manipulated inputs, and thus at frequencies where control is actually needed the manipulated effort may be very large or even reach saturation. In other words, operation with old plates is likely less controllable.

An important result in terms of resiliency limitations of TMP-refining is that regardless of plate age, the most problematic disturbance occurs when wood moisture and wood density enter the system in opposite directions.

Finally, the largest opportunity to improve the operation of the TMP-refining plant under study arises when plates are old. Indeed, for a given wood variability scenario, operation around alternative conditions can help overcome controllability problems. Accordingly, when plates are old (especially in the secondary refiner), alternative operating conditions dramatically increase the resiliency of the operation (increase in PVA).

CHAPTER 9: A DECENTRALIZED CONTROL STRUCTURE AWARE OF TMP-REFINING INTERACTIONS

"Quality has to be caused, not controlled."
Phillip Crosby (1934-2004)

9.1. Introduction

As mentioned in CHAPTER 5, the analysis of internal interactions and disturbances affecting TMP refining processes is critical as it provides an insight into some of the plant's inherent control limitations. In turn, a control structure that creates unfavourable closed-loop interactions and possesses poor *controllability* characteristics may impair pulp quality, and ultimately affect the stability of the paper machine.

Many researchers have studied and proposed various control configurations to improve the operation of TMP processes (Rogers et al., 1980; Dumont and Astrom, 1988; Fu and Dumont, 1993; Cluett et al., 1995; Evans et al., 1995; Allison et al., 1995; Du et al., 1995; Roche et al., 1996; Strand, 1998; McQueen et al., 1999; Strand et al., 2000; Strand and Edwards, 1983; Dumont and Astrom, 1988; Fu and Dumont, 1993; Cluett et al., 1995; Evans et al., 1995; Allison et al., 1995; Du et al., 1995; Roche et al., 1996; McQueen et al., 1999; Strand et al., 2000). Nonetheless, to our knowledge there has been no systematic attempt in analyzing the inherent internal interactions resulting from a given control structure. In this chapter, the controllability indices presented in section 2.6.2.1 are applied to the TMP refining process so as to propose a decentralized control structure. This analysis is made for two plate age scenarios: P119-S119 (New plates) and P602-S602 (old plates). An important outcome of this work is that it elucidates how helpful interactions can be in controlling a TMP-refining process. It is

worthwhile mentioning that in this chapter the use of PVA (section 9.6) concerns the selection of a control structure and not a controllability evaluation of different operating points such as performed in CHAPTER 8.

9.2. Process and disturbance matrices used in the analysis

The use of controllability indices requires the knowledge of the linear model of the process. The scaled steady state process and disturbance gain matrices[17] for two different plate age scenarios are presented below. Linearization is performed around the alternative operating conditions detected in section 7.2.2.

Plate age scenario P119-S119:

$$K = \begin{bmatrix} & tss & Pc_1 & Fd_1 & Pc_2 & Fd_2 \\ ML_1 & 1.06 & 1.54 & -0.75 & 0 & 0 \\ ML_2 & 0.37 & 0 & 0 & 2.55 & -0.35 \\ Co_1 & 1.78 & 2.19 & -4.22 & 0 & 0 \\ Co_2 & 0.57 & 0.54 & -1.04 & 1.24 & -0.49 \\ LF & 2.19 & 0.61 & -2.11 & -2.79 & -0.25 \\ CSF & 1.31 & -0.77 & -0.27 & -4.54 & 0.34 \end{bmatrix} \quad K_d = \begin{bmatrix} & H & \rho \\ ML_1 & 0 & 1.62 \\ ML_2 & 0 & 0.56 \\ Co_1 & -2.85 & 2.65 \\ Co_2 & -0.70 & 0.86 \\ LF & -4.23 & 3.20 \\ CSF & -0.99 & 2.16 \end{bmatrix} \tag{9.1}$$

Plate age scenario P602-S602:

$$K = \begin{bmatrix} & tss & Pc_1 & Fd_1 & Pc_2 & Fd_2 \\ ML_1 & 0.24 & 1.7 & -0.35 & 0 & 0 \\ ML_2 & 0.04 & 0 & 0 & 0.48 & -0.04 \\ Co_1 & 0.17 & 1.04 & -0.85 & 0 & 0 \\ Co_2 & 0.13 & 0.61 & -0.50 & 0.52 & -0.12 \\ LF & 0.45 & 0.59 & -0.89 & -1.17 & -0.05 \\ CSF & 0.16 & -0.38 & -0.09 & -0.78 & 0.02 \end{bmatrix} \quad K_d = \begin{bmatrix} & H & \rho \\ ML_1 & 0 & 1.10 \\ ML_2 & 0 & 0.18 \\ Co_1 & -0.96 & 0.78 \\ Co_2 & -0.57 & 0.61 \\ LF & -3.00 & 1.99 \\ CSF & -0.40 & 0.75 \end{bmatrix} \tag{9.2}$$

It is clear that when plates are old both the disturbances and the manipulated inputs affect less the system since all the corresponding gains are significantly reduced. An

[17] Disturbance scaling: $[\Delta H_{max}, \Delta\rho_{max}] = [4\ 4]$

interesting observation is that at constant production rate, freeness seems to be more affected by the two hydraulic pressures than by the two dilution flowrates, whereas long fibre content is most sensitive to changes in primary dilution and secondary hydraulic pressure.

9.3. RGA analysis

The relative gain array (RGA) matrices for the non-square plant and the two plate age scenarios are shown below.

Plate age scenario P119-S119:

$$\Lambda = \begin{bmatrix} & tss & Pc_1 & Fd_1 & Pc_2 & Fd_2 \\ ML_1 & 0.35 & \underline{0.98} & -0.36 & 0 & 0 \\ ML_2 & 0.32 & 0 & 0 & \underline{1.07} & -0.40 \\ Co_1 & 0.01 & -0.36 & \underline{1.35} & 0 & 0 \\ Co_2 & -0.16 & 0.06 & 0.06 & -0.18 & \underline{0.77} \\ LF & -0.11 & 0.06 & -0.04 & 0.50 & 0.30 \\ CSF & 0.59 & 0.26 & -0.01 & -0.39 & 0.33 \end{bmatrix} \tag{9.3}$$

Plate age scenario P602-S602:

$$\Lambda = \begin{bmatrix} & tss & Pc_1 & Fd_1 & Pc_2 & Fd_2 \\ ML_1 & 0.36 & \underline{0.99} & -0.36 & 0 & 0 \\ ML_2 & 0.30 & 0 & 0 & \underline{0.95} & -0.37 \\ Co_1 & 0.03 & -0.37 & \underline{1.33} & 0 & 0 \\ Co_2 & -0.20 & 0.10 & 0.03 & -0.13 & \underline{1.02} \\ LF & -0.18 & 0.04 & 0.02 & 0.73 & 0.20 \\ CSF & 0.69 & 0.23 & -0.02 & -0.55 & 0.15 \end{bmatrix} \tag{9.4}$$

Remark: The RGA has been calculated as a function of frequency and results are the same as those obtained using gain matrices only, i.e. RGA(K) = RGA(G).

From the above RGA matrices, the control structure that minimizes interactions between loops involves the control of motor loads by manipulating the corresponding hydraulic pressures, and the control of consistencies via the corresponding dilution flowrates. What is left to pair is the transfer screw speed (*tss*), i.e. the throughput with either long fibre content (*LF*) or freeness (*CSF*). Accordingly, two candidate (square) configurations are proposed: c-LF and c-CSF. Given that two plate age scenarios are under study, controllability analysis is from now on carried out for 4 cases:

Case (1): New plates and control configuration c-LF
Case (2): New plates and control configuration c-CSF
Case (3): Old plates and control configuration c-LF
Case (4): Old plates and control configuration c-CSF

The RGA matrices for the four square plants are:

Case (1):

$$\Lambda_{5x5} = \begin{bmatrix} & tss & Pc_1 & Fd_1 & Pc_2 & Fd_2 \\ LF & \underline{1.04} & -0.19 & -0.09 & 0.22 & 0.02 \\ ML_1 & 0.21 & \underline{1.14} & -0.35 & 0 & 0 \\ Co_1 & -0.08 & -0.28 & \underline{1.35} & 0 & 0 \\ ML_2 & 0.36 & 0 & 0 & \underline{1.12} & -0.48 \\ Co_2 & -0.53 & 0.32 & 0.09 & -0.34 & \underline{1.46} \end{bmatrix} \tag{9.5}$$

Case (2):

$$\Lambda_{5x5} = \begin{bmatrix} & tss & Pc_1 & Fd_1 & Pc_2 & Fd_2 \\ CSF & \underline{0.53} & 0.20 & -0.01 & 0.30 & -0.02 \\ ML_1 & 0.34 & \underline{1.02} & -0.36 & 0 & 0 \\ Co_1 & 0.01 & -0.34 & \underline{1.34} & 0 & 0 \\ ML_2 & 0.32 & 0 & 0 & \underline{1.16} & -0.48 \\ Co_2 & -0.2 & 0.12 & 0.03 & -0.46 & \underline{1.50} \end{bmatrix} \tag{9.6}$$

Case (3):

$$\Lambda_{5x5} = \begin{bmatrix} & tss & Pc_1 & Fd_1 & Pc_2 & Fd_2 \\ LF & \underline{1.01} & -0.17 & -0.09 & 0.24 & 0.01 \\ ML_1 & 0.21 & \underline{1.14} & -0.35 & 0 & 0 \\ Co_1 & -0.05 & -0.30 & \underline{1.35} & 0 & 0 \\ ML_2 & 0.38 & 0 & 0 & \underline{1.11} & -0.50 \\ Co_2 & -0.55 & 0.33 & 0.09 & -0.35 & \underline{1.49} \end{bmatrix} \tag{9.7}$$

Case (4):

$$\Lambda_{5x5} = \begin{bmatrix} & tss & Pc_1 & Fd_1 & Pc_2 & Fd_2 \\ CSF & \underline{0.58} & 0.18 & -0.02 & 0.26 & -0.01 \\ ML_1 & 0.34 & \underline{1.02} & -0.36 & 0 & 0 \\ Co_1 & 0.02 & -0.35 & \underline{1.33} & 0 & 0 \\ ML_2 & 0.31 & 0 & 0 & \underline{1.20} & -0.51 \\ Co_2 & -0.25 & 0.15 & 0.04 & -0.46 & \underline{1.52} \end{bmatrix} \tag{9.8}$$

The above matrices seem to indicate that process interactions are not considerably affected by plate age conditions, i.e. the reduction in process gains does not have a major impact on interactions.

In terms of control configuration, it would seem logical to control the long fibre content with the transfer screw speed (c-LF) since the corresponding RGA-element is extremely close to 1. This issue however is to discuss whether the interaction affecting the transfer screw speed loop in configuration c-CSF helps in rejecting disturbances, i.e. whether interactions in this case are favourable or not. This is analyzed via the relative disturbance gain (RDG).

9.4. RDG analysis

The RDG matrices for the four square plants are:

Case (1):

$$RDG = \begin{bmatrix} & H & \rho \\ LF & \underline{0.64} & 1.01 \\ ML_1 & \infty & 0.05 \\ Co_1 & 1.18 & -0.03 \\ ML_2 & \infty & 0.03 \\ Co_2 & 0.13 & 0.01 \end{bmatrix} \tag{9.9}$$

Case (2):

$$RDG = \begin{bmatrix} & H & \rho \\ CSF & \underline{0.22} & 0.97 \\ ML_1 & \infty & -0.03 \\ Co_1 & 1.32 & -0.05 \\ ML_2 & \infty & -0.06 \\ Co_2 & 0.02 & 0.02 \end{bmatrix} \tag{9.10}$$

Case (3):

$$RDG = \begin{bmatrix} & H & \rho \\ LF & \underline{0.62} & 1.01 \\ ML_1 & \infty & 0.04 \\ Co_1 & 1.17 & -0.03 \\ ML_2 & \infty & 0.02 \\ Co_2 & 0.12 & 0.01 \end{bmatrix} \tag{9.11}$$

Case (4):

$$RDG = \begin{bmatrix} & H & \rho \\ CSF & \underline{0.21} & 0.99 \\ ML_1 & \infty & -0.01 \\ Co_1 & 1.31 & -0.04 \\ ML_2 & \infty & -0.04 \\ Co_2 & 0.02 & 0.02 \end{bmatrix} \tag{9.12}$$

An important observation is that plate age does not seem affect the RDG. In other words, the change in the effect of disturbances caused by decentralized control will not vary with plate age conditions. In addition, although both configurations c-LF and c-CSF would be able to reject the effect of disturbances on the quality parameter under control, configuration c-CSF seems to require less input action to do so ($RDG_{1,1} > \sim 0.2$) than that corresponding to configuration c-LF ($RDG_{1,1} > \sim 0.6$). This means that the retaliatory effect from all other loops upon the loop controlling freeness in configuration c-CSF is favourable, and thus helpful for rejecting disturbances. On the other hand, controlling primary refiner consistency may be difficult and lead to input saturation if a major perturbation in wood moisture enters the system ($RDG_{3,1} > 1$). In this regard, it is clear from RDG analysis that under decentralized control, wood density is much easier to reject than wood moisture. Indeed, all elements in the last column of RDG are extremely small compared to those in the last column of K_d, i.e. the controller can potentially remove the effect of wood density from most of the outputs.

Remark: Note that the infinity values in the rows corresponding to the motor load ML_1 and ML_2 have no meaningful interpretation since the model does not account for the relationships between moisture and motor loads.

9.5. Condition number and minimum singular value

Condition numbers and minimum singular values for the four cases are shown in Table 9.1 Results indicate that plate age has a negative effect on the minimum singular value. Indeed, as plates wear the power of the manipulated input action upon all outputs weakens, and thus the system is more prone to input saturation if a control action is taken. This makes sense since the operation with old plates is closer to its input constraints, i.e. has less room for manipulation than the operation with new plates (see Table 8.3). This occurs in spite of the fact that the allowed output deviations for plate age scenario P602-S602 are larger than those of P119-S119 (see Table 8.3).

Table 9.1. Condition numbers and singular values of candidate configurations

Control configuration	Plate Scenario	
	P119-S119	P602-S602
c-LF	CN = 23.6 $\underline{\sigma} = 0.27$	CN = 57.1 $\underline{\sigma} = 0.04$
c-CSF	CN= 19.9 $\underline{\sigma} = 0.28$	CN = 51.6 $\underline{\sigma} = 0.05$

Finally, condition numbers indicate that the plant is more ill-conditioned when plates are worn out, i.e. some combinations of inputs have a strong effect on the outputs while other combinations have a weak effect (Skogestad and Postlethwaite, 1996). In terms of control configurations, one can see that configuration c-CSF shows lower condition numbers but in general results are not conclusive as they are all larger than 10.

9.6. PVA Analysis

Figure 9.1 to Figure 9.4 show that regardless of plate age, configuration c-CSF has more potential for variability attenuation i.e. is less prone to input saturation than configuration c-LF, especially at low frequencies. Moreover, when plates are old results indicate that control may not be necessary at low frequencies for most disturbance combinations. Results are given for the case of worst disturbance direction.

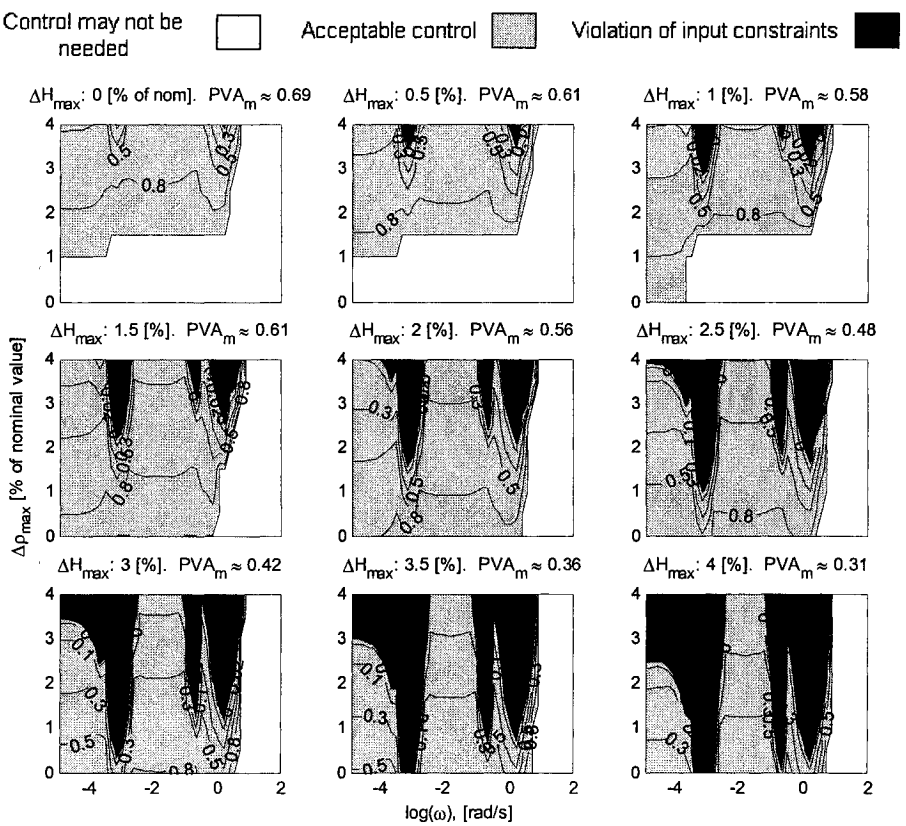

Alternative operating condition.

Figure 9.1. Dynamic PVA for configuration c-LF. Plate age scenario: P119-S119.

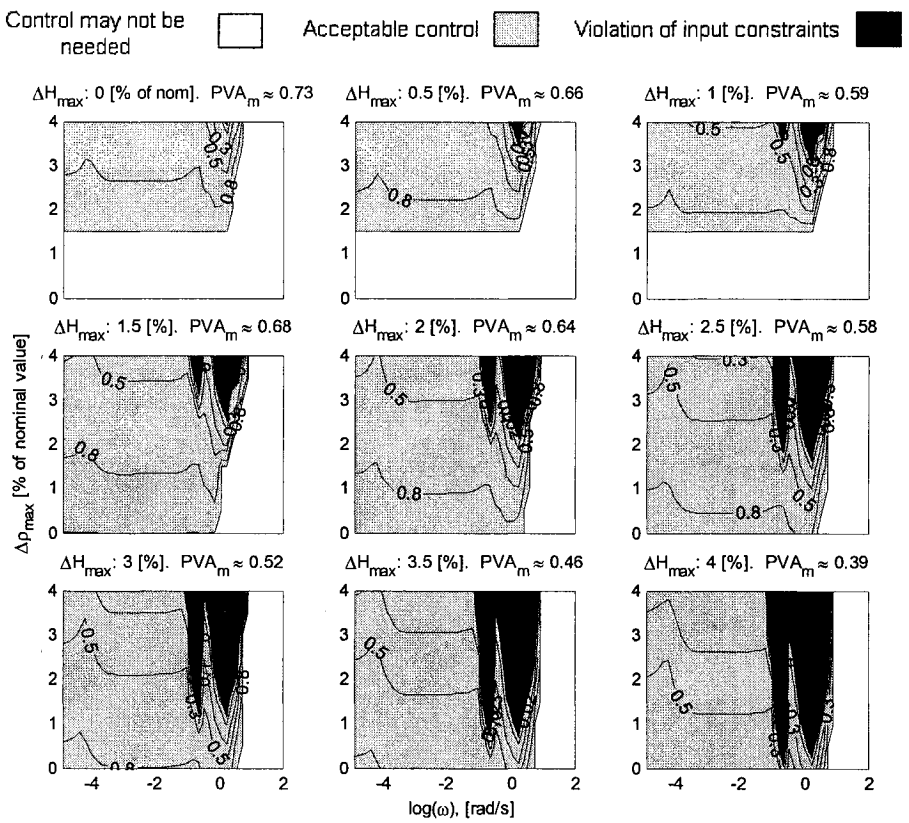

Alternative operating condition.

Figure 9.2. Dynamic PVA for configuration c-CSF. Plate age scenario: P119-S119.

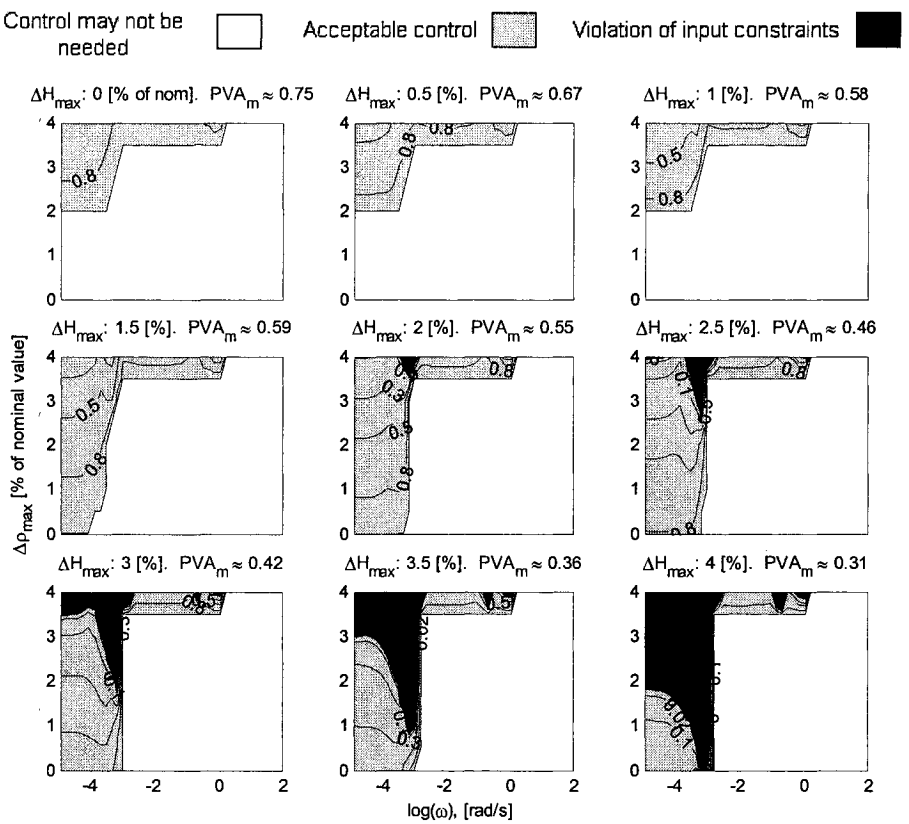

Alternative operating condition.

Figure 9.3. Dynamic PVA for configuration c-LF. Plate age scenario: P602-S602.

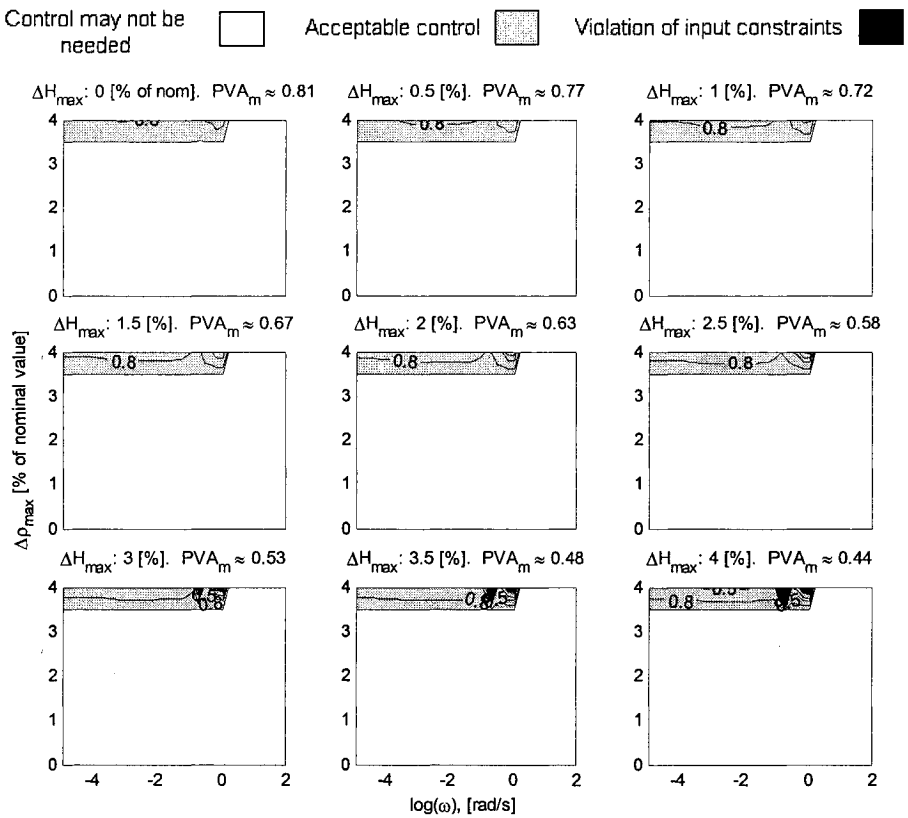

Alternative operating condition.

Figure 9.4. Dynamic PVA for configuration c-CSF. Plate age scenario: P602-S602.

In summary, the retaliatory effect from all other loops upon the loop controlling freeness in configuration c-CSF is favourable, and thus helpful when rejecting disturbances. This configuration has more potential for variability attenuation i.e. is less prone to input saturation than configuration c-LF, especially at low frequencies. Consequently, we conclude that the transfer screw speed should control freeness rather than long fibre content, i.e. c-CSF is the selected configuration. Furthermore, this configuration has been checked for any combinations of one, two and three-loop failures and in all cases the system possesses DCLI (Decentralized closed-loop integrity) according to the necessary conditions explained in 2.6.2.1.3. The Niederlinski

Index and the diagonal elements of RGA for all principal sub-matrices (or failure combinations) are given in APPENDIX D.

9.7. Closed-loop simulation

In order to validate our selection, a closed-loop simulation of the full nonlinear model has been performed around the alternative operation. A decentralized PID control structure is implemented in the model. The plate age scenario chosen is when plates are new, i.e. P119-S119. Controllers have been tuned using the IMC approximate method proposed by (Rivera et al., 1986; Morari and Zafiriou, 1989). Random variations in wood moisture and wood density with a maximum magnitude of 4% their nominal value are simulated every 11 minutes for about 17.5 hours (see Figure 9.5). No constraints are implemented during simulations in order to show the actual manipulated effort required for control. In reality input saturation occurs given the maximum magnitude of disturbance changes considered in the simulation.

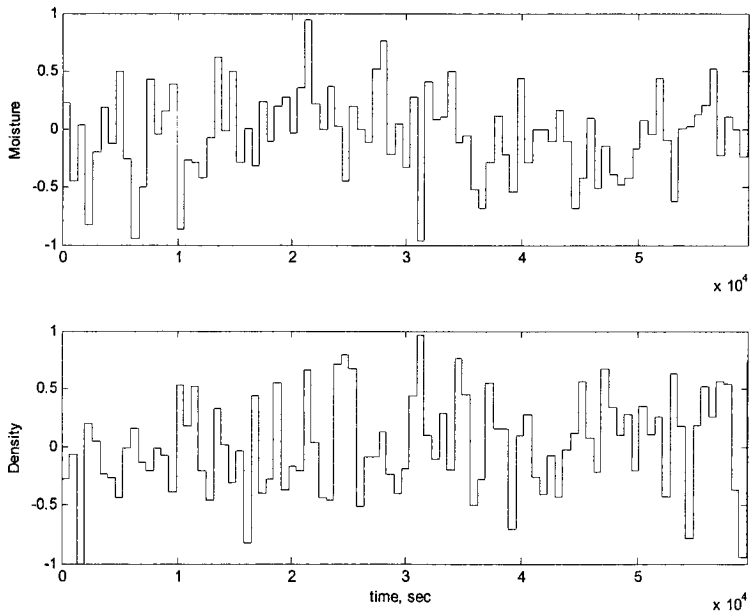

Figure 9.5. Normalized random perturbations in wood moisture and density

Results have been normalized as outlined in section 2.6.2 to facilitate comparison. In particular, the purpose is to compare the level of process variability associated with each control configuration. The performance of the *tss*-loop for both control configurations is depicted in Figure 9.6 along with the response of the uncontrolled quality parameter. Output responses for motor loads and consistencies are shown in Figure 9.7 and Figure 9.8, respectively. Input action of the remaining manipulated variables is shown in Figure 9.9 and Figure 9.10. Note: The median value appearing in the plots corresponds to the median of the absolute value of deviations.

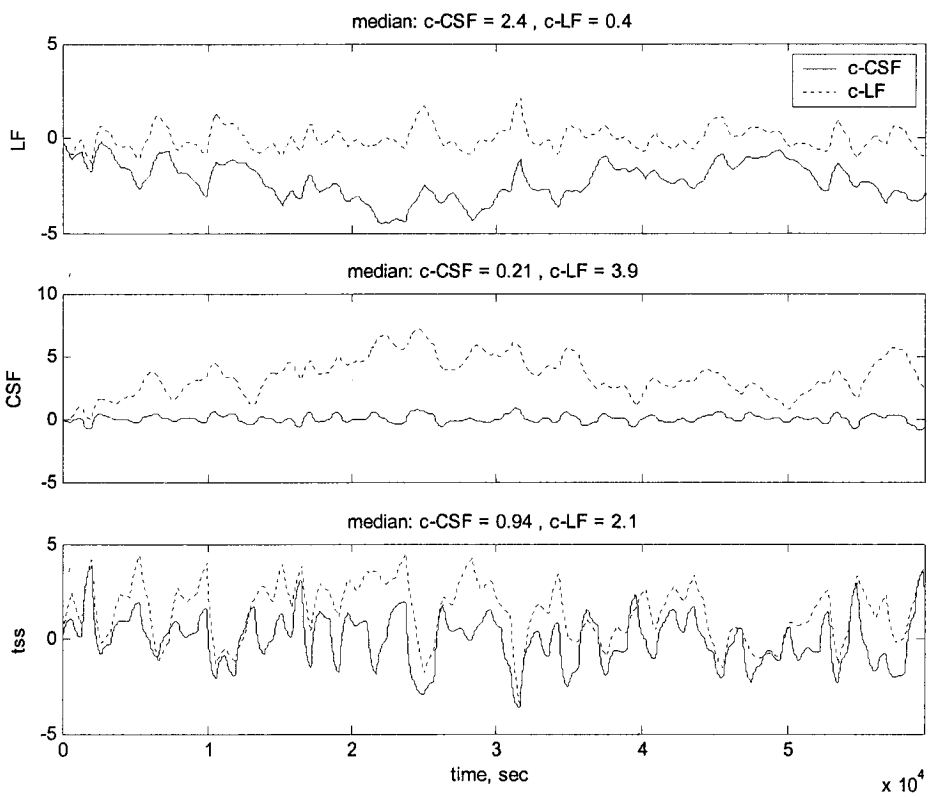

Figure 9.6. Nonlinear simulation: Pulp quality and transfer screw speed.

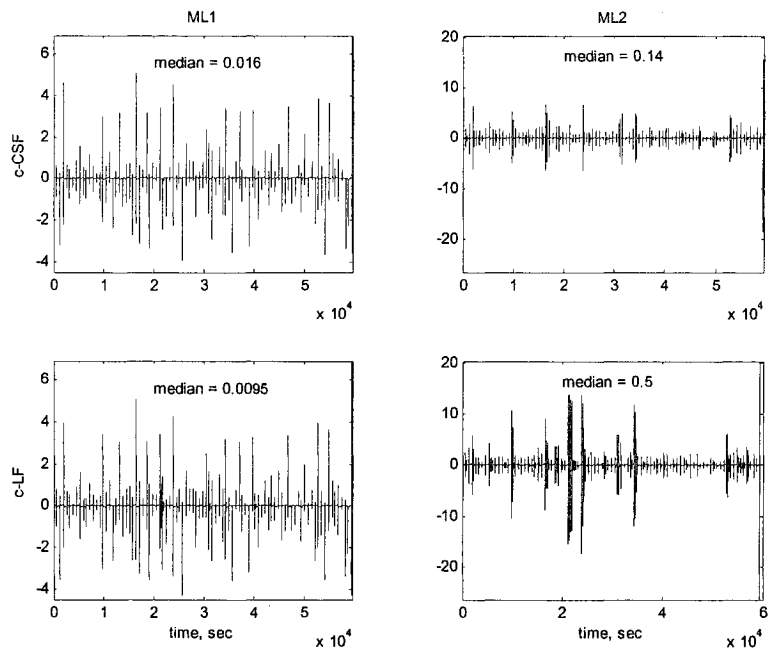

Figure 9.7. Nonlinear simulation: Motor loads.

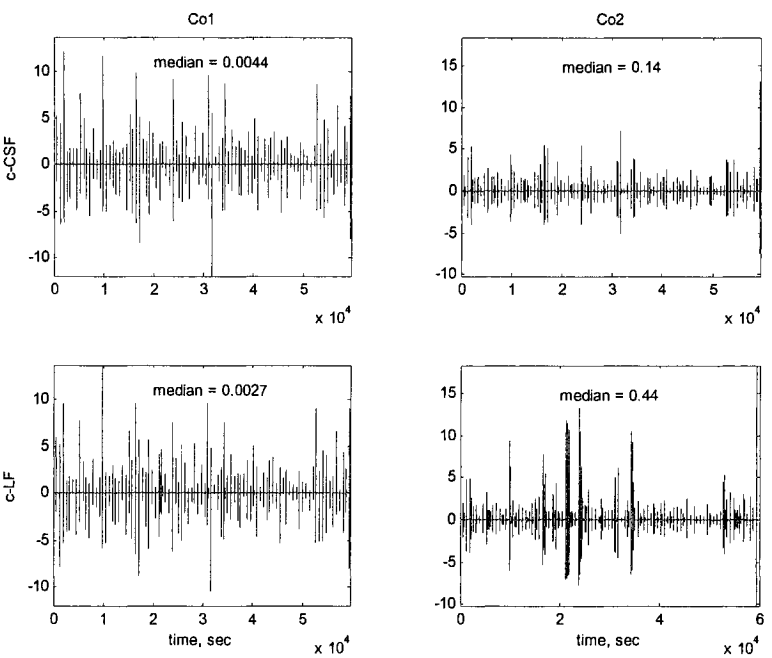

Figure 9.8. Nonlinear simulation: Consistencies.

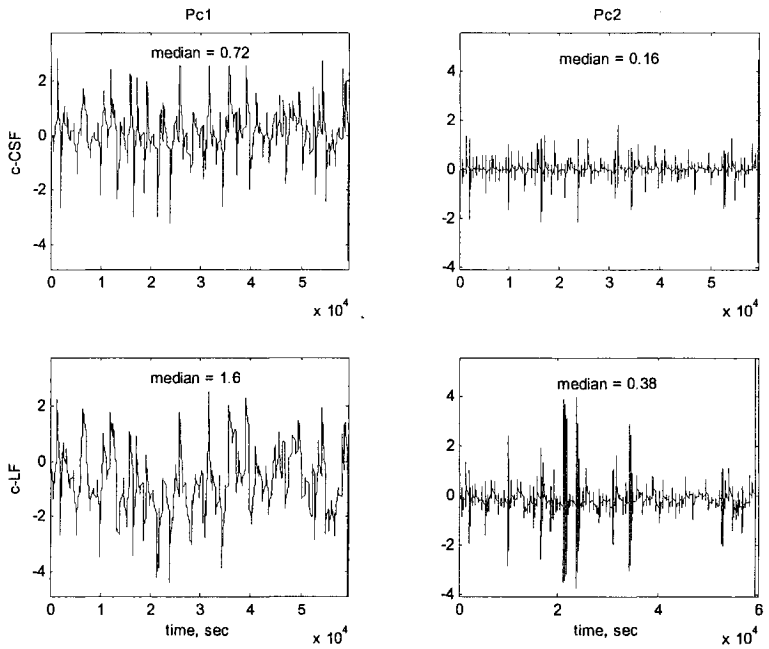

Figure 9.9. Nonlinear simulation: Hydraulic pressures.

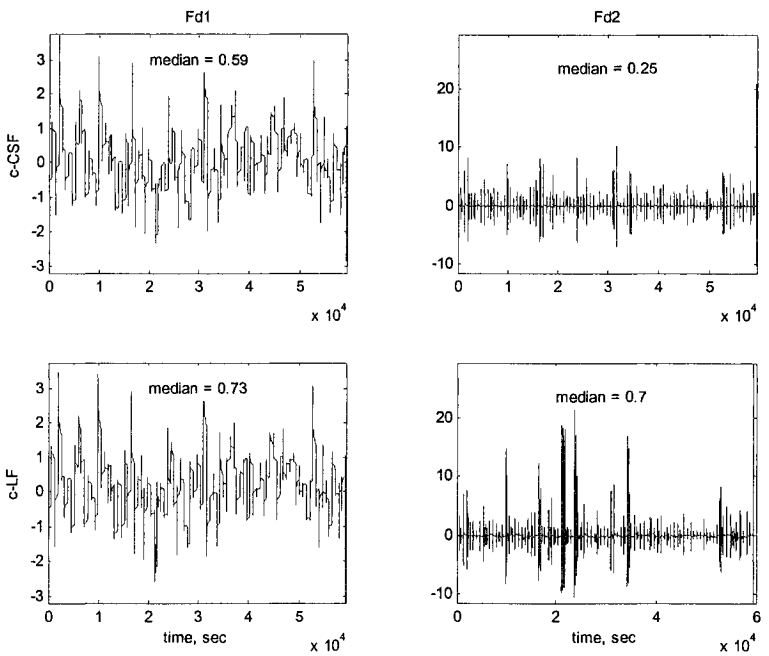

Figure 9.10. Nonlinear simulation: Dilution flowrates.

It is confirmed that configuration c-CSF requires less combined input action than configuration c-LF to control the ensemble of process outputs. In turn, controlled outputs in particular those associated to the secondary refiner and pulp quality, show more variations under configuration c-LF. Moreover, the uncontrolled variable in configuration c-CSF (long fibre content) is less affected by closed-loop interactions than freeness under configuration c-LF. Indeed, the median of the deviation for freeness when c-LF is imposed is equal to 3.9, while that for long fibre content under configuration c-CSF is equal to 2.4.

9.8. Conclusions

Results indicate that plate age does not seem to have an important effect on process interactions. In fact, the change in the effect of disturbances upon the process due to decentralized control will not vary with plate age conditions. On the other hand, as plates wear the power of the manipulated input action upon all outputs weakens, and thus the system is more prone to input saturation if a control action is taken. Accordingly, results in theory suggest for the plant to cease automatic control – or operation for that matter - when plates are extremely old since the plant becomes increasingly ill-conditioned.

Individually, wood moisture and wood density are attenuated by decentralized control in different degrees, thus wood density is much easier to reject than wood moisture.

Finally, interactions associated with configuration c-CSF have proved to be helpful in rejecting disturbances as they reduce the necessary control action. Closed-loop nonlinear simulations confirm this selection. In this regard, the proposed configuration is based for the first time on a systematic controllability analysis of the inherent interactions affecting a two-stage TMP refining process.

CHAPTER 10: CONCLUSIONS AND RECOMMENDATIONS

"Not every end is the goal. The end of a melody is
not its goal, and yet if a melody has not reached its end,
it has not reached its goal..."
Friedrich Nietzsche (1844-1900)

10.1. Contributions to the body of knowledge

A modeling methodology for TMP-Refining processes that accounts for plate age

This methodology is based on industrial data extracted from routine operations and not from designed experiments, which is the assumption most of modeling methods make when operational conditions do not allow for running controlled experiments or performing bump tests. Furthermore, this data shows non-stationary and transient parts that are ill-suited for conventional model identification. The proposed methodology pre-processes and extracts the relevant part of such data. In particular:

- The methodology takes full advantage of robust statistical techniques, long-term routine data from operations, refiner plate age, laboratory tests, and existing experimental evidence to estimate refiner motor load and pulp quality. In particular, a model structure is proposed to describe motor load behaviour in terms of plate age, production rate, hydraulic pressure and dilution flowrate.
- A practical procedure is proposed to extract refiner dynamics, specifically process time constants, from short-term uncompressed data.

- Prediction of fibre fractions after both refiners in terms of PQM values allows the evaluation of the entire refining operation –latency chest included- using a single fibre distribution standard.

Because the resulting model has to most parts a strong physical motivation and conforms to well-known process directionalities, it is a reliable basis for all the analyses made in this work.

An insight on the directionality of TMP-Refining operations

- At a given condition of plate age, dilution, and production rate, high long fibre content and freeness are attained by applying high power split ratios at low total specific energy, i.e. by charging less energy to the secondary refiner.
- Plate age increases power split and refining intensity in both stages. In addition, as plates wear it becomes increasingly difficult for the refiners to apply the same amount of energy to the pulp, especially in the secondary refiner. As for pulp quality, plate age reduces either freeness or long fibre content depending on the individual plate conditions in each refiner and the attainable total specific energy. If both refiners start operation with new plates, the pulp quality window gradually moves toward lower freeness and long fibre contents.
- Wood moisture and increased dilution conditions predominantly move the quality window toward long fibre contents.

A model-based approach to optimize TMP-refiners as plates age

The approach elucidates the effect of major drifts in wood quality and some process constraints on the optimal operation of TMP-Refiners. The formulation takes into account the long-term effect of plate age on refining to minimize total energy

consumption subject to constraints in pulp quality, primary motor load, power split and refining consistencies. Important contributions resulting from the application are:

- At constant freeness, high density wood favours energy savings. Furthermore, as plates get older optimal refining of high-density wood yields pulp of higher attainable freeness and long fibre content.
- At constant freeness and assuming that wood moisture represents seasonal conditions, the operation saves more energy during the winter than during the summer but also yields pulp of lower long fibre content.
- At constant freeness, relaxed limits – from below - in primary motor load entail considerably less energy consumption than an operation with tighter bounds. Moreover, when plates start getting old, these relaxed conditions allow for higher attainable values of freeness. On the other hand, tightening constraints in primary motor load – from below – yields higher long fibre content at constant freeness.
- Relaxing freeness specifications – from above - involves more energy savings and higher long fibre contents, particularly when plates are relatively new.

A model-based methodology to determine inherent potential for energy reduction and variability attenuation in TMP-refining operations

The methodology determines operating windows of low variability (*benchmarks*) and then verifies – through model-based optimizations - whether an improved operating condition (*alternatives*) can be found. Process constraints, fundamental internal interactions, plate age, and wood variations in moisture and density are all integrated in the problem formulation. Solutions are independent of the control configuration currently in place. In particular, the graphical way by which the potential for variability attenuation is represented allows for identifying the level of maximum wood variability the system would be able to control. Results indicate that under certain conditions of plate age and wood variability, reductions in both refining energy consumption and

process variability can be achieved simultaneously. In this context, it may be worthwhile to indicate that as a result of a recent implementation of MPC (model predictive control) strategies to a TMP-Refining (Fairbank, *personal communication*, April 2006), the operation has been able to reduce the variability in pulp freeness in about 30 to 40%, while at the same time reducing in 5% the nominal energy consumption in both refiners. This certainly confirms the validity of our results.

Among the thematic contributions resulting from the application of this methodology we have identified the following:

- The controllability of the operation with old plates is limited given its proximity to constraints. Accordingly, the older the plates in both refiners, the harder the attenuation of wood moisture and density variations becomes in the longer term. The reason is that age reduces the sensitivity of the process to input changes, and thus at frequencies where control is actually needed the manipulated effort may reach saturation. On the other hand, plate age also reduces the effect of disturbances on process outputs, and consequently refining may not require control at certain frequencies and wood variability conditions.
- Regardless of plate age, the most problematic disturbance occurs when wood moisture and wood density enter the system in opposite directions.

A proposal for a decentralized control structure based for the first time on a systematic controllability analysis of TMP-Refining interactions

In a decentralized system that controls motor loads with hydraulic pressures and consistencies with dilution flowrates, freeness is a more suitable controlled variable than long fibre content. Indeed, the retaliatory interaction from all other loops upon the loop controlling freeness is favourable for rejecting disturbances, and therefore has

more potential for variability attenuation. In this context, it is confirmed that the lack of interactions in a given control structure is not necessarily desirable.
In addition, our study reveals important aspects of the controllability of TMP-Refining processes:

- Individually, wood density is much easier to reject than wood moisture under decentralized control.
- Plate age does not have an important effect on process interactions under decentralized control. Furthermore, the change in the effect of disturbances caused by decentralized control does not vary with plate age conditions.
- As plates wear the power of the manipulated input action upon all outputs weakens, and thus the system is at risk of input saturation under decentralized control. In this context, an interesting finding is that when plates are extremely old the plant becomes increasingly ill-conditioned, and therefore potentially hard to control.

10.2. Future work

Modeling

The time constants presented in equation (3.9) are assumed invariant with respect to plate age. It would be interesting to investigate whether a significant variation occurs as plate age since this may have an impact on the dynamic PVA calculated in section 8.3.2.

The motor load model proposed in this thesis could also include wood moisture and chip size distribution as part of its structure. However, the relationship between these two variables is not clear and has not been quantified in the available literature. In this regard, recent developments in chip management systems and on-line wood quality

measurements could help clarify how the aforementioned wood characteristics should be included in the model in question.

The TMP-Refining model proposed in this thesis has been tested in Twin refiners. It would be interesting to explore the application of this modeling framework to conical disc refiners.

Lack of information on the actual volume used for mixing precluded us from modeling the latency chest as a perfectly mixed tank followed by a plug flow region. Although results should not vary significantly given the dramatic difference in dynamic scales (refiners vs. latency chest), future work should investigate the effect of the latency chest's dead volume on the potential for variability attenuation presented here.

A major conceptual assumption throughout this thesis is that plate wear is equivalent to plate age. This is not rigorously true, and thus further research must be done to elucidate the actual relationship between these two variables if optimal control is to be implemented.

Methodology

The application of steady state identification in the context of this thesis assumes for simplicity's sake that a single variable can indicate the steady state condition of the entire system. Future work could remove this assumption and directly apply multivariable steady state identification techniques provided the selected variables are not cross-correlated.

In order to simplify calculations during the optimizations we have assumed that freeness reflects the amount of fines. An interesting direction for future work would be to include the fines content in addition to freeness and long fibre content when applying

the proposed methodology. In doing so, paper properties such as tensile strength or tear index could be directly included as part of the problem formulation.

It has been assumed when optimizing the operation in CHAPTER 6 that both refining stages start operation at the same time and under the same conditions of plate age. Future work could consider the scheduling of changing plates. The model presented in this thesis can be used for this purpose since its structure allows for simulating different plate age conditions in each refiner.

Given the inherent trade-off between optimality and controllability under certain disturbance and plate age conditions, variability attenuation may be fairly limited by the additional amount of specific energy the operation is willing to consume in order to have more manoeuvrability for control. This work is thus an initial step towards developing an optimal control system capable of handling the effect of wood variations and plate wear upon pulp quality.

Most of the contributions and results contained in this thesis have also been the basis for several manuscripts, some of which have already been published or accepted for publication (Lama et al., 2006a; Lama et al, 2006b; Lama et al., 2006c), or are currently being peer-reviewed (Lama et al., 2006d; Lama et al, 2006e; Lama et al., 2006f).

REFERENCES

AFT, L.S. 1988. *Quality improvement using statistical process control.* San Diego, USA : Harcourt Brace Jovanovich. 395 p.

ALAMI, R., BOILEAU, I., HARRIS, G., LACHAUME, J., KARNIS, A., MILES, K.B. et al. 1997. "Impact of refining intensity on energy reduction in commercial refiners: Effect of primary-stage consistency". *TAPPI, J.* 80:1. 185-193.

ALLISON, B.J., CIARNIELLO, J., TESSIER, P., DUMONT, G. 1995. "Dual adaptive control of chip refiner motor load: Industrial Results". *Pulp & Paper Canada.* 96:3. T73-T79.

ALLISON, B.J., ISAKSSON, A.J., KARLSTROM, A. 1996. "Distributed parameter model of a TMP Refiner". *Proceedings of the '96 Control Systems Conference.* Halifax, Canada : PAPTAC. P. 1-4

ALLISON, B.J., ISAKSSON, A.J., KARLSTROM, A. 1997. "Grey-box identification of a TMP refiner". *Pulp & Paper Canada.* 98:4. T123-T126.

ARBIZA, M.J., BANDONI, J.A., FIGUEROA, J.L. 2003. "Use of back-off computation in multilevel MPC". *Lat. Am. Appl. Res.* 33:3. 251-256.

BERG, D., KARLSTROM, A. 2004. *Theories for decoupling 3 X 3-Systems with Application to Thermomechanical Pulp Refiners.* Sweden: Chalmers University of Technology, Department of Signals and Systems. 10 p. p.

BIALKOWSKI, W.L. 1999. "The Entech Report -Aug 1999". *Emerson Process Management* . 11:2.

BIALKOWSKI, W.L. 2000. "The Entech Report - Jan 2002". *Emerson Process Management*. 12:1.

BIALKOWSKI, W.L. 2001. "The Entech Report - Nov 2001". *Emerson Process Management*. 13:3.

BIALKOWSKI, W.L. 2002a. "The Entech Report - Mar 2002". *Emerson Process Management*. 14:1.

BIALKOWSKI, W.L. 2002b. "The Entech Report - Nov 2002". *Emerson Process Management*. 14:2.

BIALKOWSKI, W.L. 2003. "The Entech Report - May 2003". *Emerson Process Management*. 15:1.

BLEVINS, T.L., MCMILLAN, G.K., WOJSZNIS, W.K., and BROWN, M.W. 2003. *Advanced Control Unleashed. Plant Performance Management for Optimum Benefit*. Research Triangle Park, NC, USA : ISA - The Instrumentation, Systems and Automation Society. 434 p. p.

BOGLE, D., FRAGA, E. 2000. *Analysing the controllability of nonlinear process systems.* London, UK: Department of Chemical Engineering. University College London. 15 p.

BRILL, J.W. 1985. "Effects of wood and chip quality on TMP properties". *International Mechanical Pulping Conference*. Stockholm, Sweden :P. 153-161

BRISTOL, E.H. 1966. "On a new measure of interaction for multivariable process control". *IEEE Trans. Automat. Contr.* AC-11:133-134.

BRODERICK, G., PARIS, J., VALADE, J.L. 1995. "Factors affecting the optimal performance of a high-yield pulping operation". *Can. J. Chem. Eng.* 73:June. 391-399.

BROWN, P.R., RHINEHART, R. 2000. "Demonstration of a method for automated steady-state identification in multivariable systems". *Hydrocarb. Process.* 79:9. 79-83.

CAO, S., RHINEHART, R.R. 1995. "An efficient method for on-line identification of steady state". *J. Process Control.* 5:6. 363-374.

CASTRO, J.J., DOYLE III, F.J. 2002. "Plantwide control of the fiber line in a pulp mill". *Ind. Eng. Chem. Res.* 41:5. 1310-1320.

CHIU, M.-S., ARKUN, Y. 1990. "Decentralized control structure selection based on integrity considerations". *Ind. Eng. Chem. Res.* 29:369-373.

CLUETT, W.R., GUAN, J., DUEVER, T.A. 1995. "Control and Optimization of TMP Refiners". *Pulp & Paper Canada.* 96:5. T158-T162.

CUI, H. 2000. *On dynamic and controllability of Processes with recycle.* 116 p. Licenciate Thesis., Department of Signals, Sensors and Systems. Royal Institute of Technology.

DI RUSCIO, D. 1993. *Topics in Model Based Control with Application to the Thermo mechanical pulping process.* Ph D. Thesis, Department of Engineering Cybernetics. The Norwegian Institute of Technology.

DIMIAN, A.C., GROENENDIJK, A.J., KERSTEN, S.R.A. , IEDEMA, P.D. 1997. "Effect of recycle interactions on dynamics and control of complex plants". *Computers Chem. Engng.* 21:S291-S296.

DU, H. 1998. *Multivariable Predictive Control of a TMP Plant.* PhD Dissertation, University of British Columbia.

DU, H., DUMONT, G., FU, Y. 1995. "Nonlinear Control of a Wood Chip Refiner". *Proceedings of the IEEE Conference on Control Applications.* Albany, NY : IEEE. P. 1065-1066.

DUMONT, G., ASTROM, K.J. 1988. "Wood Chip Refiner Control". *IEEE Control Syst. Mag.* 8:2. 38-43.

ERIKSSON, K., KARLSTROM, A., ROSENQVIST, F., BERG, D. 2002. "The impact of different input variables in a twin-disc refiner line". *International Mechanical Pulping Conference.* Helsinki, Finland :P. 229-233

EVANS, R., SUTINEN, R., SAARINEN, K. 1995. "Refiner Control effectively accomplished through Adaptive Control". *Pulp & Paper Canada.* 96:5. T163-T166.

FISHER, W.R., DOHERTY, M.F., DOUGLAS, J.M. 1988. "The interface between design and control. 1. Process Controllability, 2. Process Operability, 3. Selecting a set of controlled variables.". *Ind. Eng. Chem. Res.* 27:597-615.

FORGACS, O.L. 1963. "The Characterization of Mechanical Pulps". *Pulp & Paper Magazine of Canada*. Convention Issue (C). T89-T118.

FRANCIS, D.W., TOWERS, M.T., BROWNE, T.C. 2002. *Energy cost reduction in the pulp and paper industry - An energy benchmarking perspective.* Montreal, Canada: PAPTAC.

FU, Y., DUMONT, G. 1993. "Chip refiner motor load adaptive control using a Nonlinear Laguerre Model". *Second IEEE Conference on Control Applications*. Vancouver, B. C. P. 371-376

GARCIA, C.E., MORARI, M. 1982. "Internal model control. 1. A unifying review and some new results". *Ind. Eng. Chem. Process Des. Dev.* 21:2. 308-323.

GOODWIN, G.C., GRAEBE, S.F., and SALGADO, M.E. 2001. *Control system design*. New Jersey : Prentice Hall. 908 p.

GROENENDIJK, A.J., DIMIAN, A.C., IEDEMA, P.D. 2000. "Systems approach for evaluating dynamics and plantwide control of complex plants". *AIChE J.* 46:1. 133-145.

GROSDIDIER, P., MORARI, M., HOLT, B.R. 1985. "Closed-loop properties from steady-state gain information". *Ind. Eng. Chem. Fundam.* 24:221-235.

HAMPEL, F.R. 1974. "The influence curve and its role in robust estimation". *Journal of the American Statistical Association*. 69:382-393.

HARRIS, T.J. 1989. "Assessment of control loop performance". *Can. J. Chem. Eng.* 67:856-861.

HAUGE, T.A., SLORA, R., LIE, B. 2002. "Model predictive control of a Norske Skog Saugbrugs paper machine: preliminary study / Control Systems 2002". *7th International Conference on New Available Technologies*. Stockholm, Sweden :P. 75-79

HAVRE, K., SKOGESTAD, S. 1998. "Performance limitations for unstable SISO plants". *Proceedings of the American Control Conference* . AACC. 5, P.3234-3238.

HOLT, B.R., MORARI, M. 1985a. "Design of resilient processing plants - V. The effect of deadtime on dynamic resilience.". *Chem. Engng. Sci.* 40:1229-1237.

HOLT, B.R., MORARI, M. 1985b. "Design of resilient processing plants - VI. The effect of right-half-plane zeros on dynamic resilience.". *Chem. Engng. Sci.* 40:59-74.

HORCH, A., ISAKSSON, A.J., ALLISON, B.J., KARLSTROM, A., NILSSON, L. 1997. "Dynamic simulation of a thermomechanical pulp refiner". *Nordic Pulp and Paper Research Journal*. 12:4. 270-275.

HOVD, M., SKOGESTAD, S. 1992. "Simple frequency-dependent tools for control system analysis, structure selection and design". *Automatica*. 989-996.

JELALI, M. 2006. "An overview of control performance assessment technology and industrial applications". *Control Engineering Practice*. 14:441-466.

JOHANSSON, K.H. 2002. "Interaction bounds in multivariable control systems". *Automatica*. 38:1045-1051.

JORGENSEN, S.B., GANI, R., ANDERSEN, T.R. 1999. Lyngby, Denmark: CAPE-Center, Department of Chemical Engineering. Technical University of Denmark. 22. http://citeseer.nj.nec.com/282387.html

KALMAN, R.E. 1960. "On the general theory of control systems". *Proceedings of the First IFAC Congress*. Moscow : Butterwoths. P. 481-492

KAMMER, L., ALLISON, B., ROCHE, A. 2005. "Performance monitoring and advanced process control in the pulp and paper industry ". *TAPPI J.* 4:1. E33-E44.

KANO, T., IWAMIDA, T., SUMI, Y. 1982. "Energy consumption in mechanical pulping". *Pulp & Paper Canada*. 83:6. T157-T161.

KAUNONEN, A., LUUKKONEN, M. 1992. "Practical experiencies using continuous freeness measurement". *TAPPI J.* 75:3. 159-164.

KUHLMANN, Ch., BOGLE, D., CHALABI, Z. 1997. "On the controllability of continuous fermentation processes". *Bioprocess Engineering*. 17:367-374.

LAMA, I., PERRIER, M., STUART, P. 2004. "Controllability analysis of a TMP-newsprint refining process". Control Systems 2004, Preprints. Quebec City, Canada: P. 99-105

LAMA, I., PERRIER, M., STUART, P.R. 2003. "Applying controllability techniques to analyze a white water network for improved productivity in integrated newsprint mills". Resources, Conservation and Recycling. 37:181-192.

LAMA, I., PERRIER, M., STUART, P.R. 2006a: "An empirical model for predicting motor load changes due to plate wear in TMP-refiners", Accepted in *Nordic Pulp and Paper Research Journal.*

LAMA, I., PERRIER, M., STUART, P.R. 2006b. "Modeling the effect of plate age on the operation of TMP-refiners", *PAPTAC 92nd Annual Meeting PrePrints.* B161-B166.

LAMA, I., PERRIER, M., STUART, P.R., 2006c. "Controllability Analysis of a TMP-Newsprint Refining Process ", *Pulp and Paper Canada* (In Press).

LAMA, I., PERRIER, M., STUART, P.R. 2006d. "Analyzing the directionality of TMP-Refining interactions", Submitted to *TAPPI Journal.*

LAMA, I., PERRIER, M., STUART, P.R. 2006e. "A methodology to model TMP-Refining processes", Submitted to *TAPPI Journal.*

LAMA, I., PERRIER, M., STUART, P.R. 2006f. "Optimal operation of TMP-Newsprint Refiners", Submitted to *Nordic Pulp and Paper Research Journal.*

LEIVISKÄ, K. 1999. "Process Control". *Papermakng Science and Technology Series.* Sous la direction de J. GULLICHSEN, H. PAULAPURO. Jyväaskylä, Finland : Finnish Paper Engineers' Association and TAPPI .

LEWIN, D.R. 1999. "Interaction of design and control". *Proc. of the 7th IEEE Mediterranean Conference on Control and Automation .*

LEWIN, D.R., BOGLE, D. 1996 . "Controllability analysis of an industrial polymerization reactor". *Computers Chem. Engng.* 20:suppl. S871-S876.

LIU, H., SHAH, S., JIANG, W. 2004. "On-line outlier detection and data cleaning". *Computers Chem. Engng.* 28:1635-1647.

LUYBEN, W.L. 1993. "Dynamics and control of recycle systems. 3. Alternative process designs in a ternary system". *Ind. Eng. Chem. Res.* 32:1142-1153.

MA, K., BOGLE, D.L. 2001. "An approach to controllability and economic design of nonlinear systems with multiplicity". *European Symposium on Computer Aided Process Engineering - 11.* Amsterdam, Netherlands : Elsevier. P. 1047-1052.

MARINO-GALARRAGA, M., MCAVOY, T.J., MARLIN, T.E. 1987. "Short-cut operability analysis. 2. Estimation of fi detuning parameter for classical control systems. 3. Short-cut methodology for the assessment of process control designs". *Ind. Eng. Chem. Res.* 26:511-531.

MCAVOY, T.J. 1983. "Some results on dynamic interaction analysis of complex control systems". *Ind. Eng. Chem. Process Des. Dev.* 22:42-49.

MCAVOY, T.J. 1999. "Synthesis of plantwide control systems using optimization". *Ind. Eng. Chem. Res.* 38:2984-2994.

MCQUEEN, S.J. 1995. *Process identification and control of a TMP wood chip refiner.* Master Thesis., Department of Chemical Engineering. University of Toronto, Canada.

MCQUEEN, S.J., CLUETT, W.R., DUEVER, T.A. 1999. "Identification of a TMP wood chip refiner with implications for process control". *TAPPI J.* 82:5. 122-129.

MEEUSE, F.M., HUESMAN, A.E.M. 2002. "Analyzing dynamic interaction of control loops in the time domain". *Ind. Eng. Chem. Res.* 41:4585-4590.

MILES, K.B. 1990. "Refining intensity and pulp quality in high-consistency refining". *Paperi ja Puu.* 72:5. 508-514.

MILES, K.B. 1991. "A simplified method for calculating the residence time and refining intensity in a chip refiner". *Paperi ja Puu.* 73:9. 852-857.

MILES, K.B., MAY, W.D. 1990 . "The Flow of Pulp in Chip Refiners". *J. Pulp & Paper Sci.* 16:2. J63-J72.

MILES, K.B., MAY, W.D., KARNIS, A. 1991. "Refining intensity, energy consumption, and pulp quality in two-stage chip refining". *TAPPI J.* 74:3. 221-230.

MOHIDEEN, M.J., PERKINS, J.D., PISTIKOPOULOS, E.N. 1997. "Robust stability considerations in optimal design of dynamic systems under uncertainty". *J. Process Control.* 7:5. 371-385.

MOHLIN, U.-B. 1980. "Latency in thermomechanical pulps". *TAPPI J.* 63:3. 83-86.

MORARI, M. 1983. "Design of resilient processing plants - III. A general framework for the assessment of dynamic resilience". *Chem. Engng. Sci.* 38:11. 1881-1891.

MORARI, M. and ZAFIRIOU, E. 1989. *Robust Process Control.* New Jersey : Prentice Hall, Englewood Cliffs. 512 p.

NIEDERLINSKI, A. 1971. "A heuristic approach to the design of linear multivariable interacting control systems". *Automatica*. 7:691-701.

OGUNNAIKE, B.A. and RAY, W.H. 1994. *Process dynamics, modeling, and control.* New York : Oxford University Press, Inc. 1260 p.

ORCCOTOMA, J.-A. 1997. *Dynamique et commandabilité du réseau d'eaux blanches dans une usine intégrée de papier journal.* 210 p. PhD. Dissertation, École Polytechnique de Montréal.

PACIFIC SIMULATION . 2000. "WinGEMS 4.5 - Reference Manual".

PEDERSEN, K., JORGENSEN, S.B., SKOGESTAD, S. 1998. *CAPE.NET project.* Lyngby, Denmark: Department of Chemical Engineering, Technical University of Denmark. 12 p.

PIKULIK, I.I., CROTOGINO, R.H. 2001. "The future of R&D in the pulp and paper industry". *87th Annual Meeting* . Montréal, QC. Canada : PAPTAC. P. B257-B261

QIAN, X. 1997. *Modeling and Dynamic Simulation of a CTMP Plant.* Ph D Dissertation, University of British Columbia.

QIAN, X., TESSIER, P. 1995. "A mechanistic model for predicting pulp properties from refiner operating conditions". *TAPPI J.* 78:4. 215-222.

QIAN, X., TESSIER, P. 2000. "Dynamic behavior of a pulp processing and reject refinng plant". *TAPPI J.* 83:4. 1-9.

QIAN, Y., LIU, H., ZHANG, X., TESSIER, P. 1997. "Optimization of wood chip refining process based on fuzzy relational models". *Computers Chem. Engng.* 21:S1137-S1142.

RIVERA, D., MORARI, M., SKOGESTAD, S. 1986. "Internal model control. 4. PID Controller design". *Ind. Eng. Chem. Process Des. Dev.* 25:252-265.

ROCHE, A., OWEN, J., MILES, K., HARRISON R. 1996. "Practical approach to the control of TMP refiners". *Proceedings of the '96 Control Systems Conference.* Montréal, Canada : TAPPI Press. P. 129-135

ROGERS, J.H., VESPA, SC., BUTLER, D.J., LEGAULT, N.D. 1980. "Automatic control of chip refining". *Pulp & Paper Canada.* 81:10. T277-T282.

ROSENBROCK, H.H. 1970. *State-space and multivariable control.* London : Nelson.

RUDIE, A.W., MORRA, J., ST. LAURENT, J.M., HICKEY, K.L. 1994. "The influence of wood and fiber properties on mechanical pulping". *TAPPI J.* 77:6. 86-90.

RUSSELL, L.W., PERKINS, J.D. 1987. "Towards a method for diagnosis of controllability and operability problems in chemical plants". *Chem. Eng. Res. Des.* 65:453-461.

SALTIN, J., STRAND, B.C. 1993. "Modeling the Effects of Refiner Operation on Newsprint Quality". *Proceedings of the 1993 International Mechanical Pulping Conference.* Oslo, Norway.

SCHWARTZ, H.M., CHANG, G., LIU, Y., PHUNG, T. 1996. "A Method of Modeling, Predicting and Controlling TMP Pulp Properties". *Proceedings of the 1996 IEEE International Conference on Control Applications*. Dearborn, MI : IEEE. P. 846-851

SEIDER, W.D., SEADER, J.D., LEWIN, D.R. 1999. "Flowsheet controllability analysis". *Process Design Principles. Synthesis, Analysis & Evaluation*. Anonyme. New York : Wiley & Sons. P. 457-499.

SEMINO, D., GIULIANI, G. 1997. "Control configuration selection in recycle systems by steady state analysis". *Computers Chem. Engng.* 21:S273-S278.

SHUNTA, J.P. 1996. "Use statistics to identify process control opportunities". *Chem. Eng. Prog.* October:47-49.

SIDHU, M.S., LAHOUAOULA, A., KOSUNEN, J., STEELE, T.H. 2005. "Advances in mechanical pulping control and measurement". *Paptac 91st Annual Meeting* . Montréal, Canada : PAPTAC. P. D751-D755

SIDHU, M.S., VAN FLEET, R., DION, M.R., ANDERSON, D.W., WEGER, B.W. 2004. "Modeling and advanced control of TMP refiner system". *Control Systems 2004 Conference, Preprints*. Quebec City, Canada :P. 107-112

SKOGESTAD, S. 2000. "Plantwide control: the search for the self-optimizing control structure". *J. Process Control.* 10:487-507.

SKOGESTAD, S., HAVRE, K. 1996. "The use of RGA and condition number as robustness measures". *Comp. Chem. Engng.* 20, Suppl.:S1005-S1010.

SKOGESTAD, S., HOVD, M. 1990. "Use of frequency-dependent RGA for control structure selection". *Proceedings of the 1990 American Control Conference.* Publ by American Automatic Control Council, Green Valley, AZ, USA. P. 2133-2139.

SKOGESTAD, S., MORARI, M. 1987a. "Design of resilient processing plants - IX. Effect of model uncertainty on dynamic resilience". *Chem. Engng. Sci.* 42:7. 1765-1780.

SKOGESTAD, S., MORARI, M. 1987b. "Effect of disturbance directions on closed-loop perfomance". *Ind. Eng. Chem. Res.* 26:2029-2035.

SKOGESTAD, S., MORARI, M. 1987c. "Implications of large RGA elements on control performance". *Chem. Eng. Res. Des.* 26:11. 2323-2330.

SKOGESTAD, S. and POSTLETHWAITE, I. 1996. *Multivariable Feedback Control. Analysis and Design.* West Sussex, England : John Wiley & Sons Ltd. 559 p.

SOLOVYEV, B.M., LEWIN, D.R. 2001. "A steady-state process resiliency index for non-linear processes". *6th IFAC Symposium on Dynamics and Control of Process Systems.* Jejudo, Korea :P. 1-5

STANFELJ, N., MARLIN, T.E., MACGREGOR, J.F. 1993. "Monitoring and diagnosing process control performance: The single-loop case". *Ind. Eng. Chem. Res.* 32:2. 301-314.

STANLEY, G., MARINO-GALARRAGA, M., MCAVOY, T.J. 1985. "Shortcut operability analysis. 1. The relative disturbance gain". *Ind. Eng. Chem. Process Des. Dev.* 24:1181-1188.

STATIONWALA, M.I., MILES, K.B., KARNIS, A. 1993. "The effect of first-stage refining conditions on pulp properties and energy consumption". *J. Pulp & Paper Sci.* 19:1. J12-J18.

STATIONWALA, M.I., MILES, K.B., KARNIS, A. 1994. "Effect of Feed Rate on Refining". *J. Pulp & Paper Sci.* 20:8. J236-J240.

STOERE, P., NAZHAD, M., KEREKES, R. 2001. "An experimental study of the effect of refining on paper formation (Tappi Journal peer reviewed paper)". *TAPPI J.* 84:7. 1-9.

STRAND, B.C. 1989. *Simulation, control and online optimization on mechanical pulping systems* . PhD Dissertation. Department of Chemical Engineering. University of Idaho.

STRAND, B.C. 1998. "Quality control of high-consistency refiners". *TAPPI J.* 81:12. 159-164.

STRAND, B.C., EDWARDS, L.L. 1983. "Optimum design, operation and control of mechanical pulping systems". *International Mechanical Pulping Proceedings*. Washington, D.C. TAPPI. P. 277-295

STRAND, B.C., FALK, B., MOKVIST, A., JACKSON, M. 1993. "The Effect of Production Rate on Specific Energy Consumption in High Consistency Chip Refining". *International Mechanical Pulping Convention*. Oslo, Norway :P. 12 p.

STRAND, B.C., FERRITSIUS, O., MOKVIST, A. 1991. "Use of simulation models in the on-line control and optimization of the refining process". *TAPPI J.* 74:11.

STRAND, B.C., HARTLER, N. 1985. "Modelling and optimization of full scale chip refining". *International Mechanical Pulping Conference*. Stockholm, Sweden :P. 46-54

STRAND, B.C., MOKVIST, A. 1989a. "The application of Comminution Theory to describe Refiner Performance". *J. Pulp & Paper Sci.* 15:3. J100-J105.

STRAND, B.C., MOKVIST, A. 1989b. "On-line modelling of Refiner Performance". *Pulp & Paper Canada*. 90:12. T499-T504.

STRAND, B.C., REICHERT, T., FILLER, A., BROOKS, Z., NUNN, B., FARMIN, D. et al. 2000. "Control and optimization of mechanical pulping systems". *TAPPI J.* 83:9. 16 pp.

SUNDHOLM, J. 2000. "Mechanical Pulping". *Papermaking Science and Technology Series*. Sous la direction de J. GULLICHSEN, H. PAULAPURO. Jyväaskylä, Finland : Finnish Paper Engineers' Association and TAPPI .

TASMAN, J.E. 1972. "The Fiber Length of Bauer-McNett Screen Fractions". *TAPPI J.* 55:1. 136-138.

TSENG, J.L., CLUETT, W.R., BIALKOWSKI, W.L. 1999. "New analysis and design tool for achieving low variability process designs". *AIChE J.* 45:10. 2188-2202.

WEITZ, O., LEWIN, D.R. 1996 . "Dynamic controllability and resiliency diagnosis using steady state process flowsheet data". *Computers Chem. Engng.* 20:4. 325-335.

WOLFF, E., SKOGESTAD, S. 1994. "Operability of integrated plants". *Proceedings of PSE'94*. P.63-69.

WOLFF, E.A. 1994. *Studies on control of integrated plants.* Ph D. Dissertation. University of Trondheim. The Norwegian Institute of Technology.

ZIEGLER, J.G., NICHOLS, N.B. 1943. "Process lags in automatic-control circuits". *Trans. A.S.M.E.* 65:433-444.

APPENDIX A: **Calculation of refiner consistency**

The inlet consistency C_i is calculated doing a simple mass balance:

$$C_i = \frac{F_c}{(W_{inlet} + F_c + F_{dil} + F_{seal})} \cdot 100 \qquad [A.1]$$

where F_{dil} is the dilution mass flowrate and F_{seal} is the seal water mass flowrate. The mass flowrate of water coming with the entering pulp is calculated as follows:

$$W_{inlet} = F_c \cdot \frac{H}{100 - H} \qquad [A.2]$$

where H is the water content of the pulp entering the refiner which also represents wood moisture in case of primary refiners.

Remark: Normally, dilution and seal flowrates are given in L/min. In order to use equation [A.1] these values must be transformed to mass units. Provided temperatures for both dilution and seal water are available, such conversion can be written as (Pacific Simulation, 2000):

$$F = 1.44 \cdot Q \cdot fac \qquad [A.3]$$

Where Q is the volumetric flowrate and the correction factor is given by:

$$fac = \frac{999.84 + 16.945 \cdot T - 0.00799 \cdot T^2 - 0.000046170 \cdot T^3 + 0.00000010556 \cdot T^4 - 0.00000000028054 \cdot T^5}{1000 \cdot (1 + 0.01687985 \cdot T)}$$

where T is the temperature of either the dilution or the seal water.

In order to calculate the outlet consistency the following mass and energy balances must be carried out:

a. Water mass balance:

$$W_{oulet} = W_{inlet} + F_{dil} + F_{seal} - W_s \qquad [A.4]$$

where W_o is the water flowrate leaving the refiner with the pulp and W_s is the saturated steam flowrate leaving the refiner.

b. Total mass balance:

$$C_{oulet} = \frac{F_{co}}{W_{oulet} + F_{co}} \qquad [A.5]$$

where F_{co} is the remaining dry production rate after a yield loss y_{loss} and is calculated as follows:

$$F_{co} = F_c \cdot \frac{(100 - y_{loss})}{100} \qquad [A.6]$$

c. Total energy balance:

Energy IN

$$\underbrace{W_{inlet} \cdot Cp_w \cdot T_{inlet} + F_{co} \cdot Cp_f \cdot T_{inlet}}_{\text{Pulp (or chips) IN}} + \underbrace{\eta \cdot ML}_{\text{Motor}} + \underbrace{F_{dil} \cdot Cp_w \cdot T_{dil}}_{\text{Dilution water}} + \underbrace{F_{seal} \cdot Cp_w \cdot T_{seal}}_{\text{Seal water}} \qquad [A.7]$$

Energy OUT

$$\underbrace{F_{co}\cdot Cp_f\cdot T_{outlet}+W_{outlet}\cdot Cp_w\cdot T_{outlet}}_{\text{Pulp OUT}}+\underbrace{W_s\cdot L_e}_{\text{Steam}}+\underbrace{e_{loss}\cdot\eta\cdot ML}_{\text{Heat Loss}} \qquad [A.8]$$

where Cp_w and Cp_f is the specific heat of water and fibre, respectively. The refiner's inlet and outlet temperatures are denoted by T_{inlet} and T_{outlet}, respectively, while the temperature of the dilution water and that of seal water are T_{dil} and T_{seal}. The efficiency of the motor is represented by η, the heat losses around the refiner by e_{loss}, and the enthalpy of the saturated steam produced during refining is calculated via interpolation from steam tables and denoted by L_e.

The total amount of steam produced can be calculated from the above energy balance, i.e. by equalizing expressions [A.7] and [A.8],

$$\begin{aligned}&W_{inlet}\cdot Cp_w\cdot T_{inlet}+F_{co}\cdot Cp_f\cdot(T_{inlet}-T_{outlet})+(1-e_{loss})\cdot\eta\cdot ML+\ldots\\&+F_{dil}\cdot Cp_w\cdot T_{dil}+F_{seal}\cdot Cp_w\cdot T_{seal}-W_{outlet}\cdot Cp_w\cdot T_{outlet}=W_s\cdot L_e\end{aligned} \qquad [A.9]$$

Substituting equation [A.4] into [A.9] gives:

$$\begin{aligned}W_s=\frac{(1-e_{loss})\cdot\eta\cdot ML}{(L_e-Cp_w\cdot T_{outlet})}&-\frac{\left[W_{inlet}\cdot Cp_w\cdot(T_{outlet}-T_{inlet})+F_{co}\cdot Cp_f\cdot(T_{outlet}-T_{inlet})\right]}{(L_e-Cp_w\cdot T_{outlet})}-\ldots\\&\frac{-\left[F_{dil}\cdot Cp_w\cdot(T_{outlet}-T_{dil})+F_{seal}\cdot Cp_w\cdot(T_{outlet}-T_{seal})\right]}{(L_e-Cp_w\cdot T_{outlet})}\end{aligned} \qquad [A.10]$$

Assumptions such that (a) the energy absorbed by water and pulp is negligible compared to the energy applied to the refiner, and (b) the latent heat of water is substantially greater than the corresponding specific heat, result in the following simplifications (Du, 1998):

$$(1-e_{loss})\cdot\eta\cdot ML >> W_{inlet}\cdot Cp_w\cdot(T_{outlet}-T_{inlet})+F_{co}\cdot Cp_f\cdot(T_{outlet}-T_{inlet})+\ldots$$
$$+F_{dil}\cdot Cp_w\cdot(T_{outlet}-T_{dil})+F_{seal}\cdot Cp_w\cdot(T_{outlet}-T_{seal}) \qquad [A.11]$$

$$L_e >> Cp_w\cdot T_{outlet}$$

Substituting the simplifications [A.11] into [A.10] gives the amount of steam produced:

$$W_s=\frac{(1-e_{loss})\cdot\eta\cdot ML}{L_e} \qquad [A.12]$$

Finally, the outlet consistency is calculated by substituting equations [A.2], [A.12], [A.6], and [A.4] into equation [A.5]:

$$C_{outlet}=\frac{F_c\cdot\frac{(100-y_{loss})}{100}}{\left[F_c\cdot\frac{H}{100-H}\right]+F_{dil}+F_{seal}-\left[\frac{(1-e_{loss})\cdot\eta\cdot ML}{L_e}\right]+F_c\cdot\frac{(100-y_{loss})}{100}} \qquad [A.13]$$

APPENDIX B: **Model estimates for pulp quality and total specific energy during LV conditions**

These figures show that almost all model estimates acceptably represent actual nominal values within the boundaries imposed by the corresponding current variability (Superimposed rectangles). In Figure- B.2, note that although estimation for plate age condition PR119-SR119 does not fall inside variability limits, it follows actual nominal trend.

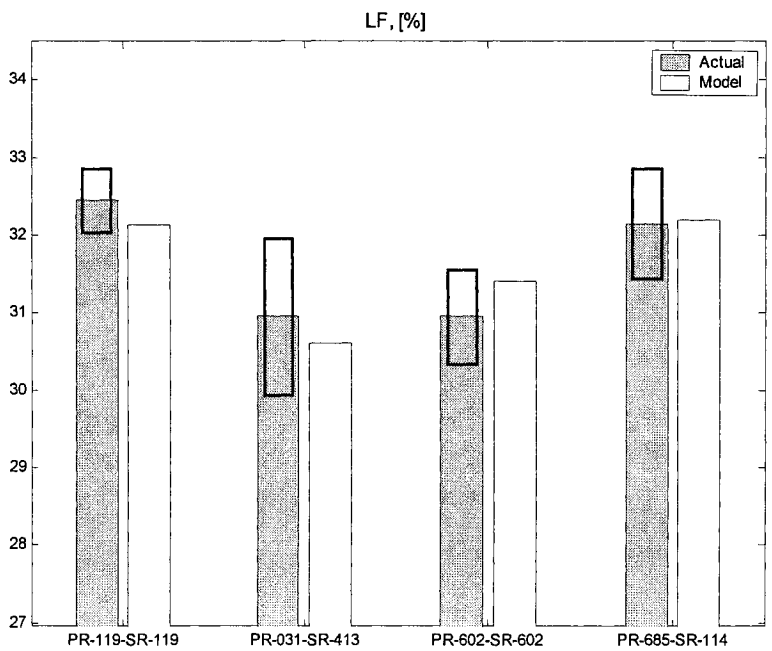

Figure- B.1. Model-mismatch in long fibre content.

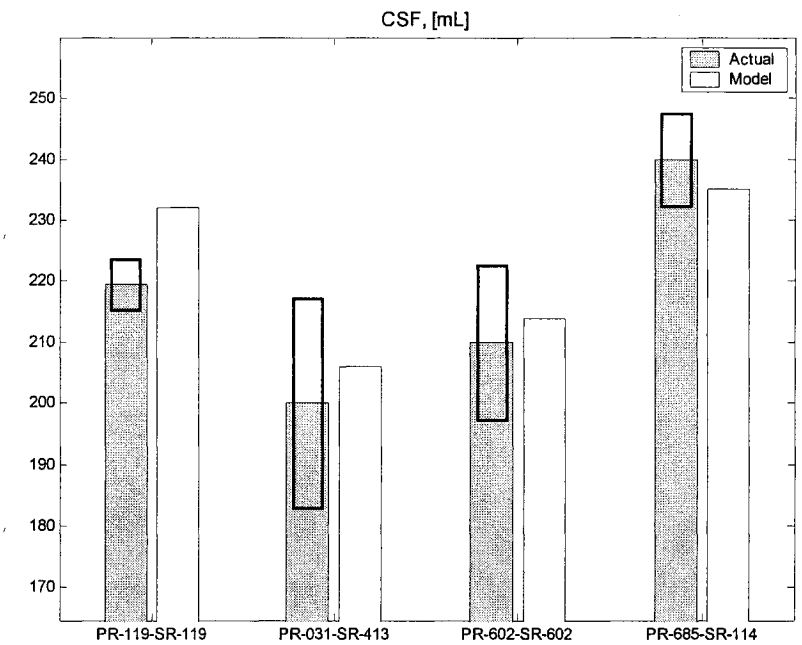

Figure- B.2. Model-mismatch in freeness.

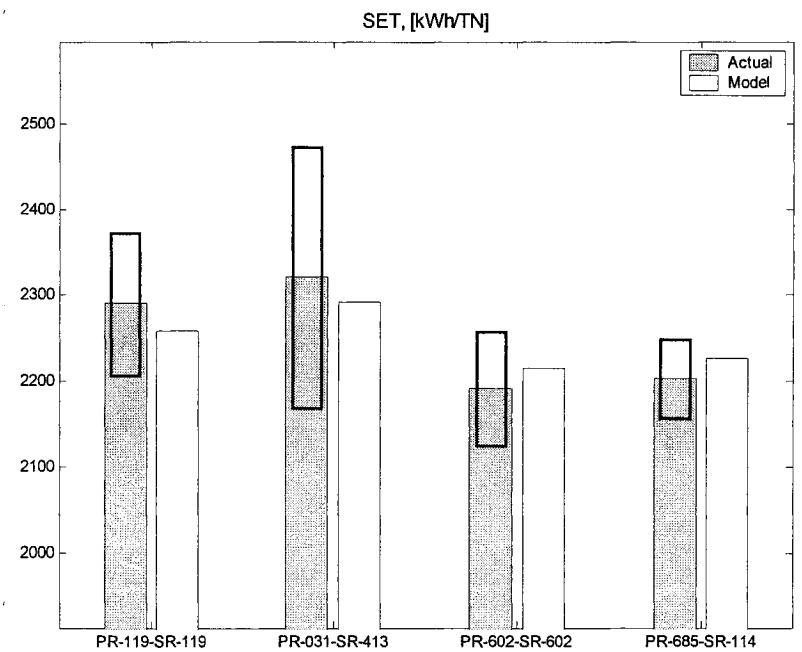

Figure- B.3. Model-mismatch in total specific energy.

APPENDIX C: **Feasibility of alternative operating conditions**

The use of a suitable back-off when searching for an optimal solution results in a operating point that has "room for manipulation without saturation" when disturbances occur:

$$\begin{aligned} NLC &= LC + (UC - LC) \cdot bk \\ NUC &= UC - (UC - LC) \cdot bk \end{aligned} \qquad [C.1]$$

where LC and UC denote the original lower and upper constraints, respectively (see Table 1.1), bk the fraction of back-off, and NLC and NUC the corresponding backed-off constraints.

At certain back-off, feasibility can be restored by relaxing both quality constraints. Accordingly, freeness and long fibre content specifications have been relaxed to various degrees so as to find more feasible alternatives to each benchmark operating condition:

$$\begin{aligned} NLC_{quality} &= LC_{quality} + (UC_{quality} - LC_{quality}) \cdot bk \cdot (1 - mov) \\ NUC_{quality} &= UC_{quality} - (UC_{quality} - LC_{quality}) \cdot bk \cdot (1 - mov) \end{aligned} \qquad [C.2]$$

where mov denotes the fraction by which back-off is relaxed. It is clear from equation [C.2] that if $mov > 1$ then both quality constraints are relaxed beyond the values given in Table 1.1. Results shown in Table- C.1 indicate that having old plates – especially in the secondary refiner- leads to unfeasible operation at high back-offs.

Table- C.1. Feasibility of alternative operating conditions under back-off and quality constraint relaxation.

Back-off, *bk* (in %)	Benchmark conditions	Quality constraint relaxation, *mov*												
		0	0.5	1	1.5	2	2.5	3	4	5	10	12	16	20
5	P119-S119	F	F	F	F	F	F	F	F	F	F	F	F	F
	P602-S602	U	U	U	U	U	U	U	U	F	F	F	F	F
	P31-S413	F	F	F	F	F	F	F	F	F	F	F	F	F
	P685-S114	F	F	F	F	F	F	F	F	F	F	F	F	F
8	P119-S119	F	F	F	F	F	F	F	F	F	F	F	F	F
	P602-S602	U	U	U	U	U	U	U	U	F	F	F	F	F
	P31-S413	F	F	F	F	F	F	F	F	F	F	F	F	F
	P685-S114	F	F	F	F	F	F	F	F	F	F	F	F	F
10	P119-S119	F	F	F	F	F	F	F	F	F	F	F	F	F
	P602-S602	U	U	U	U	U	U	U	U	F	F	F	F	F
	P31-S413	F	F	F	F	F	F	F	F	F	F	F	F	F
	P685-S114	F	F	F	F	F	F	F	F	F	F	F	F	F
13	P119-S119	F	F	F	F	F	F	F	F	F	F	F	F	F
	P602-S602	U	U	U	U	U	U	U	U	U	U	U	U	U
	P31-S413	F	F	F	F	F	F	F	F	F	F	F	F	F
	P685-S114	F	F	F	F	F	F	F	F	F	F	F	F	F
15	P119-S119	F	F	F	F	F	F	F	F	F	F	F	F	F
	P602-S602	U	U	U	U	U	U	U	U	U	U	U	U	U
	P31-S413	U	F	F	F	F	F	F	F	F	F	F	F	F
	P685-S114	F	F	F	U	F	F	F	F	F	F	F	F	F
18	P119-S119	F	F	F	F	F	F	F	F	F	F	F	F	F
	P602-S602	U	U	U	U	U	U	U	U	U	U	U	U	U
	P31-S413	U	U	U	U	U	U	U	U	U	U	U	U	U
	P685-S114	F	F	F	F	F	F	F	U	F	F	F	F	F
20	P119-S119	U	F	F	F	F	F	F	F	F	F	F	F	U
	P602-S602	U	U	U	U	U	U	U	U	U	U	U	U	U
	P31-S413	U	U	U	U	U	U	U	U	U	U	U	U	U
	P685-S114	U	U	U	U	U	U	U	U	U	U	U	U	U

F: Feasible; U: Not feasible

APPENDIX D: **Niederlinski Index and DCLI results for selected control configuration**

All results are positive, and therefore c-CSF satisfies necessary conditions for DCLI.

New plates (P119-S119):

NI = 0.92

RGA diagonal elements:

1. For all possible combinations of 3-loop failures, i.e. $l = 2$:

$\lambda_{1,1}$ =	1.52	1	1	1	1	1.34	0.77	0.67	1.1	0.71
$\lambda_{2,2}$ =	1.52	1	1	1	1	1.34	0.77	0.67	1.1	0.71

2. For all possible combinations of 2-loop failures, i.e. $l = 3$:

$\lambda_{1,1}$ =	1	1	1.34	1.34	0.81	1.02	0.71	0.66	0.53	0.73
$\lambda_{2,2}$ =	1.52	1.52	1.34	1.34	1.6	1.33	1.06	0.86	0.79	0.90
$\lambda_{3,3}$ =	1.52	1.52	1	1	1.84	0.93	0.65	0.93	0.74	1.38

Old plates (P602-S602):

NI = 0.82

RGA diagonal elements:

3. For all possible combinations of 3-loop failures, i.e. $l = 2$:

$\lambda_{1,1}$ =	1.55	1	1	1	1	1.34	0.85	0.72	1.13	0.75
$\lambda_{2,2}$ =	1.55	1	1	1	1	1.34	0.85	0.72	1.13	0.75

4. For all possible combinations of 2-loop failures, i.e. $l = 3$:

$\lambda_{1,1}$ =	1	1	1.34	1.34	0.92	1.08	0.79	0.72	0.58	0.78
$\lambda_{2,2}$ =	1.55	1.55	1.34	1.34	1.67	1.27	1.09	0.84	0.81	0.92
$\lambda_{3,3}$ =	1.55	1.55	1	1	1.98	0.96	0.69	0.96	0.77	1.39